

HOX FUNCTION IN MAMMALIAN KIDNEY DEVELOPMENT

by

Alisha Ruth Yallowitz

A dissertation submitted in partial fulfillment
of the requirements for the degree of
Doctor of Philosophy
(Cell and Developmental Biology)
in The University of Michigan
2009

Doctoral Committee:

Assistant Professor Deneen Wellik, Chair
Professor Gregory R. Dressler
Professor K. Sue O'Shea
Associate Professor Thomas M. Glaser
Assistant Professor Philip J. Gage

If we knew what we were doing,
it wouldn't be called research, would it?

Albert Einstein
1879-1955

© Alisha Ruth Yallowitz

2009

To all my colleagues, friends, and family,
especially my parents, who have put up
with me and my quirks over the years.

TABLE OF CONTENTS

DEDICATION	ii
LIST OF FIGURES	v
CHAPTER I: GENERAL INTRODUCTION.....	1
The discovery of <i>Hox</i> genes.....	1
Evolutionary conservation of <i>Hox</i> genes.....	3
Mammalian <i>Hox</i> genes	5
Hox protein function	7
Hox cofactors	9
Kidney as a model organ	10
Kidney signaling pathways.....	13
Ascent of the kidney during development	17
<i>Hox</i> genes in the kidney.....	17
Rationale.....	18
CHAPTER II: A HOX-EYA-PAX COMPLEX REGULATES EARLY KIDNEY DEVELOPMENTAL GENE EXPRESSION.....	20
Abstract.....	20
Introduction	21
Material and methods	24
Results	28
Discussion.....	37

Acknowledgements.....	41
CHAPTER III: NON-HOMEODOMAIN REGIONS CONFER ACTIVATION VERSUS REPRESSION ACTIVITIES TO MAMMALIAN HOX PROTEINS	42
Abstract.....	42
Introduction	43
Material and methods	47
Results	48
Discussion.....	63
Acknowledgements.....	69
CHAPTER IV: THE <i>HOX10</i> PARALOGOUS GENES ARE NECESSARY FOR METANEPHRIC KIDNEY MORPHOGENESIS	71
Abstract.....	71
Introduction	72
Materials and methods.....	75
Results	77
Discussion.....	89
Acknowledgements.....	92
CHAPTER V: CONCLUDING REMARKS	93
Summary of contributions	93
Discussion and future directions	94
Novel Hox cofactors.....	94
Regulatory domains of Hox proteins	95
<i>Hox10</i> genes pattern the kidney stroma	96
APPENDIX: <i>HOX</i> PATTERNING OF THE VERTEBRATE RIB CAGE.....	97
REFERENCES.....	125

LIST OF FIGURES

Figure 1.1	Homeotic genes in <i>Drosophila melanogaster</i>	2
Figure 1.2	Evolution of Hox clusters	4
Figure 1.3	Organization of mammalian <i>Hox</i> genes.....	6
Figure 1.4	Anterior homeotic transformation of the axial skeleton in <i>Hox10</i> mutants.....	8
Figure 1.5	Stages of kidney development	12
Figure 1.6	Differentiation of the metanephros.	14
Figure 1.7	Transcription factors and signals necessary for ureteric bud induction.....	15
Figure 2.1	Regulation of <i>Six2</i> expression by a Hox11-Eya1-Pax2 complex	29
Figure 2.2	Pax2 binds regions upstream of the <i>Six2</i> protein coding sequence	31
Figure 2.3	The Hox11-Eya1-Pax2 complex binds at the -450 site and is necessary for <i>Six2</i> expression.....	33
Figure 2.4	<i>Hox11-Eya1-Pax2</i> binding site is critical for kidney expression <i>in vivo</i> and the Hox-Eya-Pax network synergistically activates <i>Gdnf</i> expression.	35
Figure 2.5	Diagram of proposed mechanism of Hox11 molecular function	.38
Figure 3.1	<i>Six2</i> expression is differentially regulated in <i>Hoxa2</i> and <i>Hox11</i> mutant embryos.....	49
Figure 3.2	A single enhancer site regulates <i>Six2</i> repression in the developing periotic mesenchyme and <i>Six2</i> activation in the kidney.....	51
Figure 3.3	Differential regulation of <i>Six2</i> in reporter assays	52

Figure 3.4	Different Hox proteins can act as repressors and activators of <i>Six2</i> expression	54
Figure 3.5	Mammalian Hox protein sequence comparisons	56
Figure 3.6	Generation of chimeric Hox protein expression constructs.....	59
Figure 3.7	Non-homeodomain regions of Hox proteins are critical for differential regulation of <i>Six2</i> expression	61
Figure 4.1	<i>Hox10</i> mutant animals have severe morphological defects.....	78
Figure 4.2	<i>Hox10</i> mutants have reduced ureter branching and failure of kidney ascension affects ureter position.....	80
Figure 4.3	<i>Hox10</i> mutants have smooth muscle disorganization at the UPJ and reduced nephrogenesis	82
Figure 4.4	The <i>Hox10</i> paralogs are expressed in the nephrogenic mesenchyme and cortical stroma.....	84
Figure 4.5	Patterning of the nephrogenic mesenchyme	86
Figure 4.6	Regulation of the cortical stroma cells.....	88

CHAPTER I

GENERAL INTRODUCTION

The discovery of *Hox* genes

The fruit fly, *Drosophila melanogaster*, has eight homeobox genes, first named the *HomC* complex. This cluster of homeodomain containing transcription factors was first described in the 1970's by E. B. Lewis as determinants of body segment fate along the anterior-posterior (AP) axis. *Drosophila* have fifteen body segments partitioned into the mandibular, maxillary, and labial components in the anterior body, three thoracic segments in the medial region, and nine abdominal segments at the posterior (Figure 1.1A). The most anterior *HomC/Hox* genes, *labial (lab)*, *proboscipedia (pb)*, *sex combs reduced (scr)*, and *Antennapedia (Antp)*, are grouped into a complex called the Antennapedia complex (Ant-C) and pattern the anterior elements up to the second thoracic segment [1]. The ten caudal most segments are patterned by the posterior genes of the *HomC* cluster called the Bithorax complex (Bx-C), which consists of *Ultrabithorax (Ubx)*, *abdominal A (abd-A)*, and *abdominal B (abd-B)* homeobox genes [2].

Figure 1.1

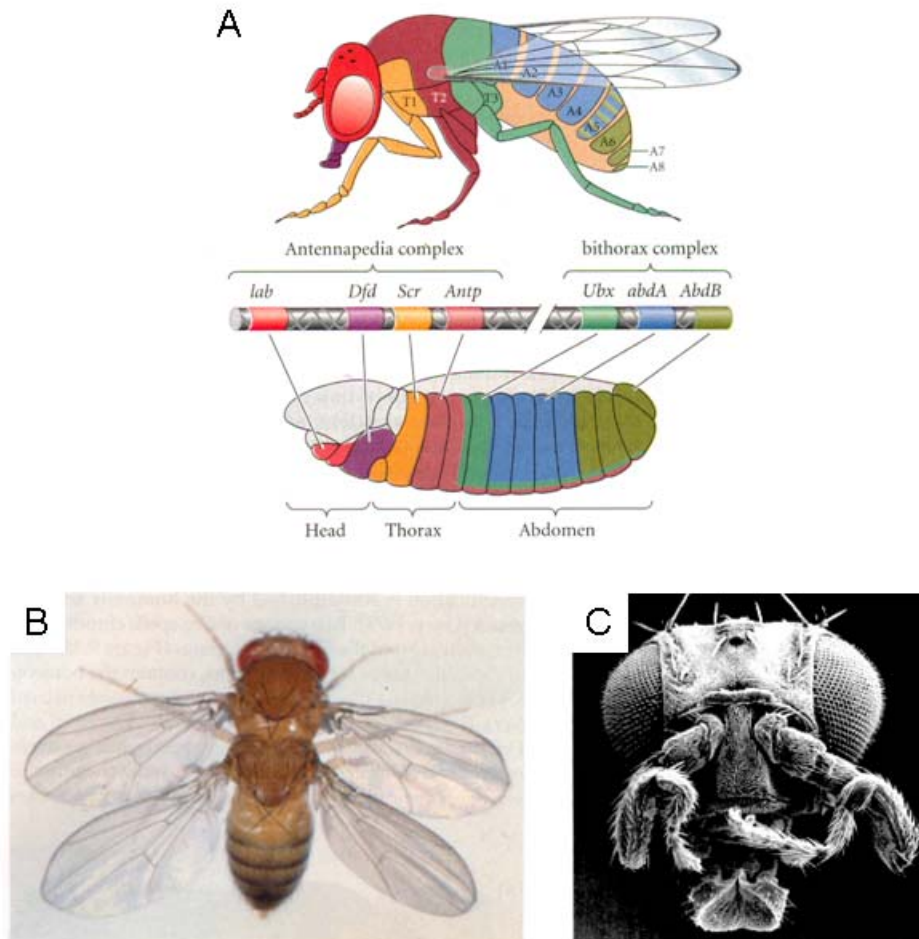


Figure 1.1. Homeotic genes in *Drosophila melanogaster*. Images adapted from [3]. (A) Expression of the *HomC* genes along the anterior-posterior body axis. Of the Antennapedia complex, the *labial* (*lab*) and *deformed* (*dfd*) genes are expressed in the head structures while *sex-combs reduced* (*scr*) and *antennapedia* (*antp*) are expressed in the first two thoracic segments (T1 and T2). Of the biothorax complex, *ultrabithorax* (*ubx*) is expressed in the third thoracic segment while *abdominal A* (*abdA*) and *abdominal B* (*abdB*) are expressed in the posterior abdominal segments. (B) Mutants with a loss-of-function of *ultrabithorax* have legs and an extra set of wings develop on the third thoracic segment instead of legs and halteres. (C) Mutants with a gain-of-function of *antennapedia* in the head grow legs instead of antennae.

HomC genes are organized in a collinear manner along the chromosome and mutations cause homeotic changes in body segment pattern [4]. Loss-of-function mutations in *Drosophila Hox* genes lead to anterior homeotic transformations. For example, *Ubx* controls the fate of the third thoracic element to create a pair of legs and structures called halteres [4]. *Ubx* mutants demonstrate an anterior shift in fate of the third thoracic segment to that of the second thoracic segment, whereby legs and wings develop on this mutant segment in place of the legs and halteres that would normally develop (Figure 1.1B). Gain-of-function mutants demonstrate posterior homeotic transformations. This is observed when *Antp* is overexpressed in the head, instead of just the first two thoracic elements, and cause legs to grow out of the head instead of antennae (Figure 1.1C) [1, 5-7].

Evolutionary conservation of *Hox* genes

Hox genes are a distinct class of clustered homeobox containing transcription factors that can be traced back to the divergence of plants and animals, about one billion years ago (Figure 1.2) [8]. Replication and divergence of initial ancestral homeobox genes along the same chromosome formed the linear arrangement of different *Hox* genes. The earliest chordate to have this linear arrangement of *Hox* genes is the *Amphioxus*, which is believed to have the ancestral *Hox* cluster for all metazoans [9-11]. A series of duplications of the original chromosomal cluster, and subsequent divergence of some of the

Figure 1.2

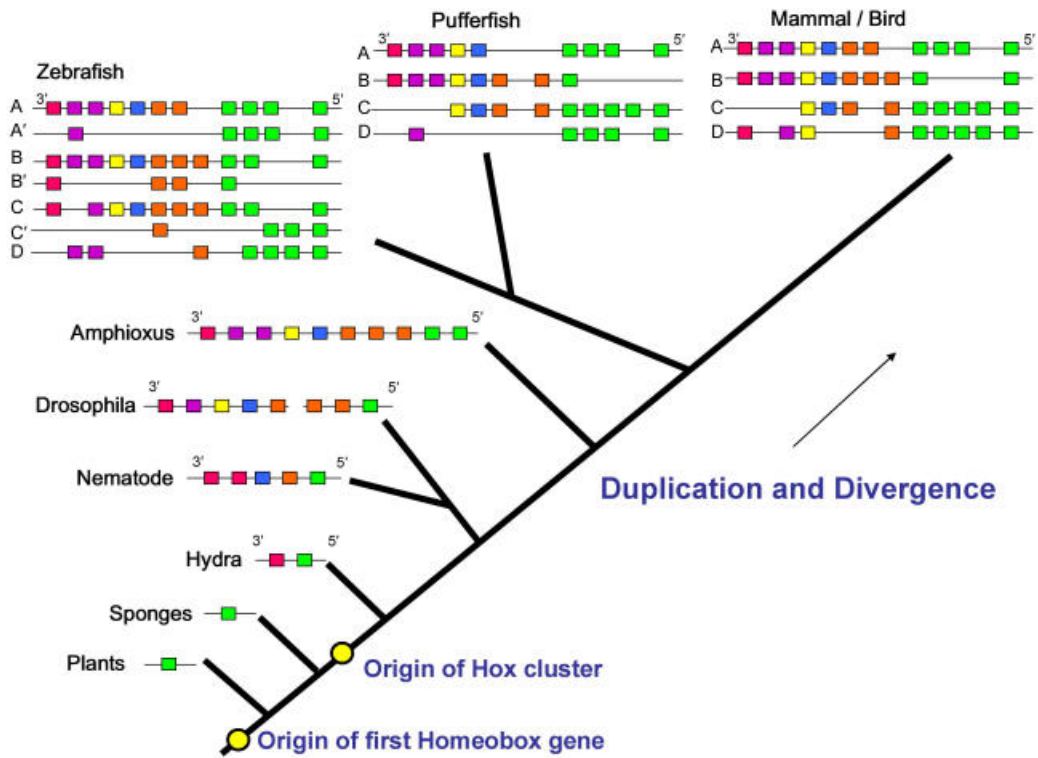


Figure 1.2. Evolution of *Hox* clusters. Figure taken from [8]. *Hox* genes are a special subset of homeobox genes that have undergone a series of duplications and divergence over time to form distinct clustered arrangements observed in higher order organisms today.

Hox genes along the replicated chromosomes, created the multiple chromosomal clusters of *Hox* genes observed in higher vertebrates today [12, 13].

Mammalian *Hox* genes

Mammals have 39 *Hox* genes arranged into four clusters. These genes are further subdivided into thirteen paralogous groups, which are designated based on similarity of the homeodomain sequence and by position along the cluster (Figure 1.3) [14]. Numerous genetic studies have demonstrated that genes within each paralogous group are functionally redundant. In many single *Hox* mutant mice, only a minimal phenotype is observed because the remaining paralogs compensate for it. When all of the genes in a paralogous group are lost, dramatic changes in patterning occur [15-27].

As in *Drosophila* and other bilateran organisms, mammalian *Hox* genes demonstrate colinearity [28, 29]. The *Hox* genes are organized in a 5' to 3' direction along the chromosomal clusters [12]. Genes that are at the 3' end have a more anterior boundary of expression, such as in the hindbrain and cervical vertebral elements, than the ones towards the 5' end of the clusters, which are expressed more caudally [30, 31]. This creates a spatial organization of *Hox* gene expression along the AP body axis. Unlike in *Drosophila*, the collinear arrangement of the mammalian *Hox* genes also results in their temporal control of expression in early embryonic development. The anterior 3' genes in a cluster are expressed earlier during development than the posterior 5' genes. This temporal control establishes the expression domains of *Hox* genes, which is

Figure 1.3

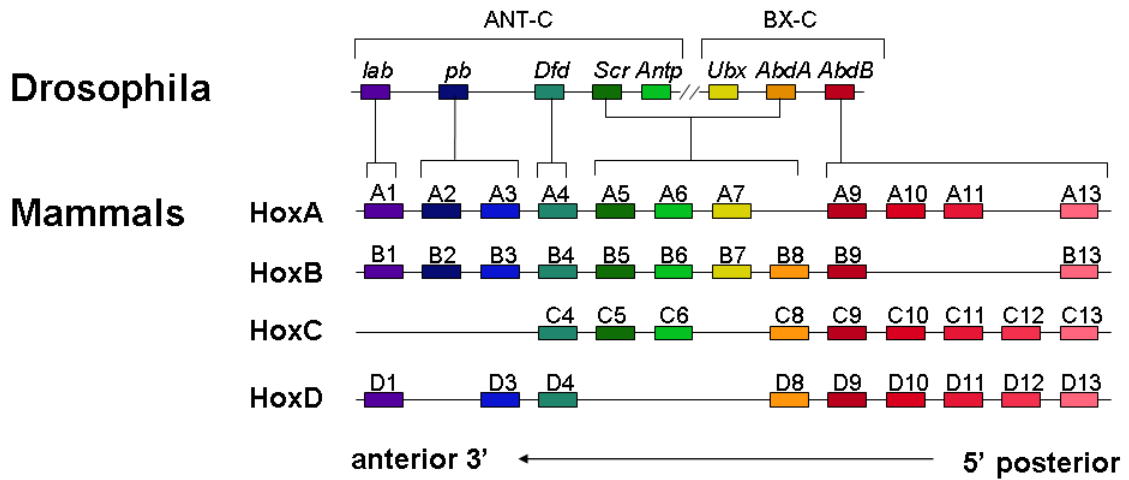


Figure 1.3. Organization of mammalian *Hox* genes. Figure adapted from [32]. Mice and humans have a total of 39 *Hox* genes found among four chromosomal clusters and organized into 13 paralogous groups (genes within a paralogous group are color-coded). The organization of the paralogous groups is similar to that observed in *Drosophila* providing spatial colinearity, with the 3' genes expressed more anterior than the 5' genes. This 3' to 5' organization also provides a temporal colinearity of the mammalian *Hox* genes, with the anterior genes expressed earlier in development than those more posterior.

observed during limb development and axial skeleton organogenesis along the AP axis [33, 34].

Hox genes are essential for the formation of numerous organ systems. One of the most well-defined roles for the *Hox* genes is the patterning of the axial skeleton [32]. Each vertebral element derives from somites, which have budded off the paraxial mesoderm. Initially, somites are morphologically identical; however they differentiate to form the distinct skeletal elements along the anterior-posterior body axis. Some of the earliest phenotypes described in *Hox* loss-of-function mutants were homeotic shifts in the axial skeleton [16, 20, 24, 35-47]. As in *Drosophila*, loss-of-function *Hox* mutants result in anterior homeotic transformations of the vertebral elements. One of the most striking examples is the anterior homeotic transformation observed in *Hox10* mutants. These mutants display an anterior homeotic transformation of lumbo-sacral vertebrae to a thoracic phenotype, with ectopic ribs forming through the posterior axial elements (Figure 1.4) [24]. In addition to the axial skeleton, *Hox* genes are also critical for patterning the limbs, hindbrain, craniofacial skeleton, and a multitude of mesodermal organs such as the parathyroid, thyroid, thymus, lungs, and kidney [48-53].

Hox protein function

Despite numerous genetic studies demonstrating that *Hox* genes are critical for many developmental processes, little is understood regarding the mechanisms by which Hox proteins function [54]. All Hox proteins contain a

Figure 1.4

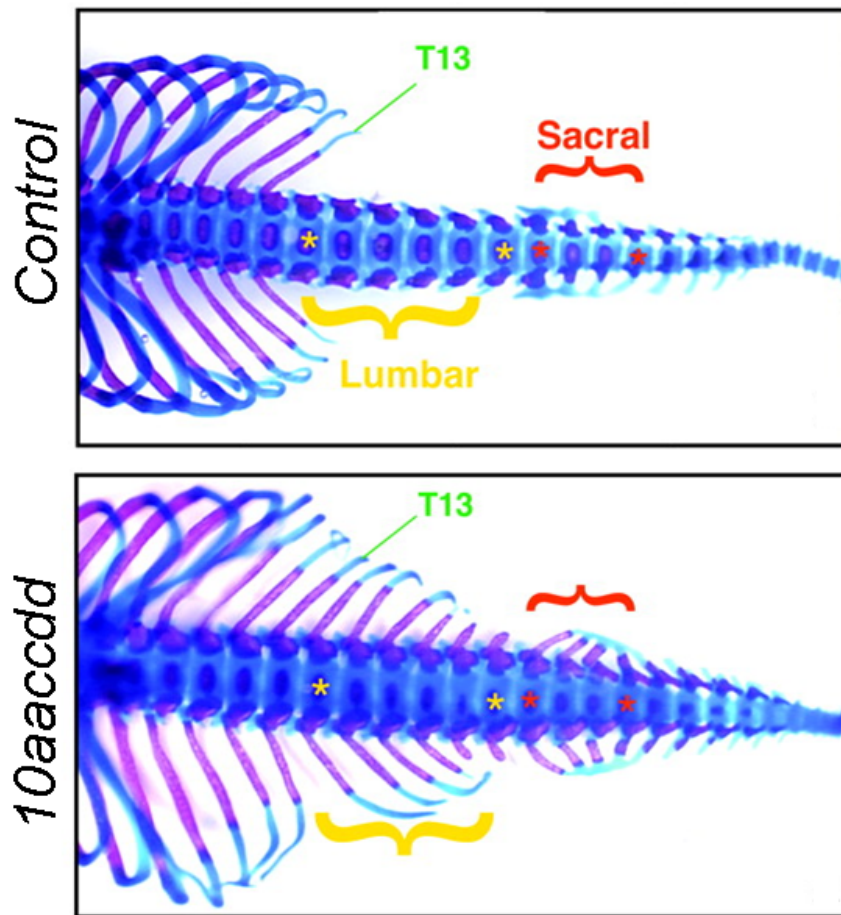


Figure 1.4. Anterior homeotic transformation of the axial skeleton in *Hox10* mutants. Figure adapted from [24]. Mice have 7 cervical, 13 thoracic, 6 lumbar, 4 sacral, and 20 or more cervical vertebrae. The green T13 indicates the rib on the final thoracic segment, yellow marks indicate the lumbar elements, and red indicates the sacral vertebrae. *Hox10* loss-of-function mutants (*10aacdd*) show ectopic ribs forming on more posterior vertebrae, demonstrating a transformation of the lumbar and sacral elements to a thoracic phenotype.

highly conserved 60 amino acid DNA binding domain, the homeodomain. All 39 mammalian Hox proteins recognize an identical, degenerate ATTA target sequence with equal affinity [55, 56]. Due to the lack of sequence recognition specificity, it has been difficult to determine what genes are downstream and how the Hox proteins regulate target gene expression [10].

Domains N- and C-terminal to the homeodomain are less well characterized, but comprise significant portions of the transcription factor coding sequence and are likely to play an important role in the regulation of downstream genes. Regions outside the homeodomain are conserved among paralogous proteins (i.e. Hoxa11, Hoxc11, and Hoxd11), but are highly variable between non-paralogous members (i.e. Hoxa2, Hoxa7, Hoxa11). Because of the lack of DNA-binding specificity of the homeodomain, interaction with cofactors is likely to promote specific target gene recognition and differential regulatory functions.

Hox cofactors

Extradenticle (Exd), a *Drosophila* TALE (three amino acid loop extension) protein, was the first described Hox/HomC regulatory cofactor [57]. Homeotic transformations are observed in *exd Drosophila* mutants, similar to those in *Antennapedia (antp)* and *Bithroax (bx-c)* complex mutants, but the expression of *Hox* genes is unaffected. *In vitro*, Exd interacts with the Hox proteins to confer DNA binding specificity, and this complex is further stabilized by another TALE protein, homothorax (Hth), [58, 59]. Downstream targets regulated by Hox-Exd-

Hth complexes have been identified in *Drosophila*, including *decapentaplegic* (*dpp*), *forkhead* (*fkh*), and *labial* (*lab*) [60-63].

The mammalian *exd* and *hth* homologs are *Pbx* and *Meis/Prep*, respectively. *Pbx* and *Prep* interact with *Hoxb1* to control the segment-specific regulation of several anterior *Hox* genes during rhombomere formation in mammals, including auto-regulation of *Hoxb1* expression [64-68]. Other than this example in hindbrain development, few other mammalian organ systems are known to rely on Hox-*Pbx*-*Meis/Prep* regulatory networks. For example, although *Pbx* and *Hox* mutants both display limb skeletal phenotypes, *Pbx* controls the spatial distribution of *Hox* gene expression and does not appear to act as a Hox cofactor [53, 69]. Additionally, genetic loss of *Pbx* or *Meis* function results in embryonic lethality with severe hematopoietic and eye defects, phenotypes that have not been reported in any combination of *Hox* mutants generated to date [70-73]. In several cases, *Pbx* interacts with non-*Hox* transcription factors, such as *Tlx1* in the spleen and *Pdx1* in the pancreas [74, 75]. Therefore, *Pbx* and *Meis/Prep* proteins appear to have broader roles in mammalian development than acting solely as Hox cofactors, and additional regulatory factors are likely to interact with Hox proteins in other developmental contexts.

Kidney as a model organ

The kidney serves as a model organ system for understanding many basic developmental patterning mechanisms. The intermediate mesoderm gives rise

to the kidney and much of the reproductive tract. Signals from the paraxial and lateral plate mesoderm induce a region of the intermediate mesoderm to begin expressing kidney specific markers, *Lim1* and *Pax2* [76, 77]. The kidney is formed through three stages, of which the first two are transitory and the third stage gives rise to the adult kidney. The first stage of kidney formation, the pronephros, begins at embryonic day 8 (E8) in mice when the primary nephric/Wolffian duct is formed, starting at the level of the twelfth somite [76, 78]. As the nephric duct extends caudally towards the cloaca, the anterior region induces the adjacent mesenchyme, the nephrogenic cord, to form pronephric tubules that degrade as soon as the mesonephros starts to form, which is the second transitory stage. The Wolffian duct induces the adjacent mesenchyme to form mesonephric tubules, which differentiate into nascent filtration structures [76, 79]. The mesonephros is a transient structure which begins to degenerate when the final stage of kidney organogenesis is beginning (Figure 1.5).

Metanephric kidney development begins at E10.5 in mice. The ureteric bud evaginates from the caudal end of the Wolffian duct and invades the metanephrogenic mesenchyme, an adjacent group of cells condensed at the posterior end of the nephrogenic cord. Signals from the metanephric mesenchyme promote ureter invasion and continued budding and branching of the ureter. Signals from the ureter promote condensations of the mesenchyme into nephrogenic cap mesenchyme, which contains nephrogenic progenitors. The nephrogenic mesenchyme undergoes epithelialization and differentiates into nephrons. The nephron is the functional unit of the kidney and consists of a

Figure 1.5

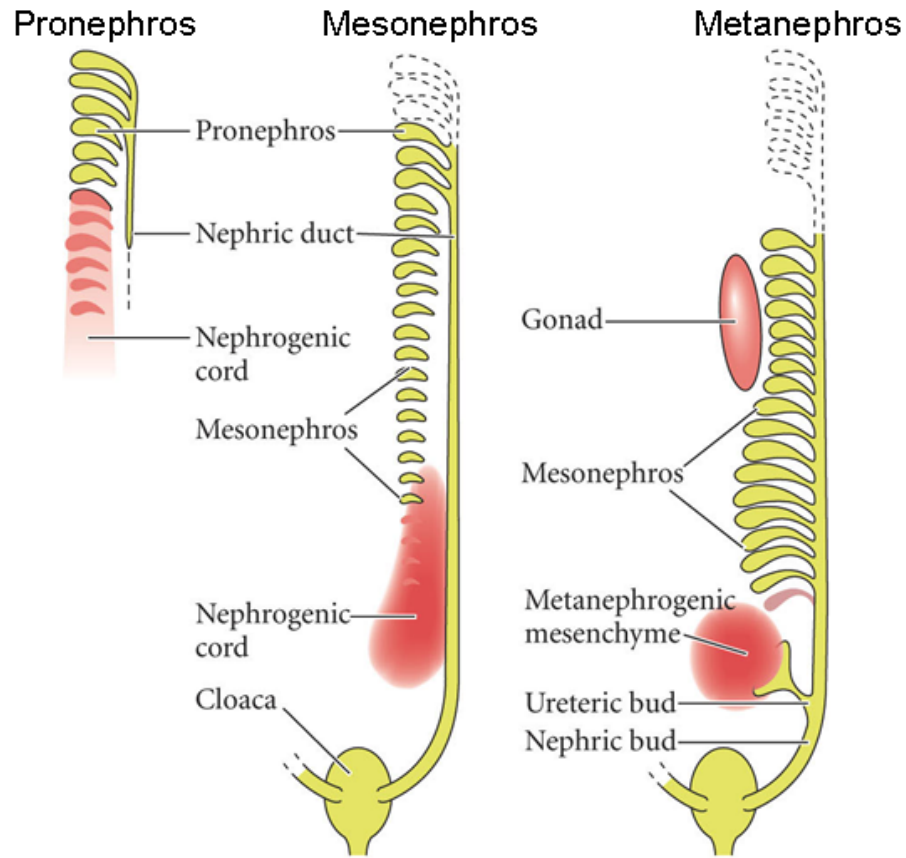


Figure 1.5. Stages of kidney development. Figure adapted from [3]. The pronephros and mesonephros are the first two stages of kidney development and are transient structures. The metanephros gives rise to the mature kidney.

glomerulus, proximal, and distal tubules (Figure 1.6) [80]. The glomerulus passes filtrate into the proximal and distal tubules, where it is further concentrated. The processed filtrate (urine) is then passed through the collecting ducts, which originate from the ureteric epithelium, and down the ureter into the bladder.

It is unclear if the metanephrogenic blastema is made up of one or multiple cell types prior to ureteric bud induction. Just after ureter invasion and condensation of the mesenchyme into nephrogenic precursors, a third cell type is observed called stromal cells. During the early branch phases of the kidney, the stromal cells make up a primary renal interstitium that surrounds the ureter branches and differentiating nephrogenic mesenchyme. Later during organogenesis, the stromal cells are localized into two compartments, the cortical stroma, which surrounds the cap mesenchyme at the kidney periphery, and the medullary stroma [81, 82].

Kidney signaling pathways

A number of signaling pathways are necessary for the initial stages of metanephric development (Figure 1.7) [76, 83]. Prior to ureteric bud induction, the condensed mesenchyme expresses a signaling factor, *Gdnf*, recognized by receptors on the ureter epithelium [84-88]. *Gdnf* is recognized by co-receptors, *Ret* and *Gfr α 1*, on the budding ureter [89-94]. The transcription factors *Hox11*, *Pax2*, *Eya1*, *Wt1*, and *Sall1* are important for promoting and maintaining *Gdnf* expression in the mesenchyme [25, 95-99]. *Foxc1*, *Foxc2*, *Robo* and *Slit* genes

Figure 1.6

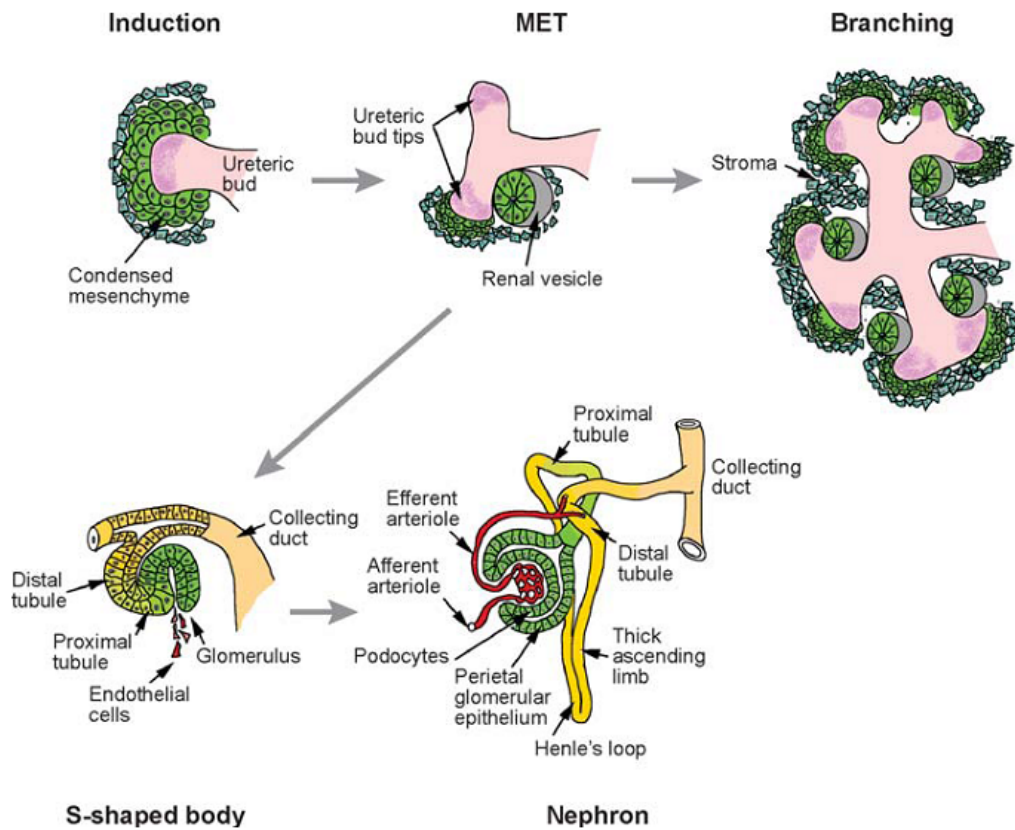


Figure 1.6. Differentiation of the metanephros. Figure from [76]. Metanephric development starts at E10.5 when the ureteric bud invades the condensed metanephric mesenchyme, a stage called induction. Signals from the ureter promote the mesenchyme to undergo a mesenchymal to epithelial transition (MET) in order to differentiate to form the collecting structures of the kidney called nephrons. Signals from the mesenchyme promote the ureter to undergo further branching. Stromal cells are also present, which help to regulate nephron differentiation and ureter branching.

Figure 1.7

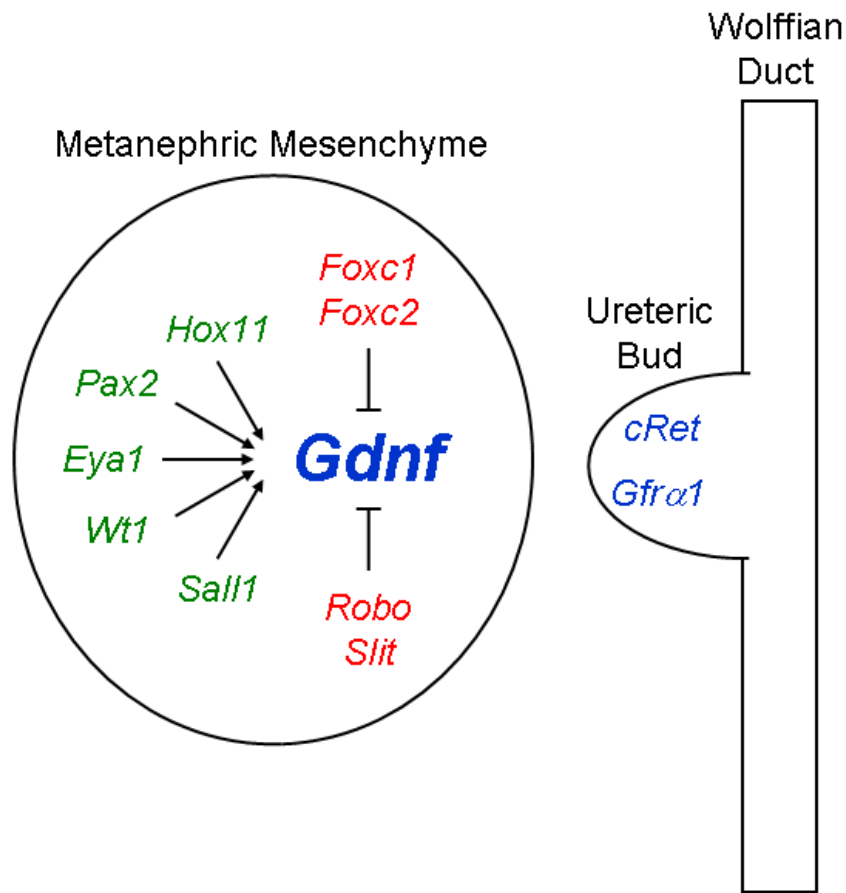


Figure 1.7. Transcription factors and signals necessary for ureteric bud induction. *Hox11*, *Pax2*, *Eya1*, *Wt1*, and *Sall1* promote *Gdnf* expression in the condensed metanephric mesenchyme prior to ureteric bud induction. *Foxc1*, *Foxc2*, *Robo*, and *Slit* limit the expression boundary of *Gdnf* in the mesenchyme. *Gdnf* is recognized by *cRet* and *Gfrα1* receptors on the ureteric bud, which forms from the Wolffian duct.

limit *Gdnf* expression to the appropriate region of the nephrogenic mesenchyme along the anterior-posterior axis of the intermediate mesoderm [100, 101]. After ureteric bud induction, the mesenchyme continues to express *Gdnf* to promote further ureter budding and branching [102, 103]. In turn, the ureter secretes *Fgf2* and *Bmp7* to promote the survival and growth of the mesenchyme [104-106]. Wnts, such as *Wnt9b*, are also secreted from the ureter and initiates mesenchyme condensations around the ureter bud tips [107, 108]. *Wnt4* is expressed in the mesenchymal condensates and promotes epithelialization and differentiation of the aggregates to form nephrons [109, 110].

More recently, another cell type in the developing kidney, the stroma, has been recognized as important for maintaining appropriate branching as well as the epithelialization of the mesenchyme. These stroma cells are first detected as a distinct sub-population in the early kidney shortly after ureteric bud invasion into the condensed mesenchyme at E11 [81, 82, 111]. The first identifiable marker of the stroma is *Foxd1*, which labels cells surrounding the condensed mesenchyme [112, 113]. *Foxd1* expressing cells become restricted to the cortical stroma at the kidney periphery at later stages. The cortical stroma uses retinoic acid signaling to regulate ureter branching and to maintain *Ret* expression in the ureter tip epithelium [114].

In addition to the cortical stroma, there are also stromal cells in the center of the kidney (medullary stroma) as well as surrounding the ureter structures. *Pod1* is expressed in both the condensed mesenchyme and the medullary stroma, and is necessary in the medullary stroma to produce signals to help

regulate nephrogenesis [115, 116]. Additional stromal cells surround the sides of the ureter and Wolffian duct. These cells express *Bmp4* to prevent ectopic ureteric bud formation [117].

Ascent of the kidney during development

The position of the kidney, relative to the rest of the body, changes during development in mammals. The condensed mesenchyme is located adjacent to the dorsal body wall in the pelvic region when the ureter initially invades ventrally at E11 in mice. By E12.5 the nephrogenic mesenchyme normally detaches from the body wall and rotates laterally such that the ureter enters the kidney from the medial aspect. At this point, the kidney also begins to ascend into the lumbar region as the pelvic region continues to elongate posteriorly. By E14.5 the kidney capsule, which is composed of fibrous tissue, surrounds the kidney and separation from the body wall is complete. At birth, the kidney has completely ascended within the abdomen and abuts the adrenal gland immediately below the liver [113]. In humans, ascension of the kidney occurs between the fifth and ninth weeks of development [118].

***Hox* genes in the kidney**

An extensive analysis of *Hox* gene expression during metanephric kidney development has recently been published [119]. Multiple *Hox* genes are expressed in the kidney, including in the ureteric bud epithelium, undifferentiated mesenchyme, and differentiated epithelial structures that are derived from the

condensed mesenchyme. However, only one set of *Hox* paralogs has been shown to be functionally important for kidney organogenesis. The *Hox11* paralog group genes are critical in the metanephric mesenchyme prior to ureteric bud induction. Loss of *Hox11* paralogous gene function leads to loss of *Six2* and *Gdnf* expression in the metanephric mesenchyme [25]. *Six2* is required to maintain the nephrogenic progenitor population, and *Gdnf* is the growth factor required to promote ureteric bud induction [84, 86, 88, 120, 121]. As a result of this loss of expression, induction of the kidney fails and no kidney develops in these mutant embryos.

Rationale

The results from numerous genetic studies highlight the importance of *Hox* gene function in the development of many different organ systems. However, little is known regarding *Hox* function at the molecular level. Using the kidney as a model organ system, the goal of my thesis is to identify novel regulatory mechanisms for *Hox* protein function.

Hox proteins have poor binding specificity. The homeodomains of all 39 mammalian *Hox* proteins recognize the same degenerate ATTA target sequence [55, 56]. Cofactors are likely to be required to promote *Hox* target gene recognition and regulatory function. The first part of my thesis describes the identification of *Pax2* and *Eya1* as novel *Hox* cofactors that form a complex with *Hox11* proteins to regulate target gene expression in the metanephric mesenchyme.

DNA binding by the homeodomain is a well described feature shared by all Hox proteins, but the functional contributions of the regions N- and C-terminal to the homeodomain are not well characterized. The second part of my thesis explains how the N- and C-terminal regions of the Hox proteins confers differential regulation of a target gene, *Six2*, using the same enhancer site.

Finally, different *Hox* paralog groups have overlapping expression in numerous organ systems [32]. It is unknown, however, if the paralog groups are expressed in the same cells or if their roles are redundant. The final part of my thesis describes how *Hox10* and *Hox11* genes are both expressed in the kidney mesenchyme, but the *Hox10* genes have unique expression and function in the kidney stromal cell population.

CHAPTER II

A HOX-EYA-PAX COMPLEX REGULATES EARLY KIDNEY DEVELOPMENTAL GENE EXPRESSION

Abstract

During embryonic development, the anterior-posterior body axis is specified by the combinatorial activities of the homeotic or *Hox* genes. Given the poor DNA binding specificity of Hox proteins, it is likely they interact with other factors to regulate target genes. However, few regulatory partners or downstream target genes have been identified. Herein, we demonstrate that Hox11 paralogous proteins form a complex with Pax2 and Eya1 to directly activate expression of *Six2* and *Gdnf* in the metanephric mesenchyme. We have identified the binding site within the *Six2* enhancer necessary for Hox11-Eya1-Pax2 mediated activation and demonstrate this site is essential for *Six2* expression *in vivo*. Furthermore, genetic interactions between *Hox11* and *Eya1* are consistent with their participation in the same pathway. Thus, anterior-posterior patterning Hox proteins interact with Pax2 and Eya1, factors important for nephrogenic mesoderm specification, to directly regulate the activation of downstream target genes during early kidney development.

Introduction

The *Hox* genes are conserved among all metazoans and specify positional information along the body axes. In mammals, 39 *Hox* genes are arranged into four chromosomal clusters, which are organized into 13 paralogous groups along the chromosome in a 3' to 5' manner. This arrangement of genes leads to spatiotemporal colinearity of *Hox* gene expression, with 3' genes expressed more anterior and earlier in development than 5' genes [29, 34]. The unique, combinatorial expression of Hox proteins is important for the regulation of anterior-posterior patterning, skeletal morphogenesis, mesodermal organ development, neural patterning and multiple other cellular and developmental processes (reviewed in [54]). Despite genetic analyses in a variety of organisms, the molecular details regarding what cofactors interact with Hox proteins to regulate transcription are poorly understood, and very few downstream Hox targets have been identified.

The mammalian kidney serves as an ideal model organ to study Hox protein function. The embryonic kidney is derived from the intermediate mesoderm and exhibits anterior-posterior patterning as it develops (reviewed in [76]). The most anterior region of intermediate mesoderm, the pronephros, is a rudimentary structure in mammals. Caudal to the pronephros are the mesonephric tubules, a linear array of nephron like structures that are transient filtering units. The most posterior intermediate mesoderm generates the metanephric, or adult, kidney, which forms adjacent to the hindlimb buds. Adult kidney development begins when the metanephric mesenchyme induces an

outgrowth, the ureteric bud, from the adjacent nephric duct epithelia. The ureteric bud invades into the metanephric mesenchyme, provides inductive Wnt signals, and subsequently undergoes branching morphogenesis to generate the radial pattern of the kidney (reviewed in [122]). In the mouse, *Hox11* paralogous genes are essential for early patterning of the metanephric mesenchyme, as loss of *Hoxa11* and *Hoxd11* results in misrouted ureters and hypoplastic kidneys, while loss of all three *Hox11* paralogs results in a complete failure of the metanephric mesenchyme to induce ureteric bud induction [18, 25, 123].

Hox proteins recognize a degenerate ATTA or TTAT sequence, which confers very little locus specificity ([124], reviewed in [54]). Thus, it is likely that co-factors interact with Hox proteins in order to promote high-affinity binding and locus specific regulatory activities. The TALE (three amino acid loop extension) proteins Pbx and Meis/Prep are known Hox co-factors that regulate target gene expression (reviewed in [66]). *Pbx1*, *Pbx3*, and *Meis1* are expressed in the kidney; however loss of *Pbx1* and *Meis* function result in less severe and later stage kidney phenotypes compared to the *Hox11* paralogous mutants [72, 125-127]. Thus, it is likely that Hox11 proteins are interacting with other co-factors to specify the early intermediate mesoderm along the anterior-posterior axis.

Prior to ureteric bud induction, the condensing metanephric mesenchyme expresses a unique combination of markers including the *Hox11* paralogs (*Hoxa11*, *Hoxc11* and *Hoxd11*), *Osr1*, *Pax2*, *Eya1*, *Wt1*, *Six1*, *Six2* and *Gdnf* [76]. In *Hox11* triple mutants, the expression of many early kidney patterning markers in the uninduced metanephric mesenchyme are unperturbed, however,

both *Six2* and *Gdnf* expression are absent [25]. *Six2* regulates metanephric progenitor cell renewal [121]. *Gdnf* ligand activates co-receptors, c-ret and *Gdnfr α* , in the Wolffian duct to promote ureteric bud outgrowth and invasion, and is a key regulator of continued branching morphogenesis [84-89, 94, 128, 129]. Mice mutant for *Pax2* have reduced levels of *Six2* expression and do not express *Gdnf* in the mesenchyme [98]. Even though *Pax2* can directly regulate *Gdnf* expression in cell culture, it is not sufficient *in vivo* as *Gdnf* expression is absent in *Hox11* and *Eya1* mutants while *Pax2* expression is normal [25, 95, 99]. *Eya1* mutants, like *Hox11* mutants, exhibit no ureteric bud induction and also lack *Six2* and *Gdnf* expression [99].

The *Pax*, *Eya*, and *Six* gene families encompass members of a common regulatory network that is conserved from *Drosophila* to mammals (reviewed in [130]). *Eya* proteins have no intrinsic DNA binding domain but can localize to the nucleus and function as co-activators of transcription [131, 132]. The *Eya1* protein also has a protein phosphatase activity which is essential for regulation of some target genes (reviewed in [133]).

Given the similarities in molecular phenotypes observed in the *Hox11*, *Pax2*, and *Eya1* mouse mutants in the developing kidney, we propose that *Hox11* proteins interact with *Pax2* and *Eya1* to regulate essential patterning genes within the posterior intermediate mesoderm. All three proteins physically interact and synergistically up-regulate *Gdnf* and *Six2* promoter activities. We identify a binding site critical for this activation within the *Six2* promoter region and demonstrate that this site is essential for driving expression within the renal

mesenchyme. Furthermore, renal development is sensitized to partial loss of *Hox11* paralogous function in an *Eya1* heterozygous genetic background, suggesting that these proteins work in the same regulatory network. These data point to a novel *Hox11*-*Eya1*-*Pax2* network that translates anterior-posterior positional information within the developing mammalian kidney. Further, our data demonstrate that *Six2* and *Gdnf* are direct downstream targets of the *Hox11* paralogous group genes.

Materials and methods

Six2 and Gdnf luciferase constructs

The 3.03 kb *Six2* promoter region, -266 to -3296 base pairs upstream of the ATG start site, was PCR amplified from a *Six2* BAC clone and inserted into a promoterless pGL3-Basic vector (Promega). A previously reported *Gdnf* promoter [95] was subcloned into pGL3-Basic. Quikchange II XL Site-Directed Mutagenesis kit (Stratagene) was used to mutate the *Pax2* binding site or delete the *Hox* binding site in the 3.03 kilobase *Six2* promoter luciferase vector.

Mutations and deletions were confirmed by sequence analysis (see

Supplementary Materials & Methods).

Protein expression vectors

The *Hoxa11* protein coding sequence (IMAGE8734051) was cloned into a p3XFlag-CMV10 expression vector (SIGMA), which places three FLAG tags at the N-terminus of *Hoxa11*. The *Eya1* protein coding sequence (IMAGE

6448408) was cloned into a pCS2+MT expression vector, which places six Myc tags at the N-terminus of Eya1 [134, 135]. The Pax2 protein expression vector was previously described [136].

Luciferase assays

MDCK cells were plated at 50,000 cells per well in a 24 well plate, cultured in MEM with 10% FBS and 10U/mL penicillin/streptomycin at 37°C, and transfected the second day with FUGENE6 (Roche). For each well, 0.64 ml of FUGENE was used per 0.32 mg of DNA, which contained 75 ng of reporter plasmid and 20 ng pRL-CMV renilla luciferase for standardization. Twenty-four hours post-transfection, cells were lysed in Passive lysis buffer (Promega). Luciferase activity was measured using a Vector3 PerkinElmer luminometer. Counts were standardized using pGL3 empty vector or co-transfected renilla luciferase (Dual Luciferase Assay System, Promega). Each transfection was performed in triplicate.

Northern blot analysis

RNA from MDCK cells was prepared using TRIZOL (Invitrogen) and resuspended in RNA Storage Solution (Ambion). 20 µg of RNA per sample was electrophoresed for 2 hours in 1% agarose denature gel (Ambion), blotted onto Hybond-N+ membrane (Amersham Biosciences), and pre-hybridized with 8 ml ULTRAhyb Ultrasensitive Hybridization Buffer (Ambion). The membrane was then hybridized at 68°C overnight with 8×10^6 cpm of a Six2 RNA probe (HindIII-

Sfol fragment from IMAGE6394139 (ATG to 346 bp of exon 1)) labeled with ^{32}P -dUTP via *in vitro* RNA probe reverse transcription. The blot was washed twice in 2XSSC + 0.1%SDS and 0.1XSSC + 0.1%SDS at 68°C and exposed to film or analyzed on a Typhoon 9400 variable mode imager (Amersham). The RNA probes for the *Hox11* paralogs, *Eya1*, and *Pax2* have been previously published [34, 137-140]

Co-immunoprecipitation assays

HEK-293 cells were transfected with *Hoxa11*-FLAG, *Pax2*-HA, and *Eya1*-Myc expression vectors and cell lysates were prepared (Complete Mini, Roche). Mouse α HA monoclonal antibody (Sigma#H9658), mouse α FLAG monoclonal antibody (M2, Sigma#F3165), or mouse α Myc monoclonal antibody (Santa Cruz#SC-40) was added to 0.5 μg lysate and incubated 4°C overnight. Mouse or Rabbit IgG (Jackson ImmunoResearch) was used as negative controls. Protein was precipitated using Protein G Agarose beads (Invitrogen), washed, and resuspended. Western Blots were probed with 1:5000 α FLAG for *Hoxa11*, 1:3000 α *Pax2* (Covance#PRB-276P) for *Pax2*, or 1:500 α Myc for *Eya1*.

Pax2-paired domain pull down and electromobility shift assays

The 3.03 kb *Six2* upstream region was digested by HpaII and used in the *Pax2*-paired domain pull down assay following methods as previously described [141].

Gel electromobility shift assays were performed as previously described with modifications [95]. Nuclear extracts from untransfected HEK-293 cells and cells transfected with the Hoxa11-FLAG, Pax2-HA, and Eya1-Myc protein expression vectors were isolated as previously described [142]. PAGE purified oligonucleotides (Invitrogen) for the wild-type and mutant probes (see Supplemental Material & Methods) were annealed and end labeled with P-32 (T4 Polynucleotide Kinase, Promega). Supershifts were performed using α Hoxa11 antibody [143] and α HA antibody (above).

Six2-LacZ transgenic mice

The 3.03 kb wild type and mutant upstream *Six2* sequences from the luciferase vectors were sub-cloned upstream the β -galactosidase gene in the promoterless pNASS β expression vectors (BDB Clontech) and were digested with NheI and KpnI to create 980 bp *Six2-lacZ* wild type and mutant pNASS β reporter vectors. DNA for injection was isolated using NheI and AseI. Purified DNA was microinjected into fertilized eggs obtained by mating (C57BL/6 X SJL) F1 or C57BL/6 female mice with (C57BL/6 X SJL)F1 male mice. Pronuclear microinjection was performed as described [144]. Embryos were collected at E11.5, genotyped for the β -galactosidase gene [145], and stained for β -galactosidase activity following standard protocols [144].

In situ hybridization and histology

In situ hybridization and histology were performed as previously described [25].

Results

As *Six2* expression is affected in *Hox11*, *Eya1*, and *Pax2* mutant metanephric mesenchyme, we tested whether these proteins can activate *Six2* expression directly. A 3 kb sequence upstream of the *Six2* ATG start site was used to determine whether *Six2* expression is regulated in cell culture by *Hox11*, *Pax2*, or *Eya1* (Figure 2.1A). In transfected cells, *Hoxa11*, *Eya1*, or *Pax2* alone were unable to substantially increase expression from the *Six2* reporter construct. However, when the proteins were co-expressed in combination, activation of the reporter was observed. Co-expression of all three proteins resulted in 50-fold activation of the *Six2*-luciferase reporter (Figure 2.1B). Expression of *Hoxc11* or *Hoxd11* vectors in place of *Hoxa11* in these experiments showed similar results, consistent with their redundant genetic function at this early stage of kidney development ([25], Supplemental Data). In MDCK cells transiently transfected with *Hoxa11*, *Pax2*, and *Eya1*, a 5-fold up-regulation of endogenous *Six2* expression is also demonstrated (Figure 2.1C). (Untransfected MDCK cells have measurable levels of endogenous *Pax2* mRNA expression, but low to undetectable levels of *Hoxa11*, *Hoxc11*, *Hoxd11*, and *Eya1* (Supplemental Data)).

Figure 2.1

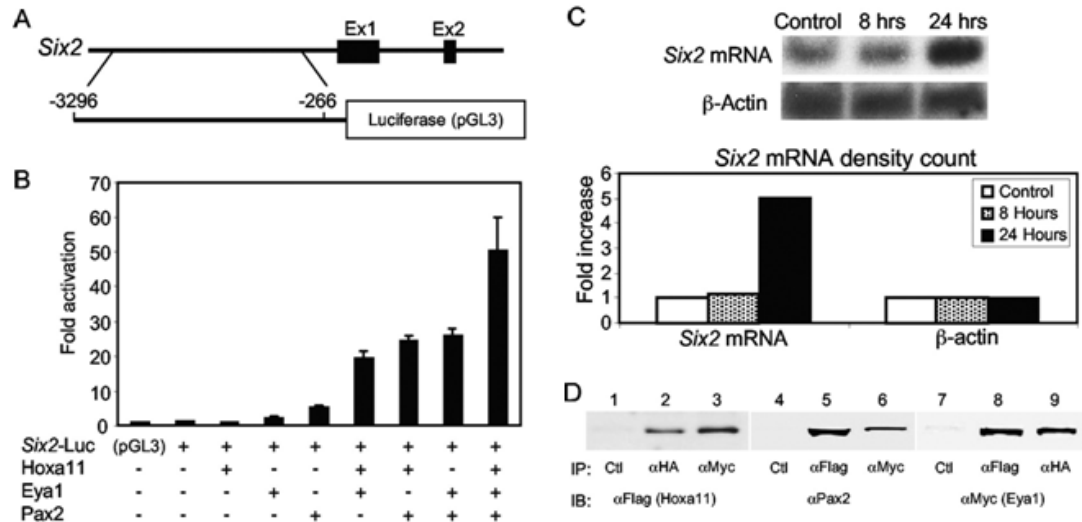


Figure 2.1. Regulation of *Six2* expression by a Hox11-Eya1-Pax2 complex. (A) Schematic of the *Six2*-luciferase vector. A fragment from 3296 base pairs to 266 base pairs upstream of the *Six2* ATG start site was subcloned into a luciferase expression vector. (B) Activity of the *Six2*-luciferase reporter plasmid in transfected MDCK cells with different combinations of Hoxa11, Pax2, and Eya1 protein expression vectors. (C) Northern blot analysis of endogenous *Six2* mRNA in MDCK cells after transfection with Hoxa11, Eya1 and Pax2, normalized to β -actin. (D) Whole cell extracts of HEK-293 cells transfected with Hoxa11-Flag, Pax2-HA, and Eya1-Myc protein expression constructs were subjected to reciprocal co-immunoprecipitations. Immunoblotting (IB) for Hoxa11 (α Flag) demonstrates co-immunoprecipitation with Pax2 (α HA) and Eya1 (α Myc) (lanes 2 and 3). Immunoblotting with Pax2 (α Pax2) demonstrates co-immunoprecipitation of Hoxa11 (α Flag) and Eya1 (α Myc) (lanes 5 and 6). Immunoblotting with Eya1 (α Myc) demonstrates co-immunoprecipitation with Hoxa11 (α Flag) and Pax2 (α HA) (lanes 8 and 9). Immunoprecipitations (IP) using mouse or rabbit IgG (lanes 1, 4, and 7) were negative controls.

The cooperative activation of *Six2* could be mediated by the formation of a Hox11-Eya1-Pax2 complex binding directly to an upstream *cis*-regulatory sequence. To test for physical interactions, we performed co-immunoprecipitation experiments using Hoxa11, Pax2, and Eya1. In cell lysates expressing Hoxa11, Eya1, and Pax2, immunoprecipitation using antibodies specific for one of the three proteins resulted in the co-precipitation of the other two proteins (Figure 2.1D). Thus, Hoxa11, Pax2, and Eya1 can form a complex and physically associate either directly or through interactions with as yet unidentified adaptor proteins within the complex.

To examine the possibility that the Hox11-Eya1-Pax2 complex could bind directly to sequences upstream of the *Six2* coding sequence, we first tested for Pax2 binding, since Pax2 is expected to have the most specificity in terms of a DNA recognition sequence and the Pax2-paired domain (Pax2-PD) has been previously shown to bind Pax2 target sequences with high affinity [95, 136]. After digestion of the 3.0 kb *Six2* reporter sequence with *Hpa*II, two fragments showed strong binding by the Pax2-PD *in vitro*: one at the 5' end of the reporter construct and another sequence 450 base pairs upstream of the *Six2* coding sequence (Figure 2.2A). Subsequent deletion analyses showed the 5' putative binding site was not required for Hox11-Eya1-Pax2 mediated activity in cell culture (data not shown). Sequence analysis of the -450 bp binding site revealed a conserved Pax2 binding sequence [95, 142, 146-148] and an adjacent putative Hox binding site (Figure 2.2B).

Figure 2.2

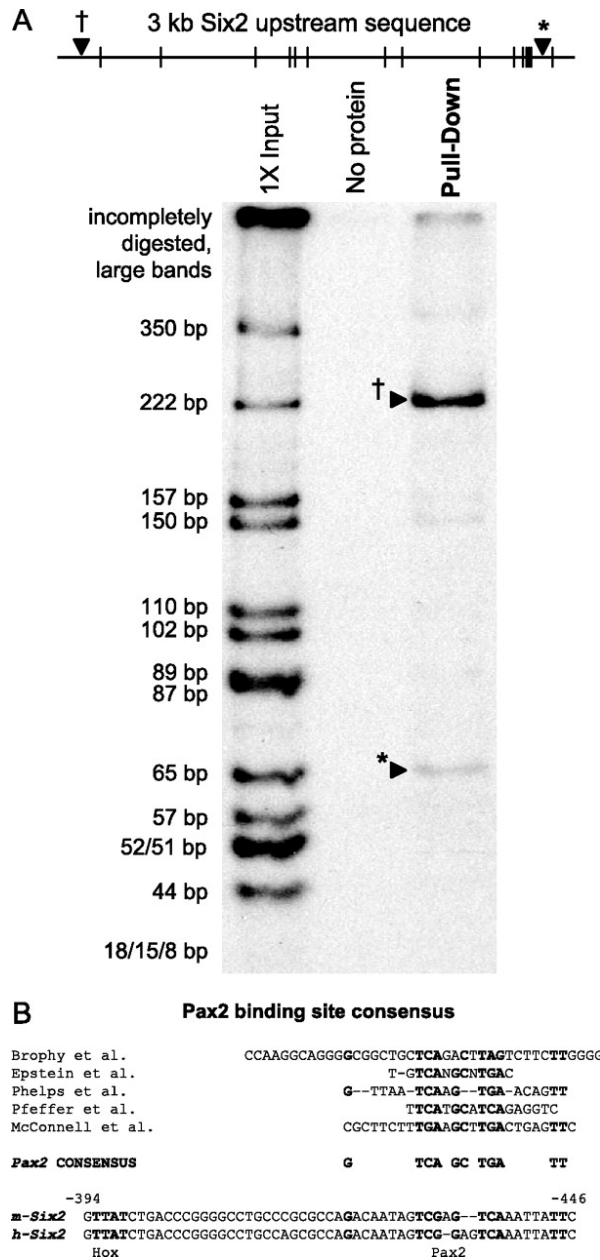


Figure 2.2. Pax2 binds regions upstream of the *Six2* protein coding sequence. (A) Pax2 paired domain (Pax2-PD) binds two regions of the *Six2* promoter *in vitro*. The black hatch marks indicate the HpaII sites in the 3.0 kb *Six2* upstream sequence. A 5', 222 bp region (†) and 3', 65 bp region (*) are pulled down only when the Pax2-PD is present. (B) Sequence analysis of the 65 bp region at -450 bp identifies a putative Pax2 binding site and a putative Hox binding site based on sequence conservation to consensus sites.

We next tested the necessity of these binding sites for reporter gene activation in our reporter assay. In addition to the wild-type 3 kb *Six2*-luciferase constructs tested previously, we generated and tested three analogous 3 kb constructs which contained a mutation of the putative *Pax2* binding site at -450 bp (*Six2/Pax2mut*), a deletion of a nearby putative *Hox* binding site (*Six2/HoxΔ*), or both mutations together (*Six2/Pax2mut-HoxΔ*). Mutation of the *Pax2* or the *Hox* binding site alone caused a decrease in Hox11-Eya1-Pax2 mediated luciferase activity compared to the wild-type *Six2* construct. However, Hox11-Eya1-Pax2 mediated expression from the *Six2* reporter is nearly abolished when both the putative *Pax2* and *Hox* sites are mutated (Figure 2.3A).

Binding at the -450 site by the Hox11-Eya1-Pax2 complex was further examined using nuclear extracts from HEK 293 cells transfected with *Hoxa11*, *Eya1*, and *Pax2* in electrophoretic mobility shift assays (Figure 2.3B). An 89 base pair fragment containing the putative binding site exhibited a slower migrating complex upon incubation with nuclear lysate expressing *Hoxa11*, *Eya1*, and *Pax2* (Figure 2.3B, lane 3). This slower migrating species was supershifted upon incubation with antibodies against *Hoxa11* or *Pax2*, indicating that these proteins are part of the DNA/protein complex (Figure 2.3B, lanes 5 and 6). The specificity of binding was demonstrated by competition with a molar excess of unlabeled wild-type competitor probe, and by loss of retention using a labeled probe containing both the putative *Pax2* and *Hox* binding sites mutated (Figure 2.3B, lanes 4 and 7).

Figure 2.3

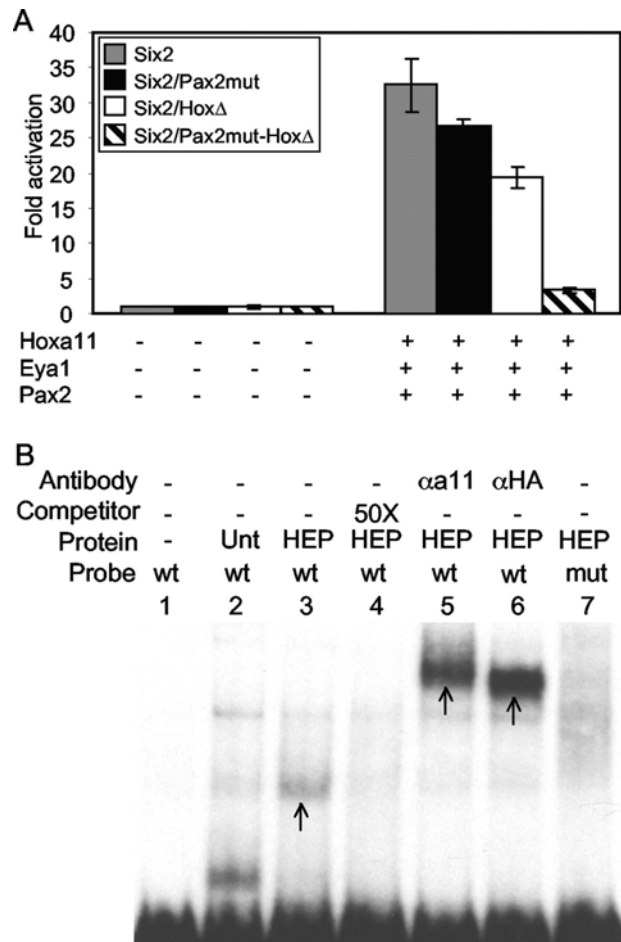


Figure 2.3. The Hox11-Eya1-Pax2 complex binds at the -450 site and is necessary for *Six2* expression. (A) Luciferase activity from the 3.0 kb wild-type *Six2* expression construct (gray bars), and constructs with the putative *Pax2* binding site mutated (black bars), with the *Hox* binding site mutated (white bars), or with both the putative *Pax2* and *Hox* sites mutated (black and white hatched bars) were compared. All plates were co-transfected with or without Hoxa11, Pax2, and Eya1 protein expression vectors in MDCK cells. (B) An 89 bp probe (wt), containing the putative *Pax2* and *Hox* binding sites of the *Six2* promoter, incubated with nuclear extracts from HEK-293 cells transfected with Hoxa11, Eya1, and Pax2 (HEP) demonstrated retention on a non-denaturing acrylamide gel (arrow in lane 3). Probe retention was not seen in untransfected extracts (lane 2). This interaction is competed with excess (50X) unlabeled competitor (lane 4) and supershifts are observed using antibodies to Hoxa11 (α Hoxa11) or to an HA tag (α HA) on the Pax2 protein (arrows in lanes 5 and 6, respectively). The transfected extract does not show retention using a probe (mut) with the *Pax2* and *Hox* binding sites mutated (lane 7).

To confirm the importance of this Hox11-Eya1-Pax2 regulatory binding site *in vivo*, we generated *LacZ*-reporter constructs using wild-type and mutant *Six2* upstream sequence to test expression within the renal mesenchyme of transgenic mice. A 980 bp *Six2* construct was used to drive *LacZ* expression and compared to expression from a construct containing mutations of the putative *Pax2* and *Hox* binding sites. The transgenic constructs were injected into fertilized mouse embryos and assayed for *LacZ* expression at embryonic day 11.5 (E11.5). The wild-type *Six2* reporter demonstrated *LacZ* expression in a pattern similar to endogenous *Six2* expression [149] in five of twelve independent transgenic lines. *LacZ* staining was prominent in the branchial arches, the otic region, and the developing urogenital mesenchyme (Figure 2.4A). Of 26 independent transgenic embryos generated with the mutant *Six2-LacZ* reporter, 19 embryos demonstrated *LacZ* staining in some region of the developing embryo, but none of the 26 mutant embryos showed any staining in the nephrogenic mesenchyme (Figure 2.4A). This confirms the Hox11-Eya1-Pax2 binding site is necessary for *Six2* expression in the nephrogenic mesenchyme *in vivo*.

Both *Eya1* and *Pax2* expression are unaffected in the condensed metanephric blastema at pre-induction stages in *Hox11* triple mutants [25]. Further, *Eya1* expression is unaffected in *Pax2* mutant mesenchyme, and *Pax2* expression is initially unaffected in *Eya1* mutant mesenchyme [99, 150]. We examined the expression of *Hoxd11* in *Eya1* and *Pax2* mutant mice and no changes in expression are seen (Figure 2.4B-E). Therefore, while the loss of

Figure 2.4

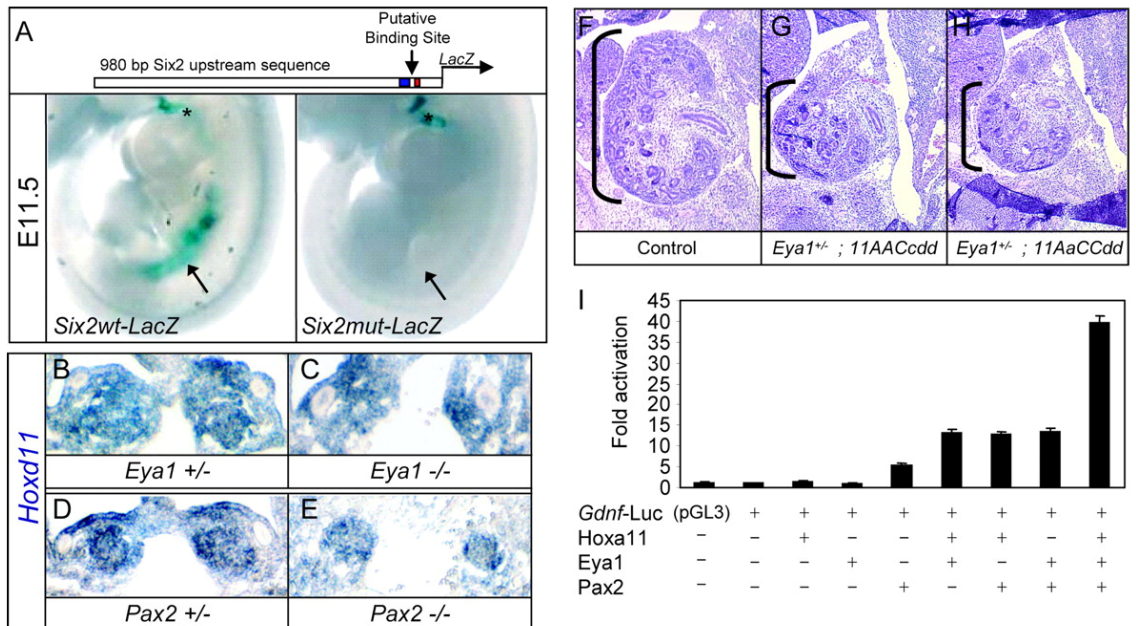


Figure 2.4. *Hox11-Eya1-Pax2* binding site is critical for kidney expression *in vivo* and the Hox-Eya-Pax network synergistically activates *Gdnf* expression. (A) *Six2*-LacZ transient transgenic mice. The top panel shows a schematic of the 980 bp *Six2*-LacZ reporters (*Hox* site in red and *Pax2* site in blue). E11.5 transgenic embryos carrying the wild-type *Six2*-LacZ constructs (left panel) exhibit staining in the nephrogenic mesenchyme (black arrow) and the branchial arches (black asterisk). Transgenic mice carrying a construct with the *Pax2* and *Hox* sites mutated retain staining in the branchial arches (right panel; black asterisk, 19 of 26), but have no nephrogenic staining (black arrow, 26 of 26). (B through E) No differences in the expression of *Hoxd11* in the posterior intermediate mesoderm are seen in *Eya1* heterozygous (B) or homozygous (C) embryos at E10.5 or in the metanephric mesenchyme of *Pax2* heterozygous (D) or homozygous (E) embryos at E10.5. (F through H) Frontal H&E stained histological sections through an E14.5 control embryo (F) and embryos with three mutant *Hox11* alleles plus one mutant allele of *Eya1* (G, H). The brackets in F - H indicate relative kidney size. (I) *Gdnf* upstream sequence driving luciferase in the presence of *Hoxa11*, *Eya1*, and/or *Pax2* in MDCK cells.

these genes individually leads to the loss of *Gdnf* expression and ureteric bud induction, they do not affect the expression of one another at early metanephric stages, consistent with their operating in parallel as transcriptional co-regulators in this system.

If the Hox11-Eya1-Pax2 complex cooperatively contributes to the expression of early kidney mesenchyme specific genes, then a reduction in gene dosage may provide genetic evidence for this interaction. *Eya1* heterozygotes or three-allele *Hox11* mutants have no histological renal phenotype at E14.5 ([25, 99] and data not shown). However, the addition of a single *Eya1* null allele to three mutant *Hox11* alleles results in hypoplastic kidneys at E14.5 (Figure 2.4F-H). This phenotype is observed regardless of which three *Hox11* alleles are missing. Thus, reduced *Eya1* gene dosage uncovers a phenotype in the *Hox11* three allele mutant kidneys similar to the phenotype reported in mutants that carry four or more mutant *Hox11* alleles [18, 25, 123]. This data provides compelling genetic evidence that Hox11 group proteins interact with Eya1.

Hox11 paralogous mutants and *Eya1* and *Pax2* mutant mice show similar kidney phenotypes with a failure to induce ureteric bud formation and loss of *Gdnf* [25, 95, 99]. Thus, we examined *Gdnf* expression as a second potential candidate for regulation by the Hox11-Eya1-Pax2 complex. The *Gdnf* reporter construct was activated by Pax2, alone, approximately 5-fold, in agreement with previously published reports [95]. However, co-expression of Hoxa11 (or Hoxc11 or Hoxd11, data not shown) and Eya1 with Pax2 increased activation of the *Gdnf*-Luciferase reporter more than 40-fold, whereas Hox11 or Eya1 alone had

no effect on activation (Figure 2.4I). These data demonstrate the Hox11-Eya1-Pax2 complex can strongly activate multiple target genes in the early renal mesenchyme.

Discussion

During the organization of the body plan, cells and tissues are specified along three axes: anterior-posterior, dorsal-ventral, and medio-lateral. The intermediate mesoderm, from which the kidney derives, is first specified along the medio-lateral axis and marks a region between the paraxial and lateral plate mesoderm shortly after gastrulation. One model proposes that Bmp signals from the lateral plate and as yet unidentified signals from the paraxial mesoderm provide positional cues to activate genes such as *Pax2*, *Osr1*, and *Lim1*, which mark the intermediate mesoderm [151, 152]. The intermediate mesoderm also has anterior-posterior patterning that is clearly represented by the pro-, meso-, and metanephric kidneys. Thus, any position within the developing mesoderm can be specified by a unique combination of anterior-posterior factors and medio-lateral factors. How these factors function cooperatively is unclear. Our results suggest a model whereby Hox11 paralogous proteins cooperate with Eya1 and Pax2 to activate *Six2* and *Gdnf*, two genes specific to the posterior intermediate mesoderm that generates the metanephric kidney (Figure 2.5). Hox11, Eya1 and Pax2 proteins physically associate, bind to a metanephric mesenchyme specific enhancer region within the *Six2* promoter, and synergistically activate reporter gene expression. Thus, the direct interactions between anterior-posterior

Figure 2.5

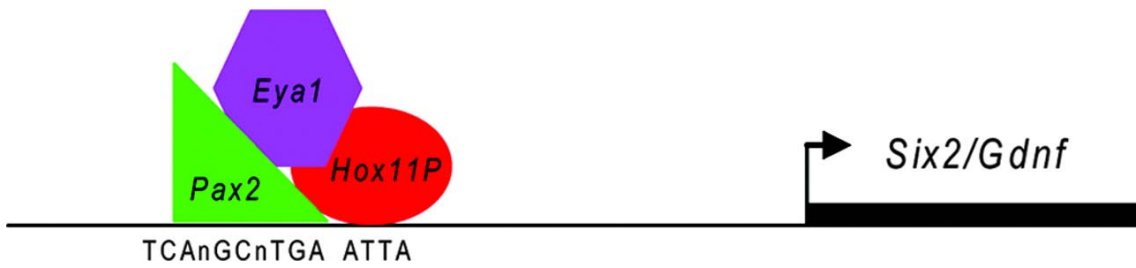


Figure 2.5. Diagram of proposed mechanism of Hox11 molecular function. Taken together, this work supports a model wherein Hox11 proteins form a transcriptional complex with Pax2 and Eya1 and directly activate the expression of *Six2* and *Gdnf* during early mammalian metanephric development.

determinants and medio-lateral determinants may be essential for specifying the positional address of the metanephric mesenchyme.

Despite the fact that targeted deletions of *Hox* genes were among the first generated [36, 153, 154] and that mutations in *Hox* genes affect numerous developmental processes (reviewed in [14]), few downstream target genes have been identified. Probably the most studied mammalian *Hox* target is *Hoxb1*, which is auto-regulated by its own expression [67, 155]. Working as a complex with Pbx and Meis/Prep, *Hoxb1* has been shown to regulate a handful of other anterior *Hox* genes [64, 65, 156, 157]. Here, we demonstrate that *Six2* and *Gdnf* are novel molecular targets of the *Hox11* genes, and identify a novel set of *Hox* regulatory partners, *Eya1* and *Pax2*, for this activity.

The Pax-Eya-Six pathway is a conserved regulatory network in organogenesis [130]. Initially found in *Drosophila*, *ey* (*Pax*) activates *eya* (*Eya*) and *so* (*Six*) expression during eye formation [158]. *Eya* can also ectopically activate *so/Six*, and *so/Six* and *eya* both feedback to regulate *ey/Pax* as well as their own expression [132]. These genes are also expressed and play important roles in mammalian development. In addition to the kidney, mutations in these genes affect development of other organ systems, such as the ear, thymus and thyroid formation as well as muscle and eye (reviewed in [130, 159, 160]). How this regulatory cassette contributes to the differentiation of so many unique structures is unclear, but presumably relies on interactions with region-specific patterning factors.

More recently, it has been shown that Hox/HomC proteins can bind ey/Pax and affect developmental processes in *Drosophila* [161, 162]. Our current work suggests this interaction is also conserved during mammalian kidney development as well. Further, it is possible that interaction between *Hox* genes and the *Pax-Eya-Six* pathway may be more generally conserved. For example, *Hoxa3* is necessary for thymus and thyroid formation, as are *Eya1* and *Six1* [163-165]. *Pax1* and *Pax9* are also expressed in the thymus and *Pax8* is expressed in the thyroid [166-168]. Similarly, during otic development, *Hoxa2* is expressed in the second branchial arch and *Hoxa2* mutant mice have middle ear defects, as do *Eya1*, *Six1*, and *Pax8* mutants [99, 169-172]. *Six2* is expressed in the first and second branchial arches and periotic mesenchyme, and a recent study shows *Six2* expression expands in these regions in *Hoxa2* mutants [149, 173]. Because of the striking similarities in the phenotypes of these mutants, it is plausible that a Hox-Eya-Pax complex is also necessary for the development of other organ systems and that *Six* genes are general developmental targets of *Hox* genes and possibly this Hox-Eya-Pax complex.

In conclusion, our results demonstrate a Hox11-Eya1-Pax2 regulatory network is necessary for *Six2* and *Gdnf* expression to promote mammalian kidney development. This study identifies new downstream targets of the *Hox11* paralogous genes as well as a novel regulatory complex in which these Hox proteins operate. It will be important to determine if this pathway is conserved in other organ systems during mammalian development.

Acknowledgements

This manuscript was written by Ke-Qin Gong, Alisha R. Yallowitz, Hanshi Sun, Gregory R. Dressler, and Deneen M. Wellik. It was published November of 2007 in *Molecular and Cellular Biology*, Volume 27, Number 21, Pages 7661-7668.

We acknowledge Galina Gavrilina and Maggie Van Keuren for preparation of transgenic mice and the Transgenic Animal Model Core of the University of Michigan's Biomedical Research Core Facilities. Core support was provided by The University of Michigan Cancer Center, NIH grant number CA46592, and The University of Michigan Center for Organogenesis. The authors gratefully acknowledge the Michigan Economic Development Corporation and the Michigan Technology Tri-Corridor for the support of this research program (Grant 085P1000815).

The *Eya1* mutant mice were a gift from Dr. Richard Maas and the Hoxa11 antibody was a gift from Dr. Honami Naora. This work was supported in part by the National Institute of Health grant R01-DK071929 and by a University of Michigan's Organogenesis predoctoral fellowship award, T32-HD007505 (AY).

CHAPTER III

NON-HOMEODOMAIN REGIONS CONFER ACTIVATION VERSUS REPRESSION ACTIVITIES TO MAMMALIAN HOX PROTEINS

Abstract

Hox genes control many developmental events along the AP axis, but few target genes have been identified. Whether target genes are activated or repressed, what enhancer elements are required for regulation, and how different domains of the Hox proteins contribute to regulatory specificity is poorly understood. *Six2* is genetically downstream of both the *Hox11* paralogous genes in the developing mammalian kidney and *Hoxa2* in branchial arch and facial mesenchyme, although loss-of-function of *Hox11* leads to loss of *Six2* expression and loss-of-function of *Hoxa2* leads to expanded *Six2* expression. Herein we demonstrate that a single enhancer site upstream of the *Six2* coding sequence is responsible for both activation by Hox11 proteins in the kidney and repression by Hoxa2 in the branchial arch and facial mesenchyme *in vivo*. DNA binding activity is required for both Hox activation and Hox repression, but differential activity is not controlled by differences in the DNA-binding homeodomains. Rather, protein domains N- and C-terminal to the homeodomain confer activation versus

repression activity. These data support a model whereby DNA binding by Hox proteins *in vivo* may be similar, consistent with accumulated *in vitro* Hox DNA binding data, and that unique functions result mainly from differential interactions with non-homeodomain regions of Hox proteins.

Introduction

Hox proteins play a critical role in patterning the anteroposterior (AP) body axis of most metazoans, but what target genes are regulated and the mechanisms by which Hox proteins direct morphological diversification are poorly understood. In most bilaterian organisms, *Hox* genes are found in closely linked clusters and their order on the chromosome reflects their expression and function along the AP axis. The most 3' genes (*la* and *pb* in arthropods; *Hox1* and *Hox2* group genes in vertebrates) are expressed most anteriorly while more 5' genes are expressed with increasingly posterior boundaries. *Hox* expression domains generally demonstrate significant overlap, with expression extending more posterior than their functional domains. All Hox proteins contain a DNA-binding domain, the homeodomain. This domain is highly conserved among all Hox proteins and this motif, along with the clustered, colinear organization of these genes on chromosomes, are defining hallmarks of this group of developmental regulators.

There is a high degree of conservation among homeodomains, and all Hox proteins bind a highly similar -ATTA- core sequence *in vitro*, providing little specificity for unique downstream target regulation [174-176]. Despite this

similarity *in vitro*, functional studies using ectopic expression of chimeric Hox proteins in *Drosophila* have provided evidence that differences in homeodomain sequence and structure may confer some degree of functional specificity to individual Hox proteins *in vivo*. In some cases, the nature of the homeotic changes induced by ectopic over-expression of Hox proteins, is altered by swapping the homeodomains between Hox proteins [177-183]. In the majority of these studies, ectopic expression of wild-type Hox protein is compared to ectopic expression of a chimeric construct in which the homeodomain is swapped with another Hox protein. However, reciprocal swaps, wherein the homeodomain remains constant and the N- and C-terminal domain are swapped, have not been systematically examined in comparison, making it difficult to assess the relative importance of the homeodomain versus the N- and C-terminal domains in these experiments. In one study by Zeng, *et al.* [183], wild-type Antp ectopic expression was compared to that of ectopic expression of Scr, and to ectopic expression of chimeric proteins in which either the homeodomain, the region C-terminal to the homeodomain or the homeodomain and C-terminal region of Scr, was swapped into the Antp protein. This study revealed that while swap of the homeodomain of Scr into the Antp protein construct results in some homeotic changes that were interpreted to mimic Scr overexpression more than Antp overexpression, the homeotic changes more closely resembled ectopic Scr when the C-terminal domain was swapped in addition to the homeodomain. Expression of chimeric protein in which only the domain C-terminal to the homeodomain of Scr was swapped into Antp still resulted in some changes that

resemble Scr-mediated homeosis [183]. While incomplete, this study supports the notion that Hox specificity may lie outside of the homeodomain.

Few domains outside of the homeodomain have been described for the Hox proteins. An important exception is the YPWM motif that is found just N-terminal to the homeodomain in Hox1 – Hox10 group proteins. The YPWM motif is critical for binding Hox cofactors, Pbx/Exd. Pbx/Exd confers DNA binding specificity and stability to Hox proteins in some contexts [57, 58]. Downstream targets regulated by Hox-Exd complexes have been identified in *Drosophila*, and include *decapentaplegic (dpp)*, *forkhead (fkh)*, and *labial (lab)* [60-62].

Mammalian Pbx and Prep interact with Hoxb1 to control the segment-specific regulation of several anterior *Hox* genes during rhombomere formation in mammals, including the auto-regulation of *Hoxb1* expression [65-68, 157]. However, a more limited number of mammalian organ systems appear to rely on Hox-Pbx-Meis/Prep regulatory complexes, and Pbx and Meis/Prep proteins appear to have broader roles in mammalian development than solely as Hox cofactors [71, 74, 75]. Therefore, it is likely that additional Hox regulatory cofactors and Hox binding interactions contribute to the wide array of Hox activities during mammalian development.

With the exception of the Pbx/Exd-binding domain, the functional specificity conferred by the non-homeodomain portions of Hox proteins has been largely unexplored. The lack of attention to the importance of the non-homeodomain portion of Hox proteins is surprising given that the amino acid sequence of Hox proteins in mammals range from 217 to 443 amino acids (in

Drosophila, the range is 270 to 782 residues), even though the homeodomain is only 61 amino acids in length.

Part of the difficulty in assessing relevant, *in vivo* functional contributions by different domains of Hox proteins, however, has been the lack of clearly defined direct downstream target genes *in vivo*, particularly those that demonstrate differential regulation by distinct Hox proteins. Recently, *Six2* has been shown to be a direct downstream target of the Hox11 proteins in metanephric kidney development. In the early metanephric mesenchyme, Hox11 proteins interact with Pax2 and Eya1 to promote the activation of *Six2* [25, 184]. *Six2* has also been shown to be a target of Hoxa2 in the branchial arches and otic mesenchyme. In this case, Hoxa2 normally represses *Six2* expression in the facial mesenchyme and the second branchial arch [173, 185]. In both cases, substantial evidence supports direct regulation by Hox proteins in *Six2* expression [173, 184, 185].

In this report, we identify a single enhancer site that promotes repression of *Six2* in anterior regions by Hoxa2 and activation of *Six2* in nephrogenic mesenchyme by Hox11 proteins *in vivo*. DNA binding is required for both Hox activation and repression activities, but differential regulation depends primarily on N- and C-terminal regions that flank the homeodomain. Specifically, repression relies on a 60 amino acid sequence C-terminal to the homeodomain, which is conserved in Hox2 and Hox3 paralogs. Activation by Hox11 requires domains both N- and C-terminal to the homeodomain, and activation is shared by a larger subset of Hox proteins.

Materials and methods

Six2-luciferase assays

The *Six2*-luciferase reporter and the *Hoxa11*, *Pax2*, and *Eya1* protein expression vectors were designed as previously reported [184]. *Hoxa2*, *Hoxb2*, *Hoxa3*, *Hoxb3*, *Hoxa5*, *Hoxa6*, and *Hoxc10* cDNAs were generated using C57Bl6 embryonic RNA using SuperScript III RNase H Reverse Transcriptase (Invitrogen), amplified by Platinum Taq High Fidelity DNA Polymerase (Invitrogen), and were cloned into p3XFlag-CMV10 expression vectors (Sigma). The *Pbx1a* and *Pbx1b* expression vectors were generously donated by Dr. Licia Selleri [69]. The *Hoxa2* and *Hoxa11* chimeric protein constructs were designed as detailed in Figure 6.

The last 63 amino acids of the *Hoxa2* C-terminal region were deleted from the *Hoxa2*-p3XFlag-CMV10 expression vector using PCR. The forward primer was designed in the p3XFlag-CMV10 vector downstream *Hoxa2* and the reverse primer was designed in *Hoxa2* upstream the sequence to be deleted. The resulting PCR product was ligated together and sequencing confirmed the deletion.

The QuikChange II XL site-directed mutagenesis kit (Stratagene) was used to mutate Hox homeodomain amino acids. The *Hoxa2* and *Hoxa11* asparagine and arginine at amino acid positions 51 and 53, respectively, were both mutated to alanines.

Luciferase assays in MDCK cells were performed as previously described [184] and the data was normalized to cells transfected with the Six2 reporter construct alone, labeled as one fold change.

In situ hybridization and transgenic expression analyses

In situ hybridization was performed as previously described [25, 186]. *Six2 in situ* probe was previously reported [149]. *Six2-LacZ* constructs and embryo analyses were previously described [184].

Results

Differential regulation of Six2 expression

Six2, a homeobox transcription factor, is expressed in multiple organ systems of the developing embryo, and *Six2* expression is altered in *Hox* mutant mice. Loss-of-function of *Hoxa2* exhibits an expansion of *Six2* expression in the branchial arches and periotic mesenchyme, and leads to malformations of the middle and external ear (Figure 3.1A, 3.1B) [172, 173]. In *Hox11* paralogous mutants, in contrast, ureteric bud induction does not occur and *Six2* expression is lost from the early metanephric mesenchyme (Figure 3.1C, 3.1D) [25]. Thus, at a genetic level, *Six2* expression is differentially regulated in these two sets of *Hox* mutant mice.

Molecular and genetic experiments have shown that expression of *Six2* in the metanephric mesenchyme is a result of direct activation by a complex of proteins that include the *Hox11* proteins, *Pax2*, and *Eya1* [25, 98, 99, 184]. We

Figure 3.1

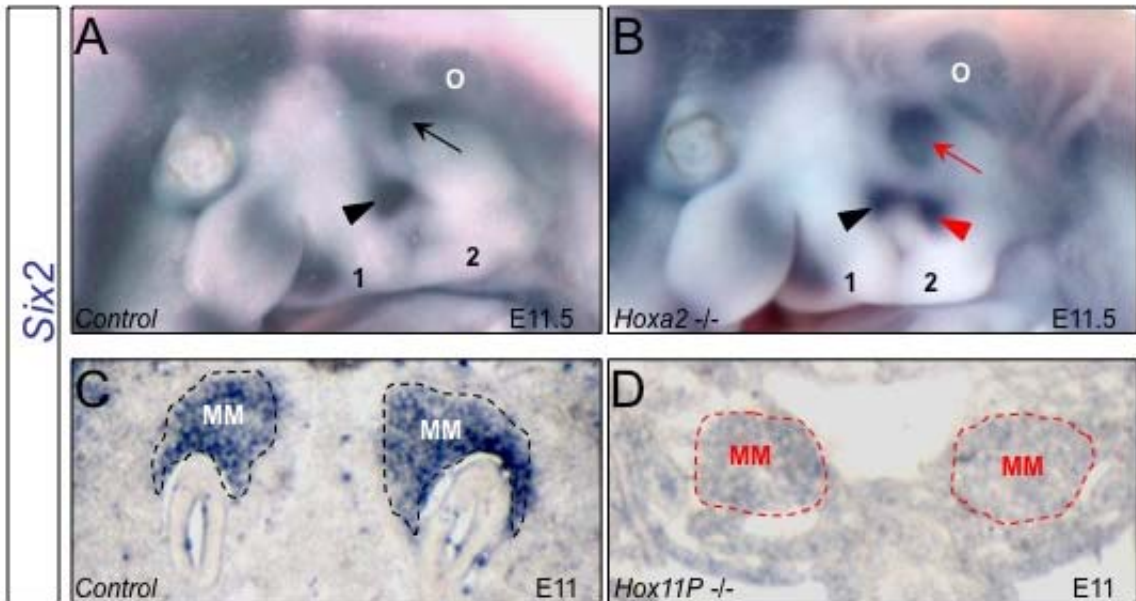


Figure 3.1. *Six2* expression is differentially regulated in *Hoxa2* and *Hox11* mutant embryos. (A) E11.5 control embryo demonstrating *Six2* expression in the first branchial arch (black arrowhead) and periotic mesenchyme (black arrow). (B) At this stage, *Hoxa2* null embryos exhibit expanded *Six2* expression in the periotic mesenchyme (red arrow) and into the second branchial arch (red arrowhead). (C) At E11.0, *Six2* is expressed in the metanephric mesenchyme in control embryos (black outline). (D) *Six2* expression is absent from the metanephric mesenchyme of E11.0 *Hox11* triple paralogous mutants (red outline). 1, first branchial arch; 2, second branchial arch; o, otic vesicle; MM, metanephric mesenchyme.

have previously shown that activation of *Six2* by *Hox11* requires a 50 bp enhancer, (gray box, Figure 3.2A, [184]). Mutation of this site *in vivo* results in loss of *Six2*-LacZ reporter expression in the nephrogenic mesenchyme (19 of 19 independent transgenic lines) (Figure 3.2B, 3.2C, red arrow). Surprisingly, mutation of this enhancer *in vivo* also results in expansion of *Six2*-LacZ expression in the periotic mesenchyme and second branchial arch in 16 of the 19 mutant transgenic embryos (Figure 3.2B, 3.2C, red arrowheads). Thus, the *Six2*-LacZ expression pattern in the transgenic embryos with a mutated Hox enhancer recapitulates the expansion observed in *Hoxa2* mutant embryos and the loss of *Six2* expression observed in *Hox11* mutant embryos, providing strong evidence that the same enhancer site confers both activation and repression by Hox proteins at this locus.

Using a reporter construct containing 3 kb of the *Six2* promoter sequence, which includes the Hox response element (HRE, Figure 3.3A, gray box), activation and repression can both be recapitulated in cell culture reporter experiments. Individually, Hox proteins have little effect on transcriptional activity. The addition of Pax2 and Eya1, cofactors for activation of *Six2* [184], results in a moderate increase in reporter expression. Addition of *Hoxa11*, *Hoxc11*, or *Hoxd11* significantly increases *Six2* activation (Figure 3.3B, and [184]). In contrast, expression of *Hoxa2* represses this activity (Figure 3.3B). Thus, the *in vivo* behavior of these Hox proteins can be recapitulated in this cell culture assay. Of note, there is no evidence that the regulatory functions of these Hox proteins are dependent on Pbx as a cofactor, as Pbx1 does not affect *Six2*

Figure 3.2

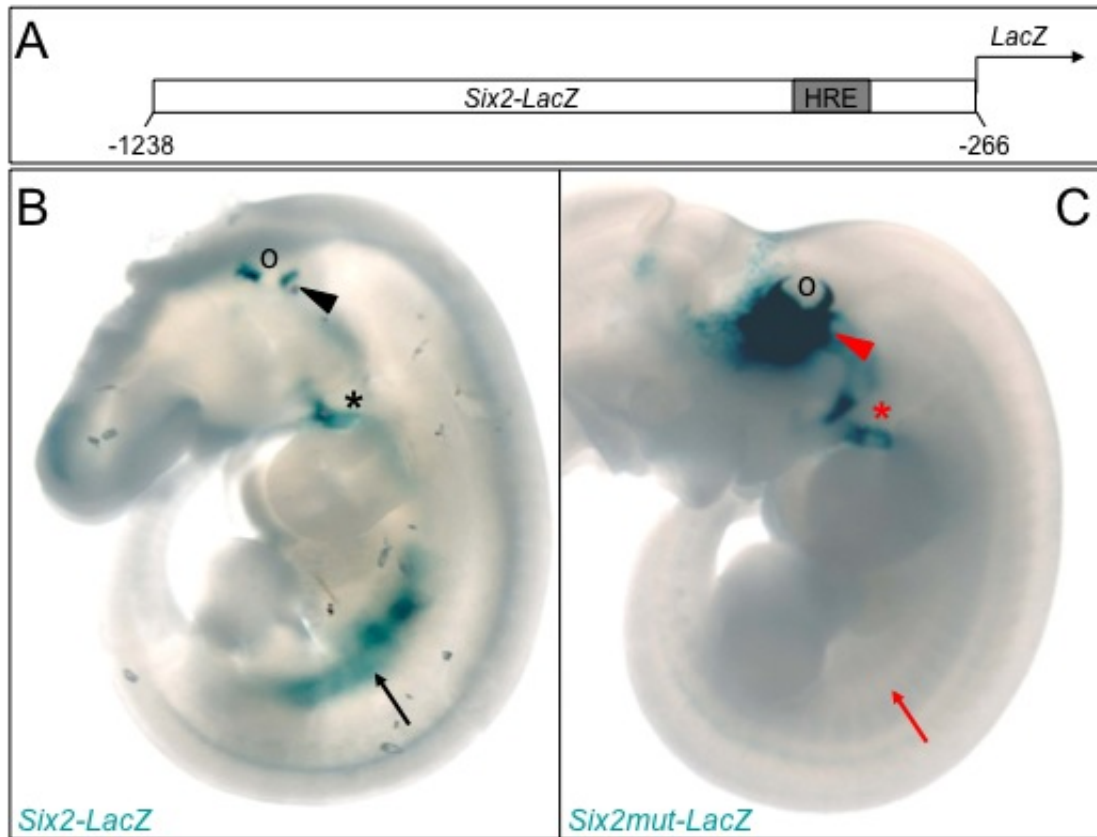


Figure 3.2. A single enhancer site regulates *Six2* repression in the developing periotic mesenchyme and *Six2* activation in the kidney. (A) Schematic of the 980 bp *Six2-LacZ* reporter construct. The Hox response element (HRE, gray box) is mutated in the *Six2mut-LacZ* construct [187]. (B) Control *Six2-LacZ* expression is observed in the periotic mesenchyme and branchial arches (black arrowhead and asterisk), as well as the posterior nephrogenic mesenchyme (black arrow). (C) Mutant transgenic embryos (*Six2mut-LacZ*) demonstrate expanded expression of *Six2* in the periotic mesenchyme and branchial arches (red arrowhead and asterisk) and loss of expression in the nephrogenic mesenchyme (red arrow). o; otic vesicle.

Figure 3.3

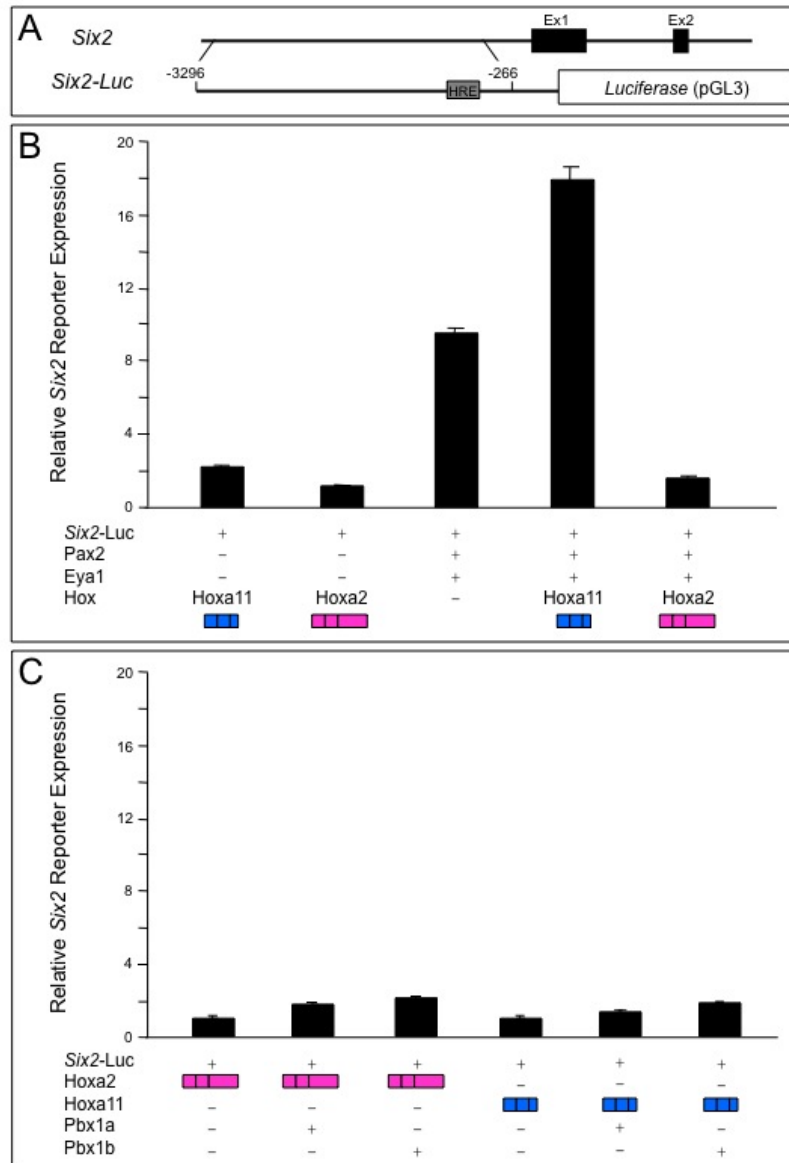


Figure 3.3. Differential regulation of *Six2* in reporter assays. (A) Diagram of reporter construct with 3 kb of *Six2* upstream sequence driving luciferase [187]. The gray box denotes the HRE. (B) Individually, *Hoxa2* and *Hoxa11* demonstrate little activity when co-expressed with the *Six2* reporter, while *Pax2* and *Eya1* in combination result in moderate up-regulation. Co-expression of *Hoxa11* with *Pax2* and *Eya1* results in a further synergistic increase in reporter activity. Co-expression of *Hoxa2*, in contrast, represses *Six2* expression. (C) Co-expression of *Pbx1a* and *Pbx1b* isoforms with *Hoxa2* or *Hoxa11* causes no significant changes in *Six2* expression levels.

reporter activity with or without Hox, Pax2 or Eya1 proteins (Figure 3.3C and data not shown).

In order to determine whether the differential activation and repression activities are unique to the Hox11 and Hoxa2 proteins or whether other Hox proteins are able to demonstrate differential activity, we examined how other Hox proteins affect *Six2* reporter activity in this assay. Members of the *Hox5*, *Hox6*, *Hox9*, and *Hox10* paralogous groups are able to mediate activation of *Six2* similar to the Hox11 paralogs. In contrast, Hoxa2, Hoxb2, as well as members of the Hox3 paralog group act as repressors in this assay (Figure 3.4 and data not shown).

Hox regulatory domains

Comparison of the protein coding sequences from all 39 Hox proteins immediately reveals a striking difference between Hox2 and Hox3 paralogs and the rest of the mammalian Hox proteins. The C-terminal regions of the Hox2 and Hox3 repressor proteins are much longer than any of the other Hox proteins (Figure 3.5A). Hoxa2, Hoxb2, Hoxa3, Hoxb3, and Hoxd3 have between 154 and 192 amino acids C-terminal to the homeodomain while the remaining 34 Hox proteins only have between 6 and 49 amino acids C-terminal to the homeodomain. Amino acid sequence alignment of the Hox2 and Hox3 paralogs reveals significant conservation in the region C-terminal to the homeodomain, especially in the most C-terminal 60 residues (Figure 3.5B, blue shading).

Figure 3.4

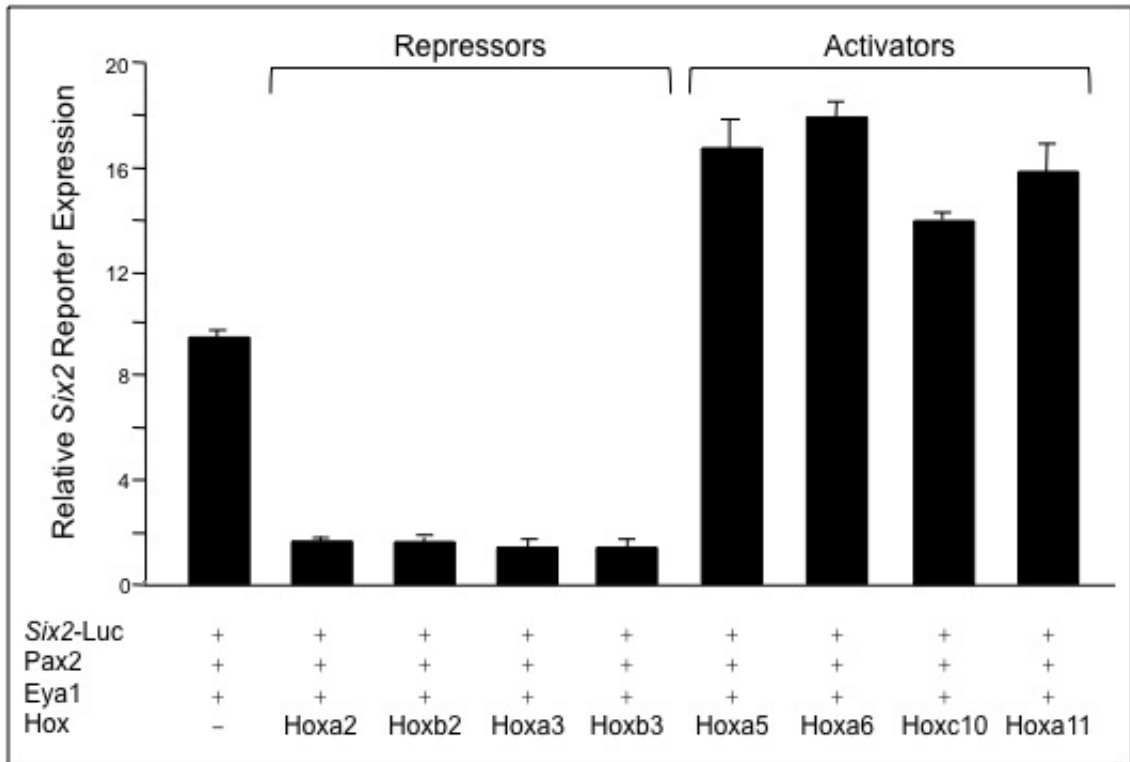
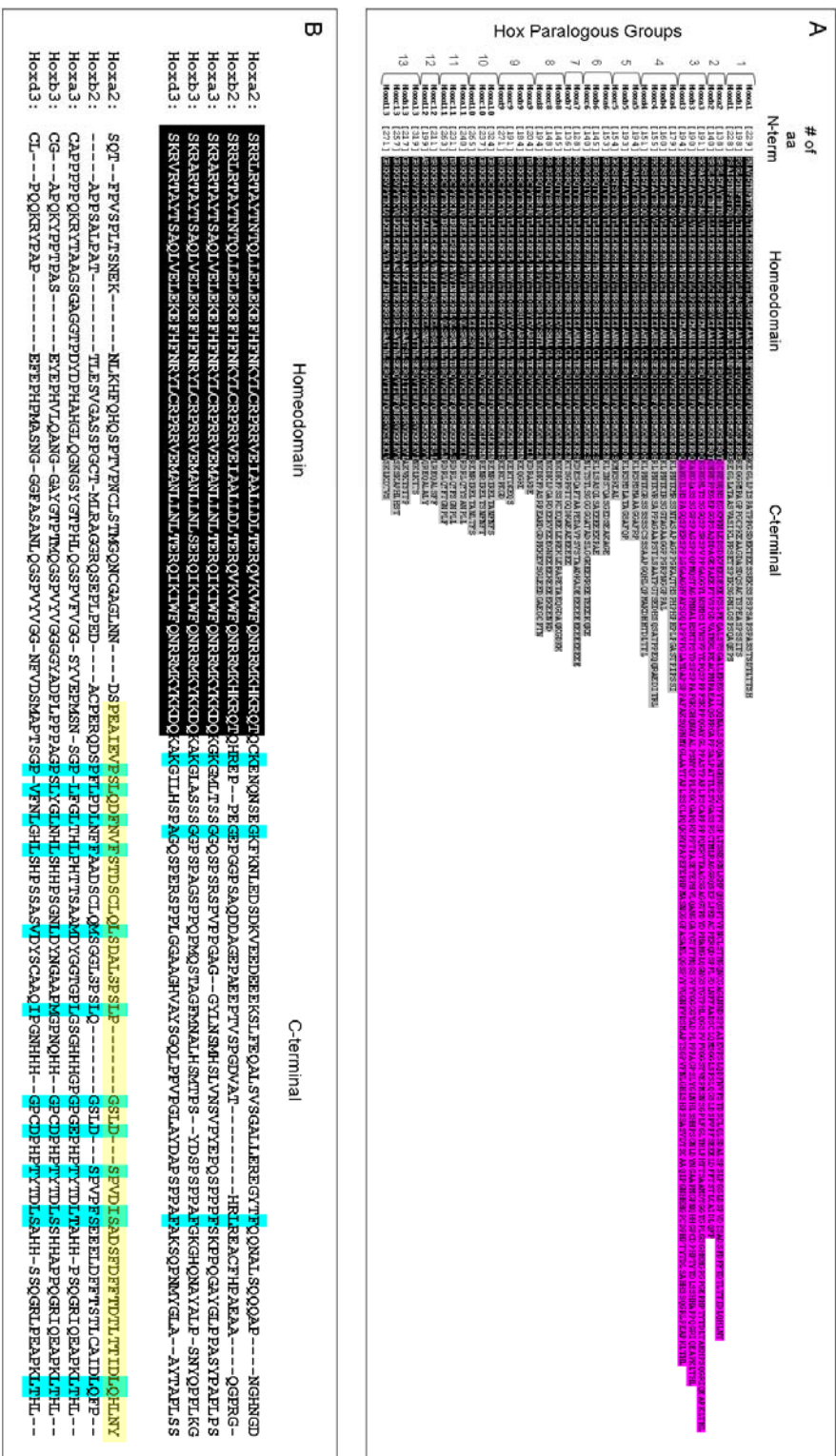


Figure 3.4. Different Hox proteins can act as repressors and activators of *Six2* expression. *Six2* is repressed by Hoxa2, Hoxb2, Hoxa3 and Hoxb3 (Repressors) in this reporter analysis. Hoxa5, Hoxa6, Hoxc10, and Hoxa11 synergistically activate *Six2* expression (Activators) in this assay.

Figure 3.5. Mammalian Hox protein sequence comparisons. (A) Alignment of all 39 Hox proteins relative to the conserved 60 amino acid homeodomain (in black background) highlights the differences in length of the regions C-terminal to the homeodomains. The C-terminal region of the Hox2 and Hox3 paralogous groups (highlighted in pink) are more than 100 amino acids longer than the C-terminal regions of any of the other Hox paralogs (highlighted in gray). The Hox proteins are ordered by paralogous group (1-13). (B) The regions C-terminal to the homeodomains of the Hox2 and Hox3 paralogs were aligned using ClustalW. Identical or similar amino acids are highlighted in blue. The yellow box indicates a conserved 63 amino acid region at the C-terminus.

Figure 3.5



To dissect the mechanistic basis for differential activation and repression by Hox proteins, we generated a series of stable chimeric protein expression constructs in which the homeodomain and/or regions N- or C-terminal to the homeodomain were exchanged between Hoxa11 (an activator Hox) and Hoxa2 (a repressor Hox, Figure 3.6 illustrates chimeric protein constructs). Replacement of the Hoxa11 C-terminal domain with the Hoxa2 C-terminal domain results in the conversion of the Hoxa11 activator to a repressor (Hoxa11N-HD+Hoxa2C, Figure 3.7A, column 5). Repression activity relies only on the identity of the C-terminal domain; whether the homeodomain region is from Hoxa11 or Hoxa2 has no effect on activity. Thus, repression activity lies within the domain C-terminal to the homeodomain of Hoxa2. The presence of an N-terminal region and the homeodomain are required as partial protein constructs without N-terminal domains or homeodomains have no activity (data not shown), but these regions are not critical for conferring repression.

To further identify the domain responsible for repression activity of the Hox2/3 proteins, we deleted only the most C-terminal 63 amino acids of Hoxa2 that exhibits the highest conservation between the Hox2 and Hox3 paralogs (yellow shaded sequence in Figure 3.5B). Deletion of this conserved region results in complete loss of repression activity of the Hoxa2 protein (Hoxa2 Δ C63, Figure 3.7, column 8). Thus, repression of *Six2* relies on a 60 amino acid sequence at the most C-terminal end of the Hoxa2 protein.

In converse chimeric activity experiments, replacing the Hoxa2 C-terminal domain with the Hoxa11 C-terminal domain does not convert this Hox protein to

Figure 3.6. Generation of chimeric Hox protein expression constructs. a11N-HD+a2C and a2N-HD+a11C: Regions C-terminal to the homeodomain were PCR amplified from full length Hoxa2 and Hoxa11 p3xFlag-CMV-10 expression vectors using primers with a KpnI restriction site 5' of the C-terminal region and an XbaI site 3' to the coding sequence. Coding sequences of N-terminal+HD regions were also PCR amplified with the same restriction site at the HD-C-terminal junction and a HindIII site upstream of the ATG. Digestion and religation to generate the chimera protein products resulted in the insertion of six bases, GGTACC, which translate to a two amino acid insertion (Gly+Thy) into the chimeric proteins. a11N+a2HD-C and a2N+a11HD-C: Regions N-terminal to the homeodomain were PCR amplified from full length Hoxa2 and Hoxa11 p3xFlag-CMV-10 expression vectors using primers with a 5' HindIII site upstream of the ATG and a 3'-end KpnI restriction site. The coding sequences of HD+C-terminal regions were also PCR amplified with the same restriction site at the N-terminal-HD junction. Digestion and religation to generate the chimera protein products resulted in the insertion of six bases, GGTACC, which translate to a two amino acid insertion (Gly+Thy) into the chimeric proteins. a2N+a11HD+a2C and a11N+a2HD+a11C: Regions N-terminal to the homeodomain were PCR amplified from full length Hoxa2 and Hoxa11 p3xFlag-CMV-10 expression vectors using primers with a 5'-end HindIII and a 3'-end BglII restriction site immediately flanking the N-terminal coding sequence. HD regions were also PCR amplified with a 5' BglII and 3' KpnI restriction sites at each junction. Regions C-terminal to the homeodomain were PCR amplified from full length Hoxa2 and Hoxa11 p3xFlag-CMV-10 expression vectors using primers with a 5'-end KpnI restriction site and 3' XbaI site. Digestion and religation to generate the chimera protein products resulted in the insertion of six bases, AGATCT (Gly+Thy), in the N-terminal-HD junction and of six bases, GGTACC (Arg+Ser), in the C-terminal-HD junction. Hoxa2 Δ C63: The yellow box with the triangle indicates the 63 amino acid deletion of the C-terminal region in Hoxa2. Hoxa2-HD^{mut} and Hoxa11-HD^{mut}: The 51* and 53* indicate the mutated amino acids in the Hoxa2 and Hoxa11 homeodomains. Hoxa2, pink; Hoxa11, blue; N, region N-terminal to the homeodomain; HD, homeodomain; C, region C-terminal to the homeodomain; asterisk, amino acid mutation. Amino acids at both positions (51, Asp and 53, Arg) were mutated to alanines.

Figure 3.6







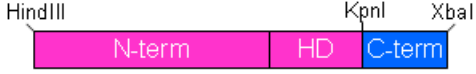





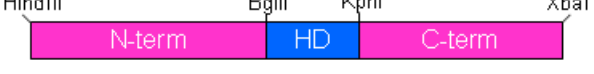

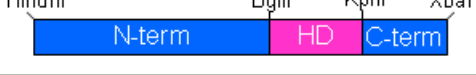







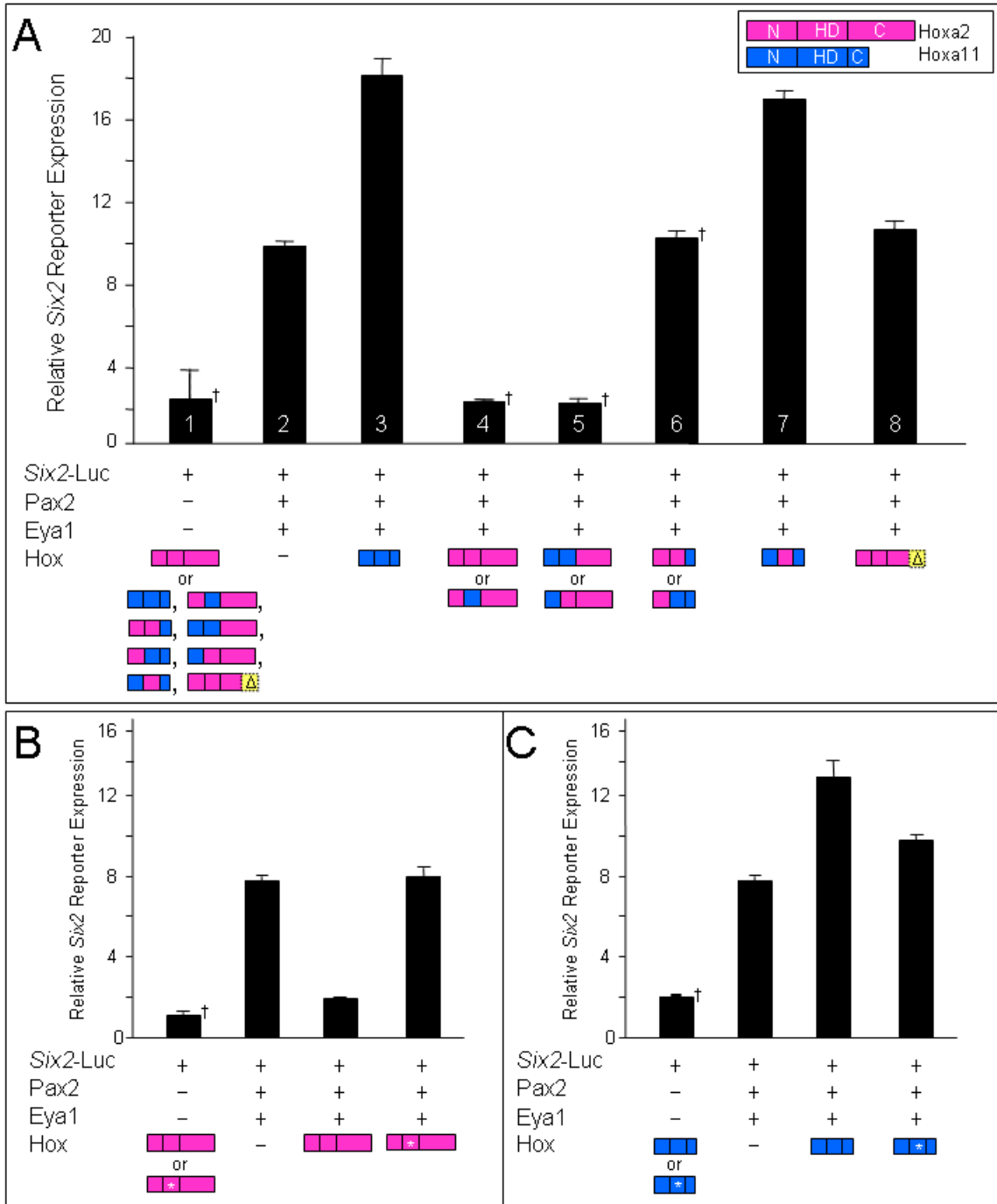
Name	Construct	Symbol
Hoxa2 (a2)		
Hoxa11 (a11)		
a11N-HD+a2C		
a2N-HD+a11C		
a11N+a2HD-C		
a2N+a11HD-C		
a2N+a11HD+a2C		
a11N+a2HD+a11C		
Hoxa2 Δ C63		
Hoxa2-HD ^{mut}		
Hoxa11-HD ^{mut}		

Figure 3.7. Non-homeodomain regions of Hox proteins are critical for differential regulation of *Six2* expression. (A) The homeodomain (HD), as well as regions N-terminal (N) and C-terminal (C) to the homeodomain, were exchanged between *Hoxa2* (pink) and *Hoxa11* (blue). Individually, chimeric protein constructs are unable to affect *Six2*-luciferase reporter activity (bar 1). Replacement of the C-terminal region of *Hoxa11* with the *Hoxa2* C-terminal domain (a11N-HD+a2C, a2N+a11HD+a2C or a11N+a2HD-C (bar 5)) represses activation of *Six2* (bar 2) in a manner similar to the full-length *Hoxa2* (bar 4), demonstrating that regions C-terminal to the *Hoxa2* homeodomain confer repression activity. Swapping the N-terminal and/or the homeodomain of *Hoxa2* into the *Hoxa11* construct abrogates activation, but does not convert this protein to a repressor (a2N-HD+a11C or a2N+a11HD-C (bar 6)). Both N- and C-terminal regions of *Hoxa11* are required to activate *Six2* expression (a11N+a2HD+a11C, bar 7). Deletion of the last 63 amino acids of *Hoxa2* C-terminal domain abrogates *Hoxa2*-mediated repression (bar 8), demonstrating this region is critical for conferring *Hoxa2* repression. (B) Mutation of the *Hoxa2*-HD (asterisk) abrogates *Hoxa2*-mediated repression of *Six2* expression. (C) Mutation of the *Hoxa11*-HD (asterisk) inhibits synergistic activation of the *Six2*-luciferase reporter compared to wild-type *Hoxa11*. Daggers (†) indicate similar fold activations were observed for the listed Hox protein expression constructs. The largest standard deviation for any single experiment is shown in the above figure where more than one construct result is represented.

Figure 3.7



an activator (Hoxa2N-HD+Hoxa11C, Figure 3.7A, column 6). However, repression is lost, consistent with the repressive activity being localized in the Hoxa2 C-terminal domain. Swapping protein domains such that both N- and C-terminal domains from Hoxa11 protein are present with the Hoxa2 homeodomain, however, is sufficient for full activation of *Six2* expression. A chimeric protein with the N-terminal portion of Hoxa11, the Hoxa2 homeodomain (HD), and the Hoxa11 C-terminal residues activates *Six2* expression similar to wild type Hoxa11 protein (Hoxa11N+Hoxa2HD+Hoxa11C, Figure 3.7A, column 7). Of note, while there are only 13 amino acids C-terminal to the homeodomain in Hoxa11 (and Hoxc11 and Hoxd11), this domain is essential for activation activity. Deletion of these 13 amino acids results in complete loss of activity (data not shown).

DNA binding is required for activation and repression

The previous set of experiments demonstrates that a homeodomain is required for activity, but that the identity of the homeodomain is not critical for differential activation and repression. In order to determine whether DNA binding is required, we generated mutations in critical homeodomain amino acids in our protein expression constructs. Previous work has shown that amino acids 51 and 53 of the homeodomain are essential for DNA binding of homeobox proteins [56, 188], so mutations at these homeodomain sites were generated for both Hoxa2 and Hoxa11 (Figure 3.6). The ability of Hoxa2 to repress (Figure 3.7B) and of Hoxa11 to activate (Figure 3.7C) *Six2* expression is significantly reduced

when the DNA binding domain of either protein is mutated, demonstrating that DNA binding is a critical component of both Hox activation and repression. Taken together, these experiments demonstrate that while DNA binding is important for transcriptional activity, the identity of the homeodomain is not critical. Rather, it is the unique domains N- and C-terminal to the homeodomain that confer differential activity.

Discussion

Despite decades of research, little is known regarding the mechanisms by which Hox proteins regulate patterning along the AP axis. Extensive genetic analyses unequivocally demonstrate the importance of these genes in controlling segment identity in *Drosophila* and many aspects of patterning along the AP body axis and the proximal-distal axis of limbs in mice [4, 18, 24, 25, 32, 36, 44, 53, 189, 190]. How these global patterning events are regulated at a transcriptional level is not well understood.

One of the main difficulties in identifying direct downstream targets of Hox genes is the poor specificity in sequence recognition exhibited by Hox proteins. The DNA binding motif is highly conserved between all Hox proteins, even over large evolutionary distances, and all Hox proteins preferentially bind a conserved -ATTA- core motif [174-176]. The low specificity and frequency with which this short sequence occurs throughout the genome makes Hox response element (HRE) prediction extremely difficult.

The poor binding specificity *in vitro* contrasts sharply, however, with the highly specific functions ascribed for individual Hox proteins *in vivo*. Initially, the notion that modest differences in binding preference by individual homeodomains contributed to *in vivo* specificity was explored and gained broad support [191, 192]. Two main lines of evidence supported this assertion. First, a number of studies were performed in which the homeodomain from Hox protein 'A' was swapped in place of the homeodomain Hox protein 'B', and Hox 'A', Hox 'B' and chimeric Hox 'B-A^{HD}' were ectopically expressed in *Drosophila* [177, 179-183, 193]. Ectopic homeodomain-swapped Hox constructs often resulted in patterning changes that were interpreted to more closely resemble phenotypes from ectopic expression of the wild-type Hox 'A' protein (the homeodomain donor) than Hox 'B', consistent with activity regulation by the DNA-binding homeodomain. Complete reciprocal experiments in which the regions N- and C-terminal to the homeodomain of Hox 'A' were used with Hox 'B' homeodomain to compare the contribution of the homeodomain to that of the non-homeodomain regions were not performed, however. Further, it was noted that many of the phenotypic changes induced by ectopic expression of Hox (chimeric or wild-type proteins) are likely to have resulted from ectopic activation of additional Hox proteins [180]; thus, how these phenotypic changes should be interpreted with respect to *in vivo* Hox function is not clear. A second set of experiments report that vertebrate proteins behave similarly to their *Drosophila* orthologs *in vivo* [194, 195]. As sequence identity between vertebrates and arthropods can be

found primarily in the homeodomain region, this was taken as further indication that the homeodomain is a primary controller of specificity *in vivo*.

The discovery that mutation in *exd*, a *Drosophila* TALE-class homeodomain gene, resulted in Hox-like homeotic changes without causing changes in *Hox* expression led to the suggestion that *exd* might be a cofactor for Hox downstream target regulation [57]. This was shown to be the case for *Ubx* in 1994 [58], and has since been shown to be operative in several contexts (reviewed in [66]). *Exd*, or *Pbx* in mammals, binds Hox primarily via a conserved hexapeptide motif N-terminal to the homeodomain [196-200]. Collectively, this work highlights the importance of at least one region outside of the homeodomain for Hox function and specificity, and has led to the identification of a subset of target genes regulated by this complex in both *Drosophila* and mammals [60-62, 65-68, 157]. However, mammalian *Pbx* proteins do not interact with the most posterior Hox paralog groups (including Hox11 proteins) and mutants for *Pbx* genes demonstrate many phenotypes not observed in *Hox* mutants (reviewed in [66]). Further, the increased specificity of the combined Hox/*Exd* consensus binding site has not led to the identification of a large number of additional target genes [201]. Altogether, it is likely that other mechanisms of conferring target gene specificity exist for Hox proteins.

Other regions of the Hox proteins, in addition to the homeodomain and the *Exd*/*Pbx*-binding hexapeptide region, might be important for Hox function. In the report by Zeng, *et al.*, swap of the C-terminal was examined in addition to the homeodomain swap [183]. Substitution of both the homeodomain and the C-

terminal regions, together, more fully recapitulated the donor protein behavior than swap of the homeodomain alone, supporting the idea that Hox specificity may lie, at least in part, outside of the homeodomain. Further, Tour, *et al.* demonstrated that while repression of *Dll* by Ubx depended on the Exd-binding YPWM motif, activation activity depended on the N-terminal 20 amino acids, which include a highly conserved SSYF motif [202].

Additional mechanisms for regulating Hox downstream targets have been proposed more recently. Notably, the idea that *Hox* genes may regulate target genes via a mechanism of ‘collaboration’, whereby Hox proteins, along with other transcription factors that bind at nearby sites, co-regulate gene expression without directly interacting with one another directly [203, 204]. This model does not incorporate how DNA binding specificity may or may not contribute to or be affected by ‘collaborative’ binding, but does assume that additional factors must be recruited by both Hox and its ‘collaborating’ co-factors [204]. Presumably, this could include differential interaction with non-homeodomain regions of the Hox proteins.

With the advent of genome sequencing and large-scale techniques, several attempts have been made to identify genome-wide Hox targets using whole organ or whole embryo approaches [205-213]. A panoply of expression changes with both loss-of-function and gain-of-function *Hox* mutants have been reported. Many of these studies note changes in expression for hundreds of genes along with distinct changes in expression for different *Hox* mutants. Together, these studies give us a sense of the broad importance of *Hox* gene

function *in vivo*, and also further demonstrate that unique regulatory contributions can be made by individual Hox proteins. A continued combination of *in silico*, computational work and *in vivo* experimentation will hopefully result in confirmation of direct downstream targets in which enhancer elements can be predicted and tested. Ultimately, these experiments may lead to a much greater understanding of Hox function, however, mechanistic details regarding Hox function await further analysis.

In this study, we demonstrate that *Hoxa2* represses *Six2* expression and *Hox11* proteins activate *Six2* expression using the same enhancer site *in vivo*. Previous work has demonstrated that *Hox11* genes activate *Six2* expression *in vivo* [25, 184] while *Hoxa2* represses *Six2* expression *in vivo* [173, 185]. Our transgenic analysis of the regulatory region upstream of *Six2* identifies a 50 bp Hox response element (HRE), and mutation of this element results in both the loss of *Six2* expression in the kidney and expansion of *Six2* expression in the facial mesenchyme. This finding, along with the ability to recapitulate these *in vivo* expression activities in cell culture with the addition of Pax2 and Eya1 (cofactors needed for activation with Hox11 proteins [184]), provides the opportunity to explore the mechanistic basis of the differential Hox regulation at this HRE.

Using reciprocal chimeric protein expression constructs of *Hoxa11* and *Hoxa2*, we show that the ability of *Hoxa2* to repress *Six2* expression lies in the domain C-terminal to the homeodomain. When this region of *Hoxa2* was exchanged with the C-terminal domain of *Hoxa11*, the resulting chimeric protein

represses *Six2* expression. Thus, with respect to this activity, the homeodomains do not contribute substantially to discriminate between activation and repression.

Further alignment and examination of the protein coding sequence of all 39 mammalian Hox proteins reveals an interesting feature shared between Hox2 and Hox3 paralogous group proteins, and not the remaining 34 Hox proteins. The C-terminal domains of each of these five Hox proteins are very large, ranging from 154 to 192 amino acids (compared to 6 to 49 amino acids in the other 34 Hox proteins). Alignment of the C-terminal regions of these five proteins revealed a conserved 60 amino acid stretch at the end of the sequence. Further functional examination revealed that the members of the Hox2 and Hox3 paralogous groups share the ability to repress expression in our assay and removal of the conserved 60 amino acids from *Hoxa2* abrogates its repressive activity, supporting the existence of a shared domain in these two Hox paralog groups important for repression.

The converse set of experiments in which either the C-terminal domain (which is only 13 amino acids) or the N-terminal domain from *Hoxa11* is used to replace the *Hoxa2* sequence does not result in conversion of *Hoxa2* into an activator. Domains both N-terminal and C-terminal to the homeodomain of *Hoxa11* are required for activation from the chimeric construct. Similar to the repression experiments, full activation was achieved independent of the homeodomain sequence present.

DNA binding, however, is required for Hox function as protein expression constructs containing 2 amino acid substitutions in the DNA binding region of Hoxa11 or Hoxa2 lost most of their activity in these assays. Together, the data suggests that the primary role of the homeodomain is to recognize a general sequence that may, indeed, be of low specificity *in vivo*, just as it is *in vitro*.

These data are consistent with the idea that the specific effects of Hox activity *in vivo* lie with its ability to interact with other proteins at the regulatory site, and it is the regions N-terminal and C-terminal to the DNA binding region that confer the proteins with these unique properties. In addition to being consistent with *in vitro* binding data, these data are also consistent with the fact that there is significant conservation of protein sequence in N- and C-terminal regions between paralogous Hox proteins, and even between orthologs. Whether Hox proteins operate largely by classically understood co-regulators, such as Exd/Pbx, or by collaboration with many other factors as has been proposed [204], this study demonstrates that domains outside of the homeodomain are likely to be critical for imparting Hox proteins with their unique properties to direct target gene regulation *in vivo*.

Acknowledgments

This manuscript was written by Alisha R. Yallowitz, Ke-Qin Gong, Ilea T. Swinehart, Lisa T. Nelson, and Deneen M. Wellik.

This work was supported in part by the National Institute of Health grant DK071929 (DW) and DK077045 (DW), by the University of Michigan's Training Program in Organogenesis T32-HD007505 (AY), and in part by the National

Institutes of Health through the University of Michigan's Cancer Center Support
Grant (5 P30 CA46592).

CHAPTER IV

THE *HOX10* PARALOGOUS GENES ARE NECESSARY FOR METANEPHRIC KIDNEY MORPHOGENESIS

Abstract

Many of the thirteen paralogous groups of Hox genes have overlapping expression patterns in different organ systems. The *Hox10* and *Hox11* genes are co-expressed in the kidney, but it is unknown if they function in similar or different pathways. Herein we have analyzed defects of metanephric kidney organogenesis in *Hox10* mutant animals. The *Hox10* genes are co-expressed with *Hox11* in the nephrogenic mesenchyme, but *Hox10* genes are also uniquely expressed in the kidney cortical stroma. *Hox10* triple paralogous mutant animals die 24 hours after birth and kidneys in these mutants display severe hydronephrosis. *Hox10* mutants have smaller kidneys than controls, with reduced ureter branching and nephrogenesis. Mutant kidneys also fail to rotate and ascend, and the kidney capsule does not form properly. *Hox10* mutant phenotypes recapitulate what is observed in other stromal cell mutants, such as *Foxd1*, indicating that the *Hox10* genes play an important role in regulating kidney stromal cell function.

Introduction

In mice, the adult kidney, or metanephros, begins development at embryonic day 10.5 (E10.5) when the ureter invades an adjacent group of metanephrogenic mesenchymal cells. The ureter emits signals that promote survival and proliferation of the condensed mesenchyme. The mesenchyme, in turn, emits signals that promote ureteric branching. As the ureter branches, the mesenchyme in direct contact with the branch tips, called nephrogenic cap mesenchyme, undergoes a mesenchymal to epithelial transition (MET) to form nephrons, the filtration units of the kidney [76, 80]. A third cell type also present at very early kidney stages are the stromal cells. Stromal cells can be detected at E11.5, just after ureter bud invasion, as a group of cells that surround the condensed mesenchyme. A role for these cells was not apparent initially, but recent evidence has demonstrated that the stromal cells provide important instructions for ureter branching morphogenesis as well as nephron maturation [81, 113, 214].

As the kidney differentiates it becomes compartmentalized into three distinct regions. The outer region of the kidney, the cortex, includes the zone of nephrogenesis where new cap mesenchyme condensations are formed around branching ureter bud tips. These structures will give rise to nascent nephrons. Cortical stromal cells are also present in the outer cortex between the mesenchymal condensations. Stromal cells appear to help give rise to a thin layer of connective tissue surrounding the outer cortex, the kidney capsule. As the kidney grows, mature nephrons, which are composed of glomeruli and

collecting tubules, can be found in the inner cortex. The innermost region of the kidney, the medulla, contains the collecting ducts, which are ureter derived epithelial structures. The interstitial cells that lie between mature nephrons and the collecting ducts in the inner cortex and medulla, respectively, are medullary stromal cells [215, 216].

Numerous signaling pathways are required for differentiation of the kidney. The interactions between the mesenchyme and ureter have been described in some detail. Prior to ureteric bud induction, the mesenchyme expresses *Gdnf* [84-88]. Receptors on the ureteric epithelium, Ret and Gfr α 1, recognize Gdnf to initiate ureter bud formation and invasion into the mesenchyme [89-94]. A myriad of transcription factors are necessary to regulate the expression of *Gdnf*, such as Pax2, Eya1, Wt1, Sall1, and the Hox11 proteins [25, 95-99, 187]. After induction, these transcription factors maintain *Gdnf* expression in the mesenchyme to promote further budding and branching of the ureter [102, 103]. The ureter expresses Fgf2 and Bmp7, which promote survival and proliferation of the mesenchyme, as well as Wnt9b to initiate formation of the cap mesenchyme around the branch tips [104-108]. The cap mesenchyme expresses Wnt4 and subsequently undergoes epithelialization to form nephrons [109, 110]. Undifferentiated cap mesenchyme expresses *Six2*, which regulates metanephric progenitor cell renewal [121]. The stromal cells, which were originally thought to provide a general supporting role, have been recently shown to express factors that are necessary for ureter branching and nephron differentiation [82, 111]. A key transcription factor important for stromal cell function is *Foxd1*, which is

exclusively expressed in the cortical stroma [112]. Loss of *Foxd1* function results in severe defects in ureter branching and kidney capsule formation [112, 113].

Multiple *Hox* genes are expressed in the kidney [119]. These genes are temporally and spatially expressed along the anterior-posterior body axis and are necessary for patterning different mesodermal organs. Currently, the only *Hox* genes that have demonstrated to be essential for kidney organogenesis is the *Hox11* paralog group [25]. The *Hox11* genes are expressed in the condensed metanephric mesenchyme prior to ureter invasion. *Hox11* triple paralogous mutants fail to express *Six2* and *Gdnf* in the condensed mesenchyme [25, 187]. Due to the absence of *Gdnf* there is no ureteric bud induction and subsequent apoptosis of the nephrogenic mesenchyme, resulting in failure of kidney formation in mutant animals.

The *Hox10* paralogs are initially expressed throughout the condensed metanephric mesenchyme and quickly become localized to the nephrogenic zone in both the nephrogenic cap mesenchyme and the cortical stroma. Herein we report that the *Hox10* paralogous genes are necessary for the proper patterning and ascension of the metanephros. *Hox10* mutant kidneys are incompletely ascended, hypomorphic, and exhibit severe hydronephrosis at birth. Ureter branching is severely reduced, the organization of the collecting structures is disrupted, and the nascent kidney capsule is not specified. The molecular phenotypes in our *Hox10* mutants are reminiscent of *Foxd1* mutants [112, 113], although *Hox10* genes do not appear to regulate *Foxd1* expression. Therefore,

our results indicate that the primary roles of the *Hox10* genes in the kidney are as regulators of the cortical stroma cells.

Materials and methods

Animals and histology

Generation of *Hox10* mutant embryos was previously described [24].

Embryos and kidneys were dissected in PBS, fixed in formalin for one to three hours, and dehydrated through graded alcohols and stored in 70% ethanol at 4°C. Embryos were vacuum-embedded in paraffin, sectioned at 5µm and stained with hematoxylin and eosin. The embryo head was used for genotyping.

Section in situ hybridization

Embryos were collected in PBS and fixed overnight in 4% paraformaldehyde in PBS at 4°C. Embryos were then rinsed in PBS and immersed in 30% sucrose at 4°C overnight prior to embedding into OCT media. 20 to 30µm frozen sections were cut and slides were stored at -80°C.

In situ hybridization was performed as previously described [111, 125]. Prior to in situ hybridization on sections of *Hoxa11*-eGFP tissue, slides were rinsed in PBS and images were taken on Olympus BX-51 upright light microscope with an Olympus DP70 camera.

The *Hoxa10*, *Hoxc10*, *Hoxd10* (EM Carpenter), *Six2*, *Eya1* (R Maas), *Pax2* (GR Dressler), *Bmp4* (R Behringer), *Raldh2*, *Sfrp1*, and *Foxd1* (CL Mendelsohn) in situ probes were generously provided. Vectors were linearized

by restriction digest and standard in vitro transcription protocol was used to produce DIG-labeled RNA probes.

Immunohistochemistry

Immunohistochemical localization of Pax2 (Covance) and pan-cytokeratin (Sigma) staining of whole organs were performed as previously described [95, 217].

α E-cadherin (R&D Systems) and α smooth muscle actin (Cy3-conjugated mouse monoclonal, Sigma) localization on slides were performed as previously described [218]. Embryos were processed as described above for section in situ.

Lectin immunohistochemistry was performed on sections of embryos processed as described above for section in situ hybridization analyses. After washing in PBS, slides were incubated in 50mM NH₄Cl in PBS at room temperature for 20 minutes, followed by a 20 minute incubation with GSP solution (0.2% gelatin+0.075% saponin (S4521, Sigma) in PBS) at 37°C. After 20 minutes of incubation with 0.075% saponin in a sodium acetate buffer (NA buffer+saponin) at 37°C the slides were incubated with 0.6 units/mL Neuraminidase (N7885, Sigma) at 37°C for 3 hours. Slides were washed at room temperature in NA buffer+saponin and incubated with GSP solution for 15 minutes. Slides were then incubated with 1:300 rhodamine labeled PNA (Vector Labs) or 1:250 rhodamine labeled DBA (Vector Labs) with 1:400 fluorescein labeled LTA (Vector Labs) at 4°C overnight in the humidifying chamber. Slides

were then incubated with GSP solution at 37°C two times for 20 minutes and rinsed in PBS+0.05% Tween at room temperature. After washing for 20 minutes with PBS, slides were mounted with Pro-Long Gold, antifade reagent (Invitrogen).

Results

Morphological phenotype

Hox10 paralogous mutant animals show a reduced viability. Double mutants, which are missing four of the six *Hox10* alleles, survive until birth but die perinatally from hydronephrosis between two weeks and three months of age (Figure 4.1B). Five-allele mutant animals occasionally survive to two to four weeks of age, while triple paralogous mutants die shortly after birth. The kidneys of triple mutants also fail to ascend towards the adrenal glands. The onset of hydronephrosis is observable at early embryonic stages in high allele mutants, starting at E16.5.

Histological sections through kidneys of E18.5 *Hox10* triple paralogous mutant embryos demonstrate a significant reduction in nephrogenesis and do not show clearly defined collecting regions. In controls, there are three distinct domains of the kidney (Fig 4.1C). The outer cortex contains a zone of nephrogenesis where mesenchymal condensates are undergoing epithelialization. The inner cortex contains mature nephrons made up of glomeruli and proximal and distal tubules. The medullary region consists of collecting ducts, derived from the ureter epithelium, that empty into the hilum of

Figure 4.1

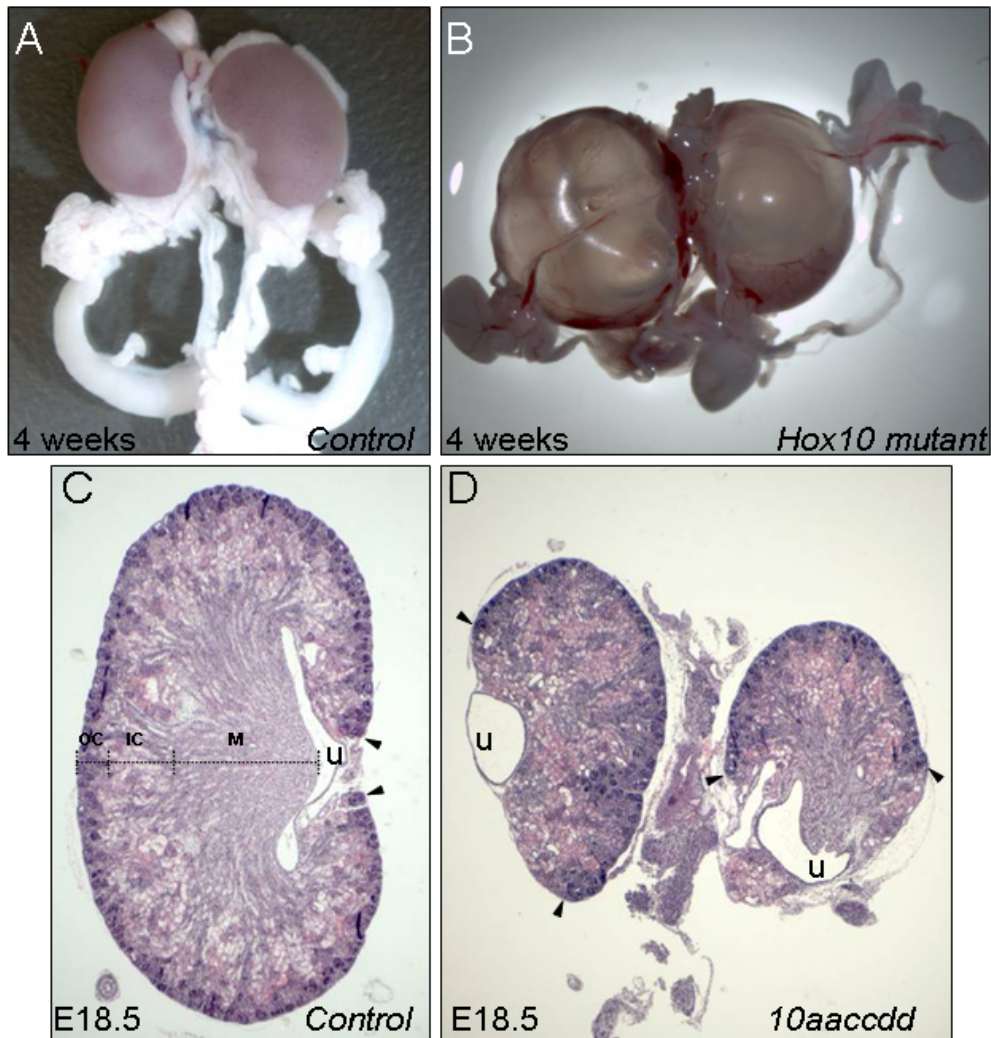


Figure 4.1. *Hox10* mutant animals have severe morphological defects. (A) Whole-mount dissection of the urogenital system of a four week control animal. (B) Whole-mount dissection of the urogenital system from a four week high-allele *Hox10* mutant animal showing severe hydronephrosis. (C) Histological section through an E18.5 control kidney. The kidney is organized into three distinct regions, the outer cortex (OC), inner cortex (IC), and medulla (M). The zone of nephrogenesis (arrowheads) is in the outer cortex and surrounds the kidney up to the point of ureter entry (u). (D) Histological section through an E18.5 *Hox10* triple paralogous mutant embryo. The nephrogenic zone in the outer cortex (arrowheads) is reduced in mutant animals and there is a reduction in the number of collecting ducts in the medulla. The ureters (u) also enter the mutant kidneys from the lateral or ventro-lateral positions.

the ureter. *Hox10* mutants have a zone of nephrogenesis in the cortex, although this region is not observed surrounding the periphery of the entire kidney as in controls (Figure 4.1D, arrowheads), and the medullary region is disorganized with fewer collecting ducts. It is also important to note a defect in ureter entry in the *Hox10* mutant kidneys. The positions of the cortical and medullary regions along the medial-lateral axes are reversed in mutant animals, with the ureter entering the kidney from the lateral or ventro-lateral position (Figure 4.1D), instead of from the medial side (Figure 4.1C) like controls.

The ureter entry defect does not appear to be a result of the ureter point of invasion into the kidney but rather from defects in kidney ascension during development. At E11.5 the ureter normally invades the metanephric mesenchyme at the ventral side of both control and *Hox10* mutant embryos (Figure 4.2A, 4.2B). Control kidneys have detached from the body wall and rotated laterally about 90° by E13.5 and E15.5 (Figure 4.2C, 4.2E, 4.2G). The rostral end of the ureter that has invaded the kidney turns laterally, resulting in medial entry of the ureter into the kidney (Figure 4.2C, 4.2E). As the kidney ascends, the caudal end of the ureter extends toward the bladder along the midline (Figure 4.2G). Kidneys in *Hox10* mutant embryos do not rotate or ascend properly. By E13.5, the kidneys have not rotated and remain dorsal to the ureter (Figure 4.2D, 4.2F). The rotational defect is due to the failure of kidney detachment from the dorsal body wall. The kidneys fail to ascend from the pelvic region and fuse with the dorsal body wall (Figure 4.2H). The physical restraint of

Figure 4.2

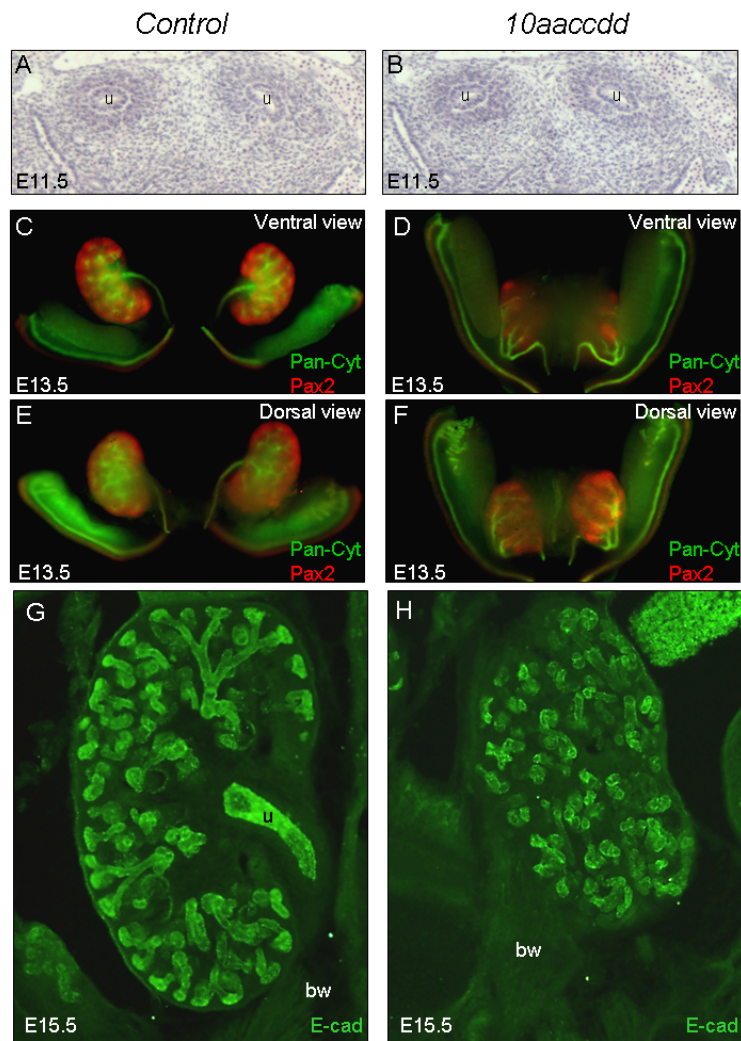


Figure 4.2. *Hox10* mutants have reduced ureter branching and failure of kidney ascension affects ureter position. (A and B) Induction of the ureter into the condensed mesenchyme at E11.5 is normal in control (A) and *Hox10* mutant (B) animals. (C through F) Dissected E13.5 urogenital systems were stained with Pax2 (red) to label the nephrogenic mesenchyme and with Pan-cytokeratin (green) to label the ureter epithelial structures. *Hox10* mutant animals have reduced ureter branching and elongated branches (D and F) compared to control animals (C and E). The kidneys of *Hox10* mutants have also failed to rotate laterally (D and F). (G and H) Sections of E15.5 control (G) and mutant (H) embryos stained with E-cadherin to label epithelial structures. The kidneys of *Hox10* mutant animals have fusions to the body wall (H) while the kidneys of control animals (G) have a distinct border separating them from other structures. u, ureter; bw, body wall.

the kidney on the rostral end of the ureter forces the ureter to elongate ventrally around the kidney to reach the bladder (Fig 4.2D, 4.2F).

After ureteric bud induction, the ureter undergoes numerous rounds of branching and bifurcation events. At E13.5, approximately six to eight branching events have occurred and the tips of the branches are surrounded by mesenchymal condensates [219] (Figure 4.2C, 4.2E). In *Hox10* mutant embryos, mesenchymal condensations are observed around the ureter tips, but there are fewer bifurcation events and the early branches are abnormally elongated (Figure 4.2D, 4.2F).

By E15.5, smooth muscle has been induced to surround the ureter along its entire length until it enters the kidney at the ureter pelvic junction (UPJ) (Figure 4.3A-4.3F). Smooth muscle is important to maintain the structural integrity of the ureter and to regulate peristaltic activity [220]. Loss of smooth muscle around the ureter results in hydroureter while loss of smooth muscle at the UPJ results in hydronephrosis [221, 222]. As hydronephrosis is observed in our *Hox10* mutants we examined smooth muscle differentiation and organization along the ureter. Despite the defects in ureter routing in *Hox10* mutants, smooth muscle surrounds the ureter from the bladder to the UPJ (Figure 4.3D, 4.3E). Organization of smooth muscle around the ureter at the UPJ in mutants, however, is absent (Figure 4.3F). This smooth muscle organizational defect at the UPJ may limit the peristaltic passage of urine from the kidney, and would therefore lead to hydronephrosis in *Hox10* mutant animals.

Figure 4.3

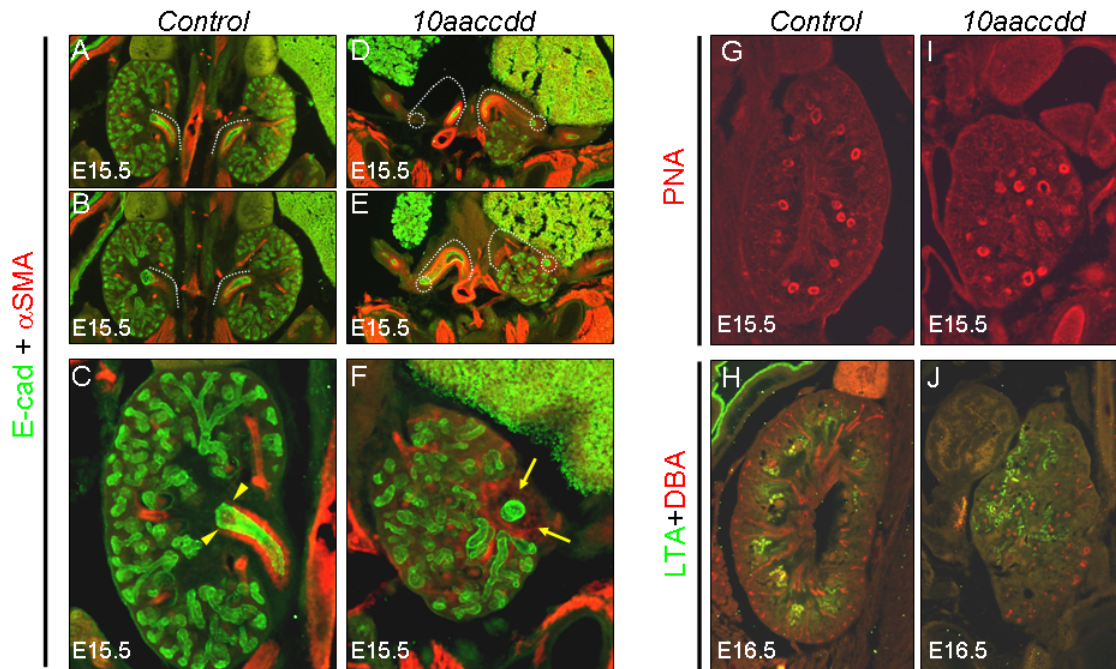


Figure 4.3. *Hox10* mutants have smooth muscle disorganization at the UPJ and reduced nephrogenesis. (A through F) Sections of E15.5 control (A through C) and *Hox10* mutant (D through F) animals stained with E-cadherin (E-cad, green) to label epithelial structures and smooth muscle actin (α SMA, red) to label smooth muscle. The white dotted line denotes the direction of the ureter entering the kidney, which is perturbed in *Hox10* mutant animals (D and E). Smooth muscle surrounds the ureter of control (A and B) and *Hox10* mutant (D and E) animals. Smooth muscle in control animals ends at the ureter pelvic junction (C, yellow arrowheads). There is no organization of the smooth muscle in *Hox10* mutant animals at the ureter pelvic junction (F, yellow arrows). (G and I) Sections of E15.5 control (G) and mutant (I) embryos stained with PNA (red) to label glomeruli. The kidneys of *Hox10* mutants have glomeruli mislocalized towards the medullary region (I). (H and J) Sections of E16.5 control (H) and mutant (J) embryos stained with LTA (green) to label proximal tubules and DBA (red) to label collecting ducts. *Hox10* mutant kidneys have mislocalized proximal tubules and a reduction in mature collecting ducts (J).

In addition to defects of ureter maturation, *Hox10* mutant embryos also showed reduced nephrogenesis and disorganization of the cortical and medullary regions (Figure 4.1D). We used lectin staining to identify structures of differentiated nephrons. Peanut Agglutinin (PNA) and Lotus Tetragonolobus Lectin (LTL) label glomeruli and proximal tubules, respectively. Glomeruli and proximal tubules, which make up part of the nephron, are localized around the kidney in the cortical region just below the zone of nephrogenesis at the periphery in E15.5 and E16.5 controls (Figure 4.3G, 4.3H). Nephron differentiation occurs in limited regions of *Hox10* mutant kidneys and mature nephrons, which should be confined to the inner cortex, are found in the medullary region (Figure 4.3I, 4.3J). There is also a reduction in the number of mature collecting ducts, as labeled by Dolichos Biflorus Agglutinin (DBA), in mutant kidneys (Figure 4.3J).

Expression of Hox10 paralogs

To dissect differences in *Hox10* and *Hox11* activity in the kidney, we analyzed the expression of the *Hox10* genes during early kidney organogenesis by in situ hybridization and compared their expression to *Hox11* [223]. At E11.5, ureteric bud invasion stages, *Hox10* genes are expressed in the metanephric mesenchyme and not the ureter epithelium, similar to *Hox11* expression (Figure 4.4A and 4.4B). By E13.5, *Hox10* and *Hox11* both remain in the condensing mesenchyme in the nephrogenic zone (Figure 4.4C, 4.4D). However, *Hox10* genes are uniquely expressed in the cells surrounding the condensing

Figure 4.4

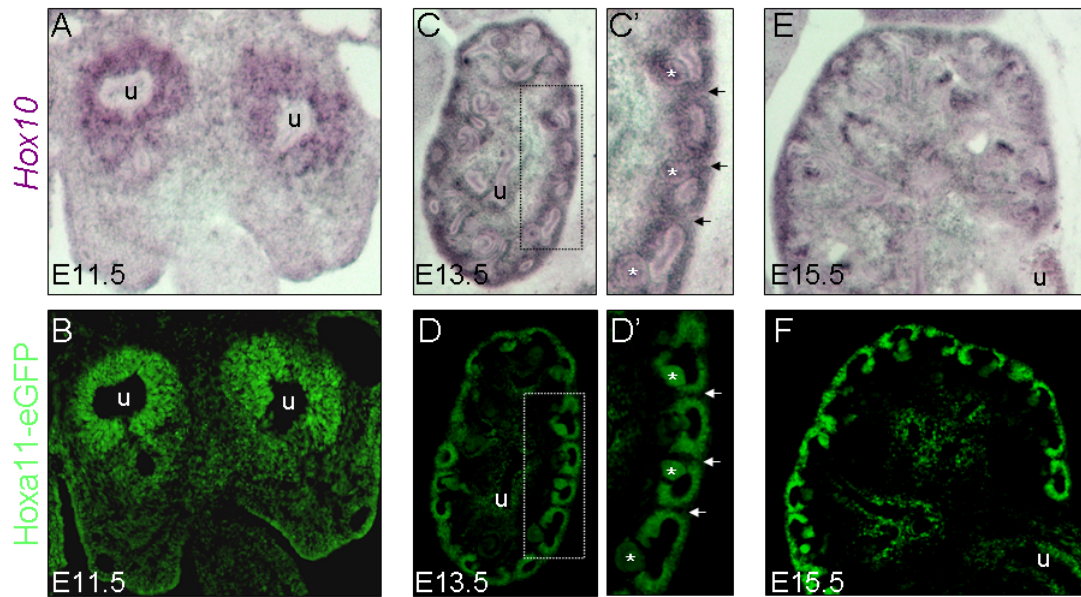


Figure 4.4. The *Hox10* paralogs are expressed in the nephrogenic mesenchyme and cortical stroma. *Hox10 in situ* analyses for all the *Hox10* paralogs were done on tissue sections from *Hoxa11-eGFP* heterozygous embryos [223]. (A and B) At E11.5, the *Hox10* genes (A) and *Hoxa11* (B, green) are expressed in the condensed mesenchyme surrounding the ureter (u). (C and D) At E13.5, *Hox10* (C) and *Hoxa11* (D) are both expressed in the nephrogenic cap mesenchyme. (C') The *Hox10* genes are also expressed in the cortical stroma (arrows) between the mesenchymal condensations and are expressed in cells that surround the initial epithelial structures of the nephrons (asterisks). (D') *Hoxa11* is expressed in the initial epithelial structures (asterisks), but it is not present in the cortical stroma (arrows). (E and F) At E15.5, the *Hox10* genes are expressed in the nephrogenic mesenchyme and cortical stroma (E), while *Hoxa11* is expressed only in the nephrogenic mesenchyme (F).

mesenchyme, in the kidney stromal cells (Figure 4.4C', black arrows). Further, while Hox11 is expressed in the early renal vesicles, the *Hox10* genes are expressed in the mesenchymal cells that surround these epithelial structures (Figure 4.4C', 4.4D', white asterisks). At E15.5 the *Hox10* genes are expressed throughout the nephrogenic zone in the nephrogenic mesenchyme and the cortical stromal cells at the kidney periphery, while Hox11 remains exclusively expressed only in the condensing nephrogenic mesenchyme (Figure 4.4E, 4.4F).

Hox10 genes are not necessary to pattern the nephrogenic mesenchyme

Despite expression in the nephrogenic mesenchyme, *Hox10* genes do not appear to be necessary for proper differentiation of this cell type of the kidney. *Six2* is a marker of the nephrogenic progenitor population and is essential for maintaining the undifferentiated type state of the mesenchyme [120, 121]. *Six2* is also directly regulated by Hox11 proteins in the nephrogenic mesenchyme [25, 187]. In controls, *Six2* is exclusively expressed in the mesenchyme that surrounds the ureter at E11.5 and in the mesenchymal condensations of the nephrogenic zone in E15.5 embryos (Figure 4.5A, 4.5C). At E11.5, the expression of *Six2* is maintained in the mesenchyme of *Hox10* mutants (Figure 4.5B). By E15.5, *Six2* expression persists in the condensing nephrogenic cap mesenchyme, although this zone of differentiation is reduced in *Hox10* mutants (arrowheads, Figure 4.5D). *Pax2* and *Eya1* are also highly expressed in the condensed nephrogenic mesenchyme [99, 137] (Figure 4.5E, 4.5G). Although at

Figure 4.5

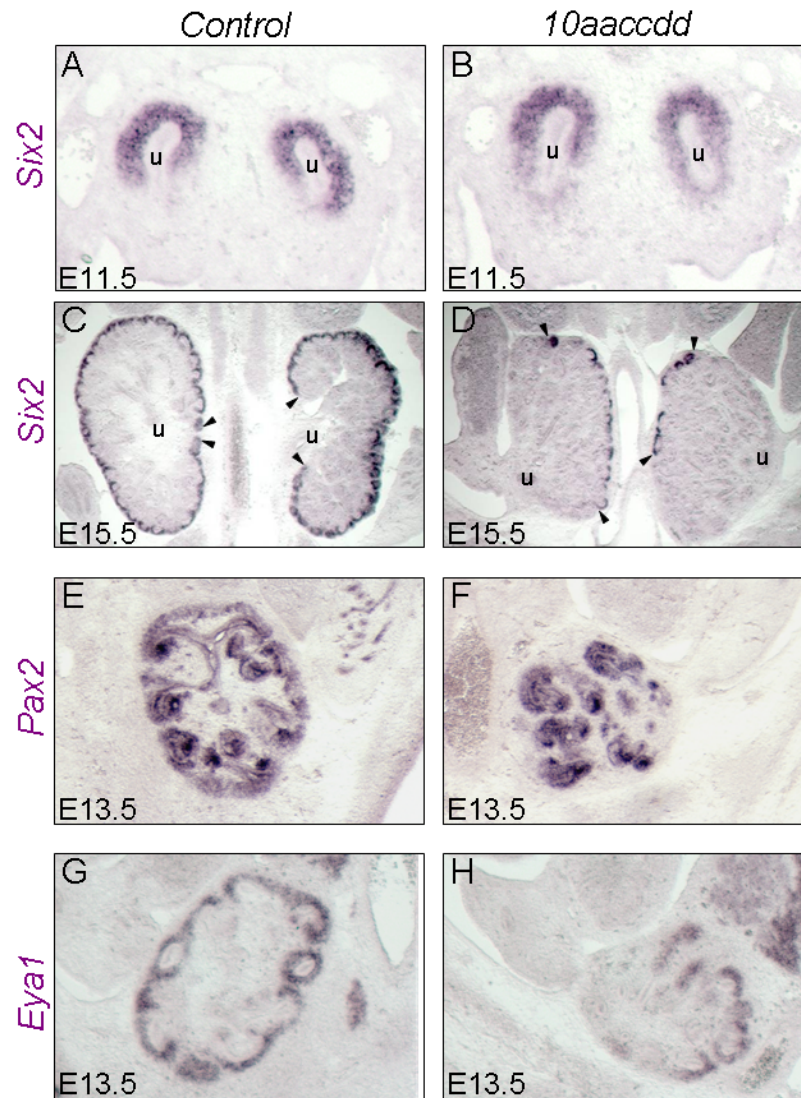


Figure 4.5. Patterning of the nephrogenic mesenchyme. (A-D) Cryosections of E11.5 (A and B) and E15.5 (C and D) control (A and C) and *Hox10* mutant (B and D) embryos stained for *Six2* mRNA expression, which labels nephrogenic progenitors. *Six2* expression is found in the condensed mesenchyme of E11.5 control (A) and E11.5 mutant (B) animals. *Six2* expression is maintained in *Hox10* triple mutants at E15.5, but the number of mesenchymal condensations in the nephrogenic zone is reduced (D). (E through H) Cryosections of E13.5 control (E and G) and *Hox10* mutant (F and H) embryos stained for *Pax2* (E and F) or *Eya1* (G and H) mRNA expression. The expression of *Pax2* (F) and *Eya1* (H) are maintained in the nephrogenic mesenchyme of *Hox10* mutant animals. u, ureter; arrowheads, zone of nephrogenesis.

E13.5 the *Hox10* mutant kidneys demonstrate defects in morphology, the expression of *Pax2* and *Eya1* are maintained (Figure 4.5F, 4.5H).

Hox10 genes play a role in stromal cell function

Unlike the *Hox11* genes, *Hox10* paralogs demonstrate a unique expression in the cortical stroma (Figure 4.4C, 4.4E). The kidney stromal cells are a distinct population from the nephrogenic mesenchyme and ureter epithelium. *Foxd1* is specifically expressed in the cortical stroma and is first detected at E11.5 just after ureter bud invasion [112] (Figure 4.6A). By E13.5 and E15.5 it is maintained in the stromal cells surrounding the condensing mesenchyme in the nephrogenic zone (Figure 4.6C, 4.6E). Many of the morphological phenotypes of *Foxd1* mutants are similar to *Hox10* mutant animals. *Foxd1* mutants have small kidneys that do not ascend, leading to secondary mis-routing of the ureter, reduced ureter branching, and disorganized cortical and medullary layers, yet nephrogenic differentiation appears to be normal [112, 113]. In *Hox10* triple mutants, *Foxd1* is expressed at E11.5, indicating that the initial stromal cell population is present (Figure 4.6B). At later stages, the stromal cell population is present in mutants as indicated by *Foxd1* expression in E13.5 and E15.5 embryos, although the stromal cell population is maintained only in a portion of the periphery of the kidney (Figure 4.6D, 4.6F).

Since *Foxd1* mutants were reported to have defects in the formation of the kidney capsule [113], we analyzed this region in our *Hox10* mutant embryos to determine if the capsule phenotype is similar to *Foxd1* mutants. *Raldh2*, a

Figure 4.6

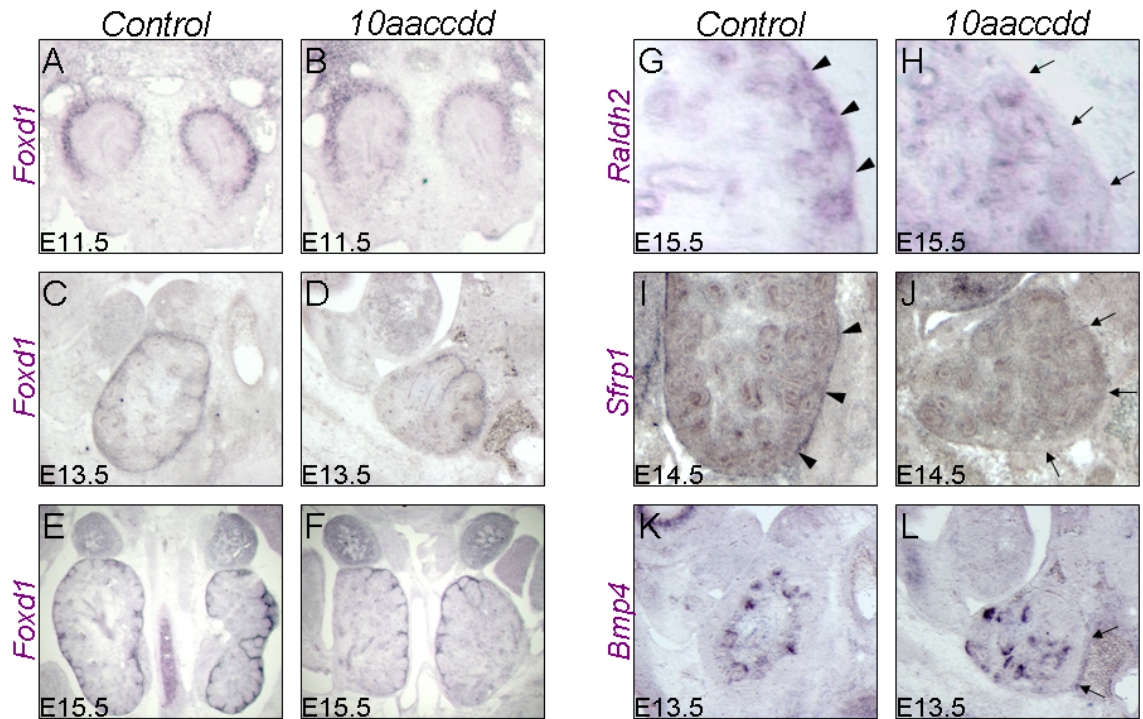


Figure 4.6. Regulation of the cortical stroma cells. (A through F) *Foxd1* mRNA expression was analyzed in the kidneys of control (A, C, and E) and *Hox10* mutant (B, D, and E) embryos at E11.5 (A and B), E13.5 (C and D), and E15.5 (E and F). *Foxd1* labels the cortical stroma cells. *Foxd1* expression is maintained in *Hox10* triple mutants at all ages tested (B, D, and F). (G and H) *Raldh2* expression in E15.5 control (G) and *Hox10* mutant (H) animals. In controls, *Raldh2* is expressed in the kidney capsule (G, black arrowheads). *Hox10* mutants have an absence of *Raldh2* expression in the kidney capsule (H, black arrows). (I and J) *Sfrp1* expression control (I) and *Hox10* mutant (J) E14.5 embryos. *Sfrp1* is strongly expressed in the kidney capsule of control animals (I, black arrowheads) and is absent in the capsule of *Hox10* mutant kidneys (J, black arrows). (K and L) At E13.5, *Hox10* mutant animals have ectopic *Bmp4* expression (L, black arrows) around the kidney periphery.

member of the aldehyde dehydrogenase family, is strongly expressed in both the stromal cells and kidney capsule [224, 225] (Figure 4.6G). *Sfrp1*, a secreted frizzled-related protein, is strongly expressed in the renal capsule [226, 227] (Figure 4.6I). Expression of both of these markers is down-regulated in *Foxd1* mutants [113]. *Hox10* mutants display the same molecular phenotype and do not express *Raldh2* and *Sfrp1* (Figure 4.6H, 4.6J). *Hox10* mutants also show ectopic expression of *Bmp4* surrounding the kidney, a defect observed in *Foxd1* mutants [113] (Figure 4.6K, 4.6L). These results indicate that the *Hox10* genes play an important role in the differentiation of the cortical stroma and kidney capsule, similar to the role of *Foxd1* [112, 113].

Discussion

Hox10 and Hox11 genes have distinct functions in the developing kidney

Differences in phenotypes, yet overlapping expression domains, have been reported for numerous organ systems in *Hox* paralogous mutants. This has been most noted in regards to patterning of the axial skeleton. For instance, *Hox10* and *Hox11* paralogs are both expressed in the somite-derived sclerotome that gives rise to the sacrum. However, the sacrum of *Hox10* mutants displays transformations towards a thoracic-type phenotype while the sacrum of *Hox11* mutants displays transformations into lumbar-like vertebrae [24]. Differences in phenotypes between adjacent and overlapping *Hox* paralogous groups have also been reported between mutants of the *Hox5* and *Hox6* group genes and the *Hox9* and *Hox10* group genes [32, 44]. It is unclear, however, if overlapping *Hox*

paralog group genes function in the same or different cell types that give rise to the vertebral elements.

Expression of the *Hox10* and *Hox11* genes overlap in the condensed metanephric mesenchyme, yet *Hox10* and *Hox11* mutant animals have distinct kidney phenotypes. *Hox10* mutants initiate kidney formation, while *Hox11* mutants demonstrate a complete loss of kidney organogenesis due to the failure of ureteric bud induction [25]. *Hox11* directly regulates both *Gdnf*, the signal necessary for ureteric bud induction, and *Six2* expression in the nephrogenic mesenchyme [25, 187]. *Hox10* mutants undergo ureteric bud induction and maintain expression of *Six2* in the nephrogenic mesenchyme. Thus, *Hox10* genes are not redundant with *Hox11* genes in induction of ureteric budding or in maintaining the nephrogenic mesenchyme. *Hox10* genes appear to function only in the cortical stroma; the region that does not overlap with *Hox11*, but that is unique to *Hox10*.

Hox10 genes regulate the stromal cell compartment

The *Hox10* genes have a unique expression pattern in the cortical stroma. The cortical stromal cells are present in the zone of nephrogenesis interspersed between the mesenchymal condensations. A transcription factor that is exclusively expressed in the cortical stroma is *Foxd1* [81, 82, 112]. Although *Foxd1* expression is maintained in *Hox10* mutants, many of the *Hox10* phenotypes overlap with those described for *Foxd1* mutant animals. Like *Hox10*

mutants, *Foxd1* mutant kidneys fail to rotate and ascend, exhibit reduced ureter branching, and demonstrate severe kidney disorganization [112].

Foxd1 and *Hox10* mutants retain cortical stromal cells [112]. Thus, these genes regulate the function of the stromal cells and not their formation. One of the roles of the stromal cells is to regulate the formation of the kidney capsule [113]. *Foxd1* and *Hox10* mutants have capsule defects as evidenced by the loss of *Raldh2* and *Sfrp1* expression surrounding the kidney, as well as loss of separation between the kidney and body wall [112, 113]. This alteration of the capsule opens the kidney to aberrant signals that will affect maturation and affects the kidney's ability to rotate and ascend to its proper position. One such signal is *Bmp4*, which remains ectopically expressed surrounding the kidneys in both *Hox10* and *Foxd1* mutants [113].

To summarize, we show that *Hox10* paralogous genes have a role in kidney development distinct from the previously reported phenotype for *Hox11* mutant mice [25]. In *Hox10* mutant animals, ureter induction is normal, but branching events are perturbed resulting in hypomorphic kidneys with fewer nephrons. While nephron differentiation is maintained in mutants, the medullary and cortical regions are disorganized, likely secondary to defects in the cortical stromal cells. *Hox10* mutants exhibit severe hydronephrosis, which likely results from the disorganization of the collecting duct structures as well as the loss of smooth muscle at the ureter-pelvic junction. Many of the structural and molecular defects in *Hox10* mutant mice phenocopy the loss of *Foxd1* function,

which suggests *Hox10* and *Foxd1* are in the same or parallel pathways that regulate the function of the cortical stroma.

Acknowledgements

This work was supported in part by the National Institute of Health grant DK071929 (DW) and DK077045 (DW), by the University of Michigan's Training Program in Organogenesis T32-HD007505 (AY), and in part by the National Institutes of Health through the University of Michigan's Cancer Center Support Grant (5 P30 CA46592).

CHAPTER V

CONCLUDING REMARKS

Summary of contributions

Hox proteins are required for many different developmental processes, but their functions at the molecular level are not well understood. All Hox proteins have a highly conserved 60 amino acid DNA binding domain called the homeodomain. The homeodomains of Hox proteins, however, recognizes the same degenerate ATTA DNA element, which has made it difficult to identify Hox target genes [54]. Further, many Hox proteins repress or activate genes depending on developmental context. Thus, Hox proteins presumably require cofactors to regulate genes, of which the only known Hox cofactors are the TALE-group proteins [66]. The aim of my thesis was to further explore the molecular roles of the Hox proteins using the kidney as a model organ system. With help from my colleagues, we have identified novel Hox cofactors and direct target genes. We have additionally shown that regions outside of the homeodomain confer the regulatory specificity of the Hox proteins, at least in some contexts, and that the *Hox10* paralogous genes regulate the function of the cortical stroma in the developing kidney.

Discussion and future directions

Novel Hox cofactors

The *Hox11* genes were previously shown to be necessary for the initial stage of metanephric kidney organogenesis, whereby the ureter is induced to bud from the Wolffian duct and invade the metanephric mesenchyme [25]. Hox11 proteins regulate the expression of *Six2*, a transcription factor that maintains proliferation and regeneration of the nephrogenic mesenchyme, and of *Gdnf*, the protein secreted from the metanephric mesenchyme to initiate ureteric bud induction. In the absence of Hox11 function, *Six2* and *Gdnf* expression are not initiated, resulting in the failure of ureter induction and leading to the subsequent absence of kidneys in *Hox11* mutants. The same phenotype is also observed in *Eya1* and *Pax2* mutant animals [98, 99].

My work provides evidence that the Hox11 paralogs interact with Eya1 and Pax2 to directly regulate *Six2* and *Gdnf* in the metanephric mesenchyme. Co-immunoprecipitation and cell culture assays demonstrate that Hox11, Pax2, and Eya1 physically interact to synergistically regulate *Six2* and *Gdnf* expression. Sequence and mutational analyses led to the identification of an enhancer in the *Six2* promoter necessary for Hox11-Eya1-Pax2 mediated activity *in vitro* and *in vivo*. Thus, we provide evidence that Pax2 and Eya1 are novel cofactors for Hox11 proteins and we identified the enhancer sequence that regulates *Six2* expression in the kidney.

As members of the *Hox*, *Eya*, and *Pax* gene families are genetically required for the formation of numerous other organ systems, such as the thymus

and thyroid [163-168], it is important in the future to determine if the Hox-Eya-Pax regulatory network is conserved during embryogenesis.

Regulatory domains of Hox proteins

As all Hox proteins have a highly conserved 60 amino acid DNA binding domain that recognizes a similar ATTA sequence, it has been difficult to identify direct target genes for these proteins. One gene that has been shown to be genetically downstream of two distinct paralogous *Hox* groups *in vivo* is *Six2*. Hox11 promotes *Six2* expression in the kidney mesenchyme whereas Hoxa2 represses *Six2* in the periotic mesenchyme and branchial arches [25, 173, 184, 185]. Using Six-lacZ transgenic reporters we demonstrate that Hox11-mediated activation and Hoxa2-mediated repression require the same Hox response element (HRE) to regulate *Six2* expression.

By recapitulating Hoxa11-mediated activation and Hoxa2-mediated repression in cell culture, we developed a system in which we could analyze the regulatory functions of the Hox protein domains. DNA binding by the homeodomain is required for Hox function, but it does not confer differential activity. Hoxa2-mediated repression of *Six2* requires the last 60 amino acids of the C-terminal region, and the C-terminal region of Hoxa2 is sufficient to convert an activator Hox to a repressor Hox when swapped into a chimeric construct. The Hoxa11 N- and C-terminal regions are both required to confer activation activities to a Hox protein. Together, our work provides strong evidence that regions outside of the homeodomain confer regulatory specificity to the Hox

proteins. Knowing this, we can pursue the identification of novel cofactors that co-regulate Hox target genes.

***Hox10* genes pattern the kidney stroma**

Formation of the kidney requires inductive interactions between multiple cell types. The best understood cross-talk is between the ureter epithelium and metanephric mesenchyme. Signals from the ureter to the mesenchyme promotes nephrogenesis while signals from the mesenchyme regulate ureter branching [76]. More recently, a third cell type, called the stromal cells, has also been shown to regulate signals necessary for kidney organogenesis [81].

We demonstrate that the *Hox10* paralogous genes are expressed in both the nephrogenic mesenchyme, like the *Hox11* genes, as well as uniquely in the cortical stromal cells. We provide evidence that the *Hox10* genes regulate stromal cell function. Using morphological and molecular analyses, we show that the kidneys of *Hox10* mutants are hypoplastic, have reduced and abnormal ureter branching, have disorganization of the cortical and medullary regions, and do not properly form the renal capsule. *Hox10* mutant phenotypes are similar to those described for *Foxd1* mutants [112, 113]. Since *Foxd1* expression is maintained in *Hox10* mutants, it is possible that *Hox10* and *Foxd1* interact in the same pathway to regulate signals from the cortical stroma. Future work will determine how *Hox10* and *Foxd1* function in the same pathway of kidney development and what genes are directly downstream of them in the cortical stroma.

APPENDIX

HOX PATTERNING OF THE VERTEBRATE RIB CAGE

Abstract

Unlike the rest of the axial skeleton, which develops solely from somitic mesoderm, patterning of the rib cage is complicated by its derivation from two distinct tissues. The thoracic skeleton is derived from both somitic mesoderm, which forms the vertebral bodies and proximal ribs, and from lateral plate mesoderm, which forms the sternum and sternal ribs. By generating mutants in *Hox5*, *Hox6* and *Hox9* paralogous group genes, along with a dissection of the *Hox10* and *Hox11* group mutants, several important conclusions regarding the nature of the 'Hox code' in rib cage and axial skeleton development are revealed. First, axial patterning is consistently coded by the unique and redundant functions of *Hox* paralogous groups throughout the axial skeleton. Loss of paralogous function leads to anterior homeotic transformations of colinear regions throughout the somite-derived axial skeleton. In the thoracic region, *Hox* genes pattern the lateral plate-derived sternum in a non-colinear manner, independent from the patterning of the somite-derived vertebrae and vertebral ribs. Finally, between adjacent sets of paralogous mutants, the regions of

vertebral phenotypes overlap considerably, however, each paralogous group imparts unique morphologies within these regions. In all cases examined, the next most posterior *Hox* paralogous group does not prevent the function of the more anterior *Hox* group in axial patterning. Thus, the 'Hox code' in somitic mesoderm is the result of the distinct, graded effects of two or more *Hox* paralogous groups functioning in any AP location.

Introduction

Differences in the anteroposterior (AP) patterning of the axial skeleton result in an enormous diversity of body plans in vertebrates. *Hox* genes were first described in *Drosophila* for their ability to cause segmental homeotic transformations of the body plan [228, 229], and have since been found to be conserved throughout vertebrate evolution, suggesting their importance in patterning the vertebrate body plan. While flies have eight *Hox* genes located in a single cluster, mammals have 39 *Hox* genes arranged in four clusters, which are further subdivided into thirteen paralogous groups based on sequence similarity and position within the cluster.

Hox expression along the vertebrate anterior-posterior (AP) axis exhibits overlapping expression domains with unique and increasingly posterior limits of expression [34, 230, 231]. As a result of this colinear expression, more posterior axial regions express greater numbers of *Hox* genes. The existence of a vertebrate 'Hox code' was proposed that would assign morphologies to each vertebra as a result of the combination of the *Hox* genes functioning in each

region [232, 233]. Based on several studies, including early work on changes in *Hox* expression in the retinoic acid-treated limb, ectopic expression of mammalian *Hox* genes in *Drosophila*, and early genetic experiments which showed that loss-of-function of single *Hox* genes generally resulted in changes in only the vertebra at the most anterior limit of expression, the model of 'posterior prevalence' has been put forth, which holds that posteriorly-expressed *Hox* genes are functionally dominant over more anteriorly-expressed genes [234-237].

A number of studies have shown that functional redundancy has been retained among *Hox* paralogous genes [238-248]. Horan, *et al* showed that while single mutants for *Hoxa4*, *Hoxb4* and *Hoxd4* resulted in incompletely penetrant phenotypes in the second or third cervical vertebra, loss-of-function of three of the four *Hox4* genes caused extensive cervical transformations, with C2 through C5 transformed towards a C1 phenotype [242]. Complete removal of paralogous function of the *Hox10* and *Hox11* group genes has also been reported. These mutants display regional anterior homeotic transformations of the posterior axial skeleton [245]. Loss of *Hox10* paralogous function results in conversion of the entire lumbosacral region to a thoracic-like morphology. When the *Hox11* paralogous genes are removed, the entire sacral region undergoes transformation to a lumbar-like morphology.

Hox function in the thoracic region, however, has not been as clearly defined. First, both anterior and posterior homeotic transformations have been reported in this region for single *Hox* mutant animals. Single mutants in *Hox5* and

Hox6 paralogous groups have both resulted in phenotypes at the cervicothoracic transition. While mutants for *Hoxa5* and *Hoxa6* both exhibit an ectopic rib at C7 - a posterior homeotic transformation, single mutants of *Hoxb5*, *Hoxb6* and *Hoxc6* demonstrate partially penetrant loss of rib formation at T1 – an anterior homeotic transformation [249-252]. As C7 and T1 are affected in both the *Hox5* and the *Hox6* single mutants, colinearity is not immediately apparent for these genes, however, paralogous mutants have not been examined for these groups. Mutants in the *Hox7*, *Hox8* and *Hox9* genes have also been examined [238, 240, 253]. The reported defects in these mutants also show no clear colinearity. The phenotypes in these animals are reported to localize at both cervicothoracic and at thoracolumbar transition points, not to distinct AP regions of the axial skeleton. These combined results suggest that there are alternative mechanisms by which *Hox* genes govern patterning of the thoracic region.

Part of the difficulty in understanding patterning of the rib cage is due to the nature of the development of the thoracic skeleton. The thoracic vertebrae have a primaxial component that is derived from somitic mesoderm like the rest of the axial skeleton. This includes the axial vertebral elements as well as the proximal ribs. Unlike the rest of the axial skeleton, however, the thoracic skeleton also has an abaxial component – the sternum and sternal ribs, which are derived from the lateral plate mesoderm [254-256]. Thus, the phenotypes in the thoracic region must be interpreted with respect to the distinct derivation of the tissues that comprise this portion of the axial skeleton.

In order to more completely understand how *Hox* genes pattern the vertebrate axial skeleton, including the rib cage, we have generated triple paralogous mutants in the *Hox5* and *Hox6* group genes as well as quadruple paralogous mutants in the *Hox9* group genes and characterized their phenotypes in the axial skeleton. We have also examined and compared the complete axial phenotype of the *Hox10* triple mutants and the *Hox11* triple mutants with the newly generated paralogous mutant groups. Each set of the paralogous mutants demonstrates functional redundancy in axial patterning and *Hox5*, *Hox6*, and *Hox9* paralogous mutants display dramatic effects on rib cage morphology. Anterior homeotic transformations occur in distinct AP domains in the somite-derived primaxial skeleton for each set of paralogous mutants and these defects demonstrate clear colinearity. While the AP boundaries of the vertebral transformations for each adjacent set of paralogous mutants overlap considerably, each paralogous mutant group imparts unique morphologies to the overlapping regions. Thus, the simplest interpretation of posterior prevalence in which the next-most posterior *Hox* group is functionally dominant over the more anterior group is not supported by these results. Further, the lateral plate-derived abaxial phenotypes in these mutants overlap almost completely and these phenotypes are not colinear, suggesting an independent role for *Hox* genes in patterning the lateral plate-derived axial skeleton.

Materials and methods

Mutant animals in the *Hox5*, *Hox6*, and *Hox9* paralogous colonies were generated using standard genetic crosses [238, 239, 249-252, 257]. Skeletal preparations were performed on E18.5 embryos throughout the study. *Hox10* and *Hox11* mutants were generated as described previously [245].

Mouse embryos were skinned and eviscerated, fixed for four days in 95% ethanol, and prepared by alkaline digestion before staining with alcian blue 8GX for cartilage and alizarin red S for ossified bone. Embryos were then dissected and photographed in 97% glycerol [245].

Embryos were genotyped using PCR and the results were analyzed on agarose gels. For *Hox5*, *Hox6* and *Hox9* paralogous genes, analyses were conducted using 12.5µl reactions with the following conditions: 32 cycles of 94°C for 30 seconds, 64°C for 30 seconds, and 72°C for 30 seconds. Primers for each genotype are detailed in Supporting On-Line Table 1. Genotyping for *Hox10* and *Hox11* mutants were as described previously [245].

In situ hybridization analyses were performed as published previously [25, 258]. The *Hoxd11* probe was previously published [34]. The *Hoxb6* probe and the *Neof* probe were generated using PCR amplification. T3 sites were incorporated into the reverse primers, and the PCR product was used in an *in vitro* transcription reaction to produce DIG-labeled RNA probes. Sequences used for probe generation can be found in Supplemental On-Line Table 1.

Results

Whole skeletal analyses of the *Hox5*, *Hox6* and *Hox9* paralogous mutants at E18.5 reveal patterning defects throughout the rib cage. *Hox5* and *Hox6* mutants have shortened sternums and are missing a complete first rib (Figure 1A, B). In *Hox5* mutants, an eighth rib attaches to the sternum (Figure 1A, E), and fusions are observed in the cervical vertebrae (black arrows, Figure 1A). In *Hox9* quadruple mutants, the first rib forms but does not always attach to the sternum. Growth of the posterior ribs is abnormal and rib attachment to the sternum continues past T7 to T13 or 'T14'. Additionally, four vertebrae posterior to T13 form ribs (Figure 1D and data not shown).

A ventral view of the intact rib cage (Figure 1E-H) demonstrates the sternal defects in the three sets of mutants. *Hox5* mutants are missing the manubrium, and the second rib often fuses with the third before attaching to the sternum (Figure 1E). The clavicles are attached by connective tissue to the rib cage, but do not articulate with it directly (green asterisk, Figure 1E). In the *Hox6* mutants, distal rib fusions are seen from T2 to T4, the sternabrae are poorly formed or missing, and the xiphoid process is reduced or absent (orange asterisk, Figure 1F). *Hox9* mutants exhibit distal rib fusions of the anterior-most ribs, and extensive growth and fusion of extra posterior ribs to the sternum (Figure 1H). Distinct sternabrae do not form. Rather, the sternum is ossified and mispatterned along its entire AP length. From views of the whole skeleton, defects are apparent throughout much of the rib cage in each set of mutants, but colinear defects are not immediately apparent.

Appendix Figure 1

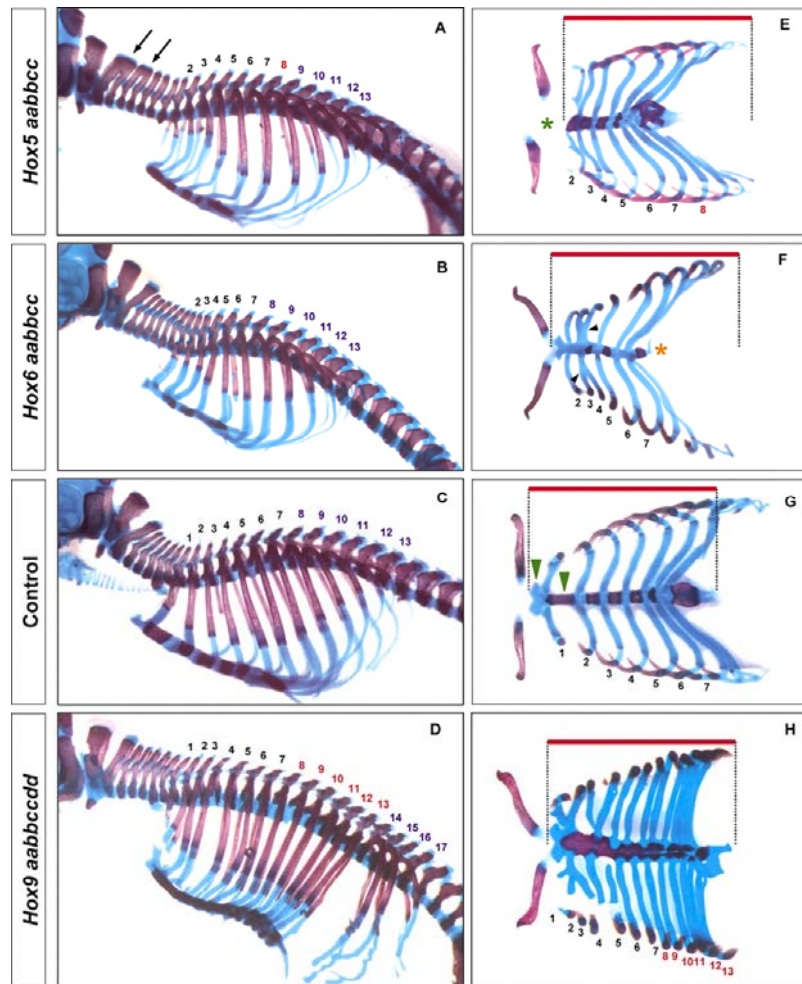


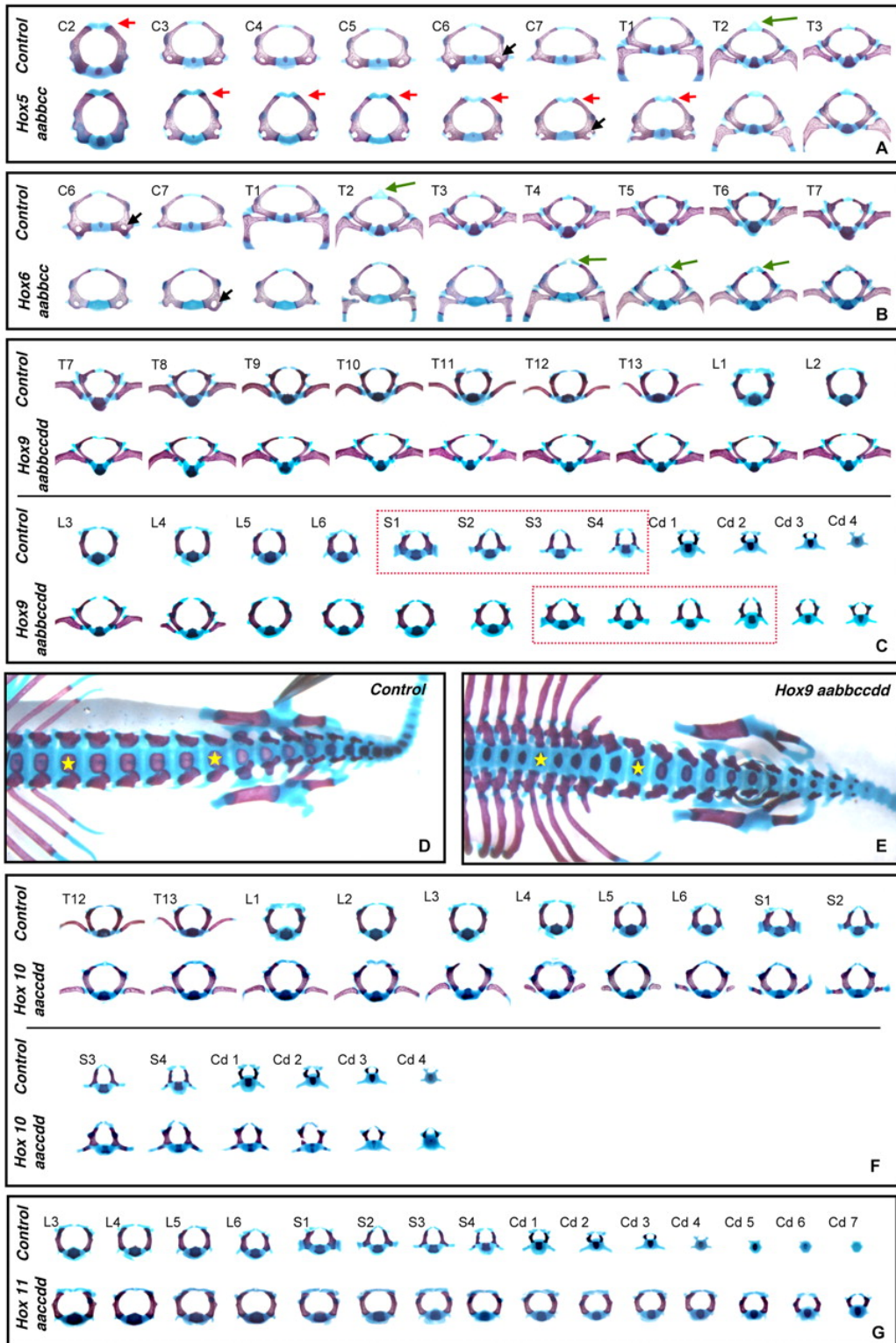
Figure 1. Whole skeletal phenotypes from *Hox5*, *Hox6* and *Hox9* paralogous mutant mice. Lateral and ventral views of the rib cages of *Hox5* (A, E), *Hox6* (B, F), wild-type (C, G) and *Hox9* (D, H) paralogous mutant mice, at embryonic day 18.5 (E18.5). In panels showing a lateral view (A through D), all vertebrae having visible ribs are numbered, whereas in panels showing a ventral view (E through H) only those that articulate with the sternum are numbered. The rib cages in panels E through H are intact (white paper inside the rib cage hides the dorsal aspects of the rib cages). The red bar in panels E through H provides a size reference for the length of the sternum. Black numbers indicate ribs that normally connect with the sternum, red numbers indicate extra ribs connecting to the sternum and blue numbers indicate floating ribs. Black arrows in panel A mark fused cervical vertebrae. The green asterisk in panel E marks connective tissue in place of missing manubrium and first sternabra. The orange asterisk in panel F denotes missing xiphoid process. Green arrowheads in panel G denote wild-type manubrium and first sternabra.

Upon dissection and examination of individual vertebral elements, it is apparent that the somite-derived, primaxial skeletal defects occur with distinct AP boundaries for each of the three sets of paralogous mutants. In *Hox5* mutants, C3 through T2 demonstrate anterior homeotic transformations (Figure 2A). C3 through T1 in the *Hox5* mutants display characteristics normally associated with C2, the axis. Notably, the dorsal cartilage is thickened and forms a distinct curvature at the top of the vertebra (red arrows, Figure 2A) and the rounded shape of the vertebral elements is maintained. The anterior projection that normally forms on T2 (green arrow, Figure 2A) does not form completely, but appears similar to controls by T3. The vertebral foramina extend beyond the normal posterior limit of C6 to C7 (black arrow, Figure 2A) and ribs initiate but do not extend on T1 (100% penetrance).

Anterior homeotic transformations of the primaxial elements in the *Hox6* mutants, in contrast, begin at C6 and continue through T6 (Figure 2B). C7 shows a continuation of the vertebral foramina as in the *Hox5* mutants (Figure 2B, black arrow). T1, however, has no partial rib formation, appearing identical to C7 in controls (100% penetrance). The morphology of the first three thoracic vertebral bodies are similar to cervical vertebrae, and the anterior projection normally found on T2 is not apparent until T4 and continues through T6 (Figure 2B, green arrows). Importantly, the posterior thoracic, lumbar and sacral skeleton is completely normal in appearance and position in both *Hox5* and *Hox6* paralogous mutants.

Figure 2. Anterior homeotic transformations of vertebral elements in *Hox5*, *Hox6*, *Hox9*, *Hox10* and *Hox11* paralogous mutants. Anterior views of individual vertebrae from controls (top row) and mutants (bottom row) for each set of paralogous mutants for *Hox5* (A), *Hox6* (B), *Hox9* (C), *Hox10* (F), *Hox11* (G). The position of each vertebra in controls is indicated by a C (cervical), T (thoracic), L (lumbar), S (sacral), or Cd (caudal), followed by a number identifying its position in each region. Vertebral elements anterior and posterior to those shown in the figure appear identical to controls. Dorsal views of the control (D) and a *Hox9* quadruple mutant (E) axial skeleton. In the control (D), the sacrum is immediately caudal to six lumbar vertebrae (which are indicated by yellow stars on L1 and L6). In the *Hox9* mutant (E), the lumbar region is extended by two vertebral elements. The yellow stars in Panel E mark control positions of the first and sixth lumbar vertebrae.

Appendix Figure 2



Primaxial defects in the *Hox9* quadruple mutants evidence anterior homeotic transformations throughout the posterior thoracic skeleton and into the lumbar region (Figure 2C). The morphology of T8 through L2 displays transformations to a T7-like phenotype. By L5, the axial skeleton has resumed normal patterning. However, unlike other *Hox* paralogous mutants (*Hox5* and *Hox6* above, and *Hox7*, *Hox8*, *Hox10* and *Hox11* [240, 245, 253]), the axial skeletons of the *Hox9* mutants posterior to the observed transformations are shifted caudally by two vertebral segments. The vertebra at the level of L5 in the *Hox9* mutants looks indistinguishable from the L3 in controls, and normal patterning continues posterior to this element, but offset by two vertebral elements (Figure 2C). Dorsal views of whole skeletons show the shift of the axial skeleton posterior to the anterior homeotic transformations (Figure 2D and E). Yellow stars indicate the normal position for L1 and L6. Note the posterior shift of the sacrum, thus displacement of pelvic attachment in the *Hox9* quadruple mutant. Nonetheless, the *Hox9* mutants have an average of two less caudal vertebrae than controls, so the total number of vertebrae formed is unchanged in these animals.

As the posterior region of the defects in the quadruple *Hox9* mutants demonstrates extra rib formation on the first four lumbar vertebrae, we compared the individual vertebral phenotypes of these animals with those from the *Hox10* triple mutants, which we previously reported to have rib formation on all lumbar vertebrae [245]. In *Hox10* triple mutants, rib formation is seen on all six lumbar vertebrae and even the sacral vertebrae show conversion of the sacral lateral

processes to rib-like outgrowths (Figure 2F). However, the shape of the lumbar vertebral elements in the *Hox10* mutants looks similar to lumbar vertebrae in controls, and the rib projections on all lumbar vertebrae in *Hox10* mutants are quite small, much like the most posterior thoracic vertebrae. In contrast, in *Hox9* quadruple mutants, the early lumbar elements that have rib projection have vertebral bodies that appear morphologically similar to more anterior thoracic vertebrae and the rib projections on these elements are very long and also appear similar to more anterior thoracic vertebrae (compare Figures 2C and 2F). Thus, while the phenotype of rib outgrowth occurs in the first four lumbar vertebrae of both *Hox9* and *Hox10* paralogous mutants, these phenotypes are not identical, but rather represent phenotypes from different levels of the thoracic vertebrae.

Individual vertebral elements from the *Hox11* triple mutant animals allow a comparison of the overlapping sacral phenotypes between the *Hox10* mutants and *Hox11* mutants. Both mutants demonstrate clear phenotypes throughout the sacral region, but while the *Hox10* mutants show primarily a conversion of the normal lateral processes to those of a thoracic or rib-like character (Figure 2F), the *Hox11* mutants show a transformation of this entire region to a lumbar-like phenotype (Figure 2G). Again, the morphological changes associated with the sacral vertebrae in these two sets of mutants are quite distinct.

Hox5, *Hox6* and *Hox9* mutants all have smaller rib cages than controls. As the size of the rib cage is a product of contributions from both the somite-derived, primaxial vertebral bodies and proximal ribs, as well as the lateral plate-derived,

abaxial sternal skeleton, thoracic elements with the ribs intact were examined. In *Hox5* mutants (Figure 3A, left column), T1 has incomplete rib projections and ribs from T2 extend but often do not reach the sternum (64%). Yet the primaxial vertebrae and rib angles are largely normal posterior to T1, suggesting the smaller rib cage is due primarily to the severe defects in the lateral plate-derived sternum. In contrast, the *Hox6* mutants show significant defects in the somite-derived, thoracic vertebral elements as well as in the sternum. Anterior homeotic transformations of the rib projections in the *Hox6* mutants extend from T2 through T6 (Figure 3A, right column). Red arrows show that T2 through T4 have proximal rib angles similar to those of T1 in control skeletons. These defects, along with the severe defects in the lateral plate-derived sternal skeleton (Figure 1B, F) result in the large decrease in the size of the rib cages in *Hox6* mutants.

The somite-derived vertebrae from the anterior thoracic skeleton (T1 – T7) of the *Hox9* mutants are patterned normally although fusions at the distal portion of the first three ribs are observed (Figure 3B and 1H). Anterior homeotic transformations of the somite-derived skeleton are seen from T8 through L4. Unlike controls, ribs from T8 through T13 in this *Hox9* mutant continue to grow distally and attach to the sternum, similar to more anterior vertebrae (Figure 3B). Despite many extra fused ribs, the rib cage is smaller than controls due to apparent growth constraints from crowding at the sternum.

Redundancy continues to play a key role in understanding *Hox* function. *Hox5* and *Hox6* mutants possessing any combination of five of the possible six

Appendix Figure 3

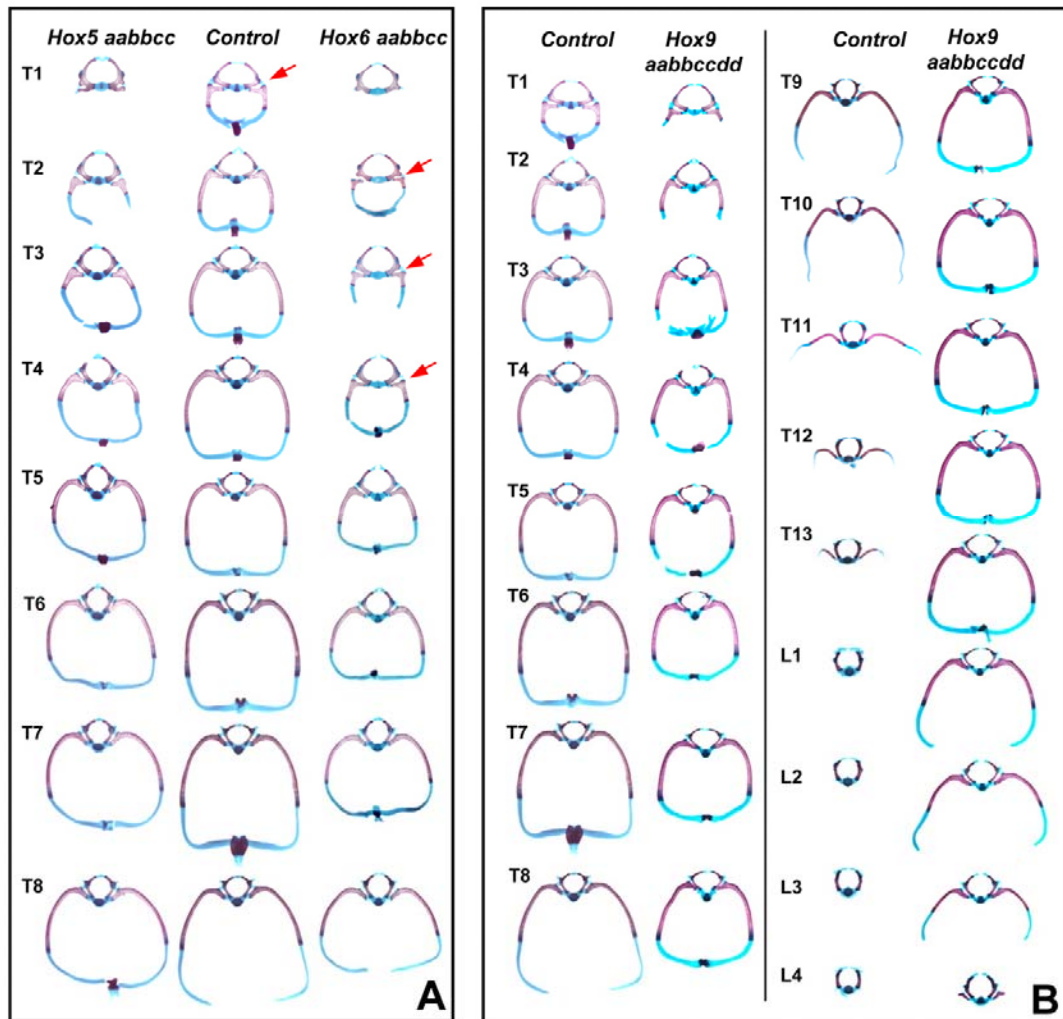


Figure 3. Rib and sternal abnormalities in the *Hox5*, *Hox6* and *Hox9* paralogous mutants. (A) Individual skeletal elements, dissected with ribs attached, from the upper thoracic region of *Hox5* paralogous mutant, wild type and *Hox6* paralogous mutant mice. The first column shows the 1st through 8th thoracic elements from a *Hox5* mutant mouse (the ventral ribs on T2 in this animal are incompletely formed). The second column depicts the same elements from a wild-type control mouse. The elements in the third column are from a *Hox6* mutant mouse (T3 in this animal was fused with T4, and so appears incompletely formed). Red arrows denote the rib angle of control T1 and the phenotypic similarity in *Hox6* mutant T2 through T4. (B) Individual skeletal elements, with ribs attached, from the thoracic and lumbar regions of a *Hox9* paralogous mutant mouse (right column) are compared to those of a wild type control (left column).

mutant alleles are much less affected than the paralogous mutants (Figure 4A-C). Similarly, the 7-allele *Hox9* mutant in Figure 4D has a much less severe phenotype, with only two extra ribbed vertebrae, T8 and T9, attached to the sternum.

Because of the overlap in phenotypes between the *Hox5* and *Hox6* paralogous mutants, we generated trans-triple heterozygous embryos (*5AaBbCc/6AaBbCc*) to examine whether *Hox5* and *Hox6* paralogous groups are functionally equivalent in their respective patterning roles. Trans-triple heterozygotes have a less severe phenotype than either *Hox5* or *Hox6* triple mutants in both the primaxial and abaxial skeleton despite containing the same number of mutant alleles (Figure 4A, E), demonstrating that the two paralogous groups do not function redundantly in axial patterning.

Phenotypes in overlapping regions of adjacent paralogous mutants are distinct from one another in all of the cases we have examined to date, suggesting the phenotypes are not due to changes in the expression of more posterior *Hox* paralogous genes. To test for this possibility, we performed *in situ* hybridization to determine whether the anterior limit of expression of the next most posterior group *Hox* genes are perturbed in *Hox* paralogous mutants. In *Hox5* triple mutants the expression of *Hoxb6* is observed at the same anterior limit as controls at E11.5 (Figure 5A, B). Similarly, in more posterior regions of the embryo, the anterior limit of *Hoxd11* expression in *Hox10* triple mutants is also unchanged compared to controls (Figure 5C, D). This data supports the

Appendix Figure 4

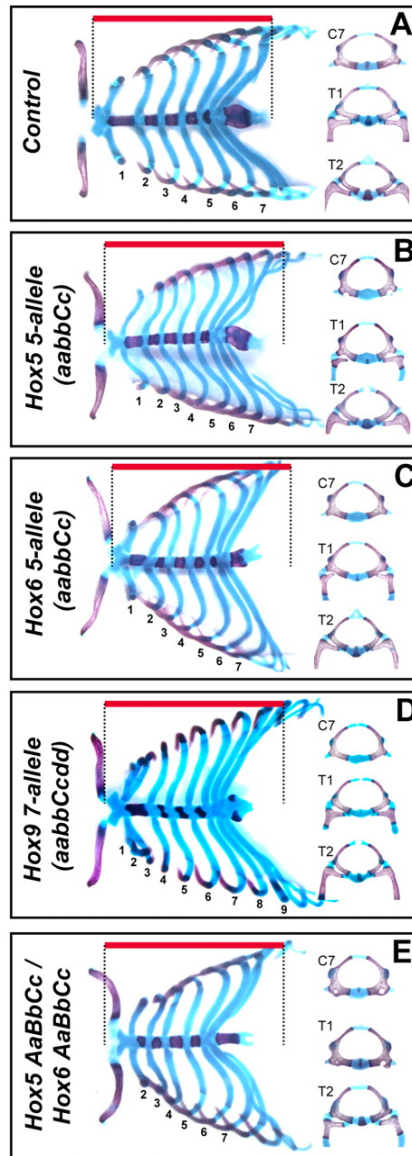
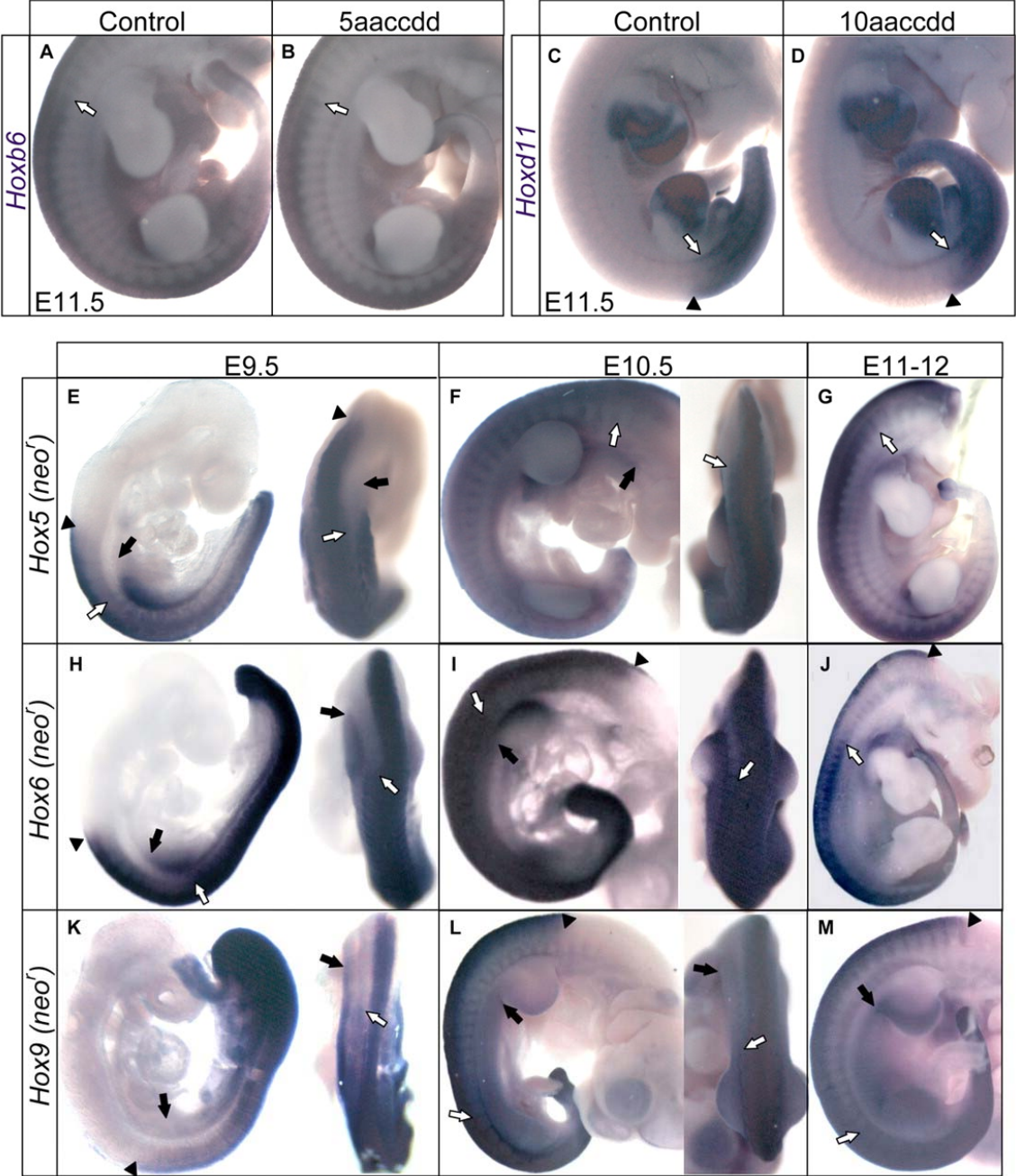


Figure 4. Defects in the rib cage of *Hox* mutant mice show functional redundancy. Ventral views of the skeletal phenotypes from wild-type (A), *Hox5* 5-allele (B), *Hox6* 5-allele mice (C), *Hox9* 7-allele mice (D) and *Hox5/Hox6* trans-triple heterozygous mice (E). Numbers below the rib cage in each panel indicate the thoracic vertebrae with ribs that fuse to the sternum. The red bar in each panel is included as a size reference. Note that any combination of five mutant alleles of *Hox5* or *Hox6* (*Aabbcc*, *aaBbcc* and *aabbCc*) shows very similar phenotypes to the ones shown in Panels D and E. In the *Hox9* paralogous group, however, *Hoxc9* contributes more strongly to extra sternal rib growth and fusion than the other *Hox9* genes (data not shown).

Figure 5. *Hox* expression during axial patterning. The anterior boundary of *Hoxb6* expression at E11.5 is the same in control (A) and *Hox5* paralogous mutant mice (B). The anterior boundary of *Hoxd11* expression in control (C) and *Hox10* paralogous mutants are also equivalent. In Panels E through M, an ISH probe to *Neof* has been used to demonstrate the anterior expression boundaries of the entire paralogous group in triple heterozygous animals (in the case of *Hox5* and *Hox6* embryos) or quadruple heterozygous mutants (for *Hox9* embryos), all of which have no phenotype. (Each mutant allele has *Neof* inserted into the *Hox* coding sequence.) Somite anterior expression limits are marked with a white block arrow and lateral plate anterior expression limits are marked with a black block arrow. (The anterior expression limit for the neural tube, marked with a black arrowhead in these embryos, is often far anterior to the somite expression boundary as published for the individual *Hox* genes referenced in the text.) In panels E, F, H, I, K and L, embryos are shown in lateral and dorsal view. In panels G, J and M, embryos are shown in lateral view only.

Appendix Figure 5



conclusion that adjacent *Hox* paralogous genes are co-expressed and have distinct functions in overlapping AP regions.

Further, the rib cage phenotypes of the *Hox5*, *Hox6* and *Hox9* paralogous mutants demonstrate differential phenotypic boundaries for the somite-derived vertebral elements and the lateral plate-derived sternum. The genetic results suggest that expression and function in the somites may be distinct from expression and function in the lateral plate mesoderm. To ascertain whether expression levels correlate with the genetic results, we examined the expression pattern of these paralogous group genes at several developmental stages. We found that *Hox* expression is dynamic during these early developmental time points, particularly in the lateral plate. The anterior expression boundary in the somites of the *Hox5* paralogous group genes appear to be at approximately the level of the ninth developing somite at E9.5 (Figure 5E, white arrow), with the lateral plate expression limit slightly anterior to this, including in the early limb bud. (Figure 5E, black arrow). By E10.5, somite staining can be visualized more anteriorly, with the expression limit at somite five (Figure 5F, white arrow). Lateral plate staining can still be seen along the entire lateral plate anterior to the forelimb and between the forelimb and hindlimb, consistent with sternal defects throughout the AP length of the sternum (Figure 5F). By E12.5, intense staining in the somite can be detected up to an anterior limit at somite 6/7 (Figure 5G, white arrow), although fainter staining can be detected in two anterior somites. This expression in somites correlates with the observed genetic phenotypes beginning at C3, and is also in complete agreement with reports of *Hoxa5*, *Hoxb5*

and *Hoxc5* somite expression boundaries, which were examined previously at the later time point [259, 260]. Further, lateral plate expression cannot be clearly detected after E11.5. It cannot be discerned whether expression of these genes are absent or has just fallen to very low levels.

The anterior limits of somitic expression for *Hox6* appear to be more similar in all of the stages examined, approximately at the somite 12 boundary (Figure 5H – J, white arrows). This is consistent with previous reports for these genes at E12.5 and E13.5 time points [251, 259, 261], and also consistent with the genetic phenotypes reported here which begin at C6. Lateral plate expression is visible from the forelimb area to more posterior regions through E10.5 (Figure 5H, I, black arrows), but expression decreases below background at later developmental stages, similar to the observation for the *Hox5* genes. This suggests that the contribution from *Hox5* and *Hox6* genes to patterning the sternum is an early developmental event, but functionally significant expression levels that are too low to detect cannot be ruled out without conditional functional analyses.

The expression profile of *Hox9* during these developmental time points differs significantly from *Hox5* and *Hox6*. At E9.5, expression is intense in the tailbud and becomes fainter more anteriorly with no clearly established anterior boundary. Expression in the lateral plate mesoderm reaches levels just posterior to the developing heart (black arrow, Figure 5K). By E10.5, a boundary at somite 23 can be seen in the paraxial mesoderm (white arrow), but the lateral plate expression remains intense far anterior to this, in the entire region between the

forelimbs and hindlimbs (black arrow, Figure 5L). The somitic boundary at somite 23 becomes even sharper by E11.5, in agreement with previous reports on these genes (white arrow, Figure 5M [231, 259, 262, 263]). (*Hoxd9* has been reported to have more posterior somitic boundaries, but this would be masked by more anterior expression of the remaining three paralogs [231, 259]). Unlike the *Hox5* and *Hox6* genes, strong *Hox9* expression persists in the lateral plate at this and later stages (Figure 5M and data not shown). This expression pattern is consistent with the possibility that later expression in the lateral plate is important for *Hox9*-mediated repression of growth and attachment of posterior ribs to the sternum. Consistent with this, the anterior most somitic boundary of *Hox9* expression is at somite levels well below that of the thoracic skeleton where distal rib phenotypes occur, with the exception of the E9.5 time point during early boundary formation (Figure 5K, [259, 262]). Clearly, conditional genetic analyses will be required to understand the contributions to sternal phenotype.

Discussion

Comparisons of the phenotypes in the paralogous mutant groups are diagrammed in Figure 6 and lead to several important conclusions about the nature of the *Hox* code in vertebrate axial patterning. First, loss of paralogous *Hox* function consistently exhibits functional redundancy among *Hox* paralogous genes, and all paralogous mutant phenotypes in the primaxial skeleton can be clearly categorized as anterior homeotic transformations. As previously shown for the *Hox10* and *Hox11* paralogous genes, leaving just one wild-type allele in

the absence of five alleles (in the case of *Hox5*, *Hox6*, *Hox10* and *Hox11*) or seven alleles (in the case of the *Hox9* genes) results in a much less severe phenotype than removing all functional copies in a given paralogous group. Further, these phenotypes show clear colinearity with more anteriorly expressed *Hox* genes affecting more anterior regions of the somite-derived axial skeleton and more posterior *Hox* genes affecting increasingly posterior regions.

While anterior homeotic transformations in each paralogous mutant have distinct AP boundaries, the vertebrae that exhibit transformations in adjacent paralogous mutant groups significantly overlap (Figure 6, red-shading indicates the AP region demonstrating anterior homeotic transformations; overlapping phenotypic regions between adjacent paralogous mutants are highlighted in yellow). Within the overlapping affected regions in adjacent paralogous mutants, however, the observed phenotypes are distinct, suggesting that each *Hox* paralogous group imparts unique morphological characteristics to the vertebrae. For example, whole skeletons of both *Hox5* and *Hox6* mutants each appear to be missing the first rib. However, inspection of the T1 element shows that *Hox5* mutants have transformations of the dorsal aspects of this element towards a C2 fate with small ribs initiating with complete penetrance (12 of 12, Figure 2A). T1 from *Hox6* mutants, in contrast, show an anterior transformation to a C7 phenotype, with no likeness to C2 and no indication of rib initiation (11 of 11, Figure 2B). In another example, both *Hox10* and *Hox11* paralogous mutants display phenotypes in all sacral vertebrae. While loss of *Hox10* function results in a conversion of the sacral lateral wings to rib-like projections that fuse laterally,

Appendix Figure 6

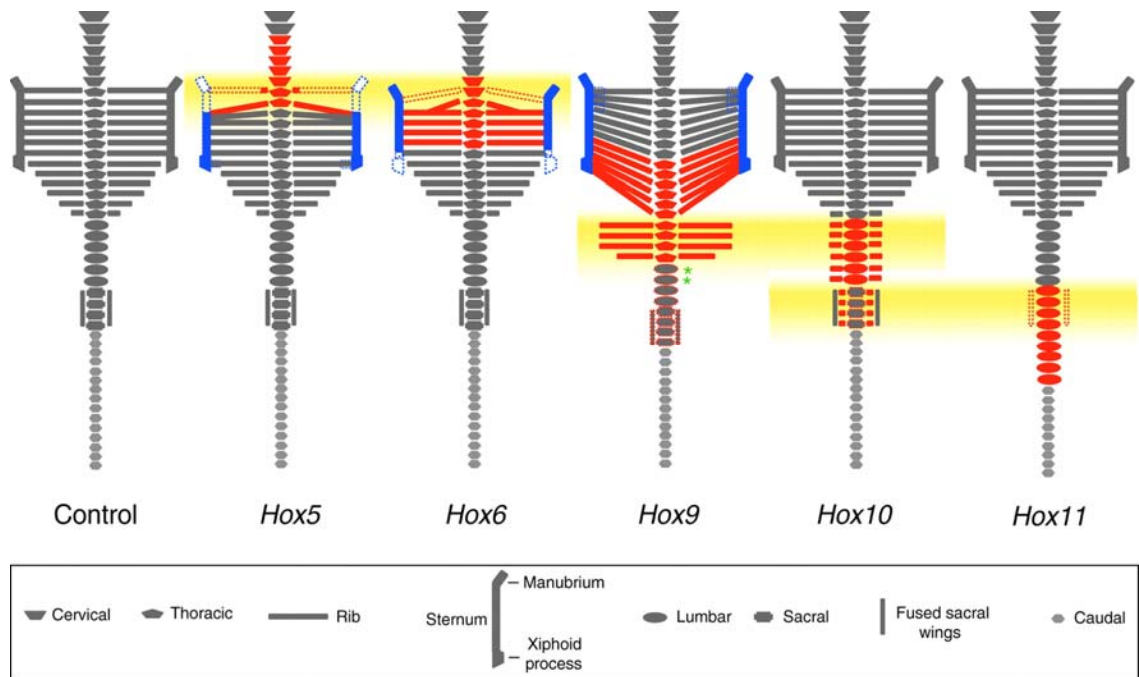


Figure 6. Schematic representation of paralogous *Hox* axial skeleton phenotypes. Somite-derived, primaxial skeletal elements that exhibit anterior homeotic transformations in paralogous mutants are shaded red. Lateral plate-derived, abaxial structures affected in paralogous mutants are shaded blue. Note that *Hox5*, *Hox6* and *Hox9* mutant phenotypes are offset in their AP extent for defects in the somite-derived primaxial (red) and lateral plate-derived abaxial (blue) skeleton. The yellow shading highlights somite-derived AP regions that are affected in adjacent paralogous mutant groups. In each case, the overlapping regions of phenotype display distinct vertebral morphologies for each paralogous mutant. The green asterisks in the *Hox9* mutant panel reflect the posterior shift of the axial skeleton. Mice normally possess 28-30 caudal vertebrae. Only 15 are represented in this schematic for simplicity. Despite changes in the number of caudal vertebrae in *Hox9* and *Hox11* paralogous mutants, the same average total numbers of vertebrae are present in all of the paralogous mutants depicted in this diagram and are the same as in control animals.

loss of *Hox11* results in transformation of sacral vertebrae to a lumbar-like morphology with no sacral wing projections and no lateral fusions (Figure 2F, G and [245]). We also show that removal of the function of an entire paralogous groups does not significantly affect the expression of the next most posterior group genes (Figure 5A-D).

The current data strongly support the idea that the genetic function of each of the paralogous groups of *Hox* genes in axial patterning is distinct, and that the 'Hox code' is a combination of the unique morphological contributions imparted by each of the two or more paralogous groups functioning in a given AP region. This data is not in simple agreement with the posterior prevalence model, which has held that the patterning information at a given AP region relies on a single *Hox* gene or paralogous group [237] and that patterning information, in the cases of overlapping expression of two or more *Hox* genes (or paralogous groups), is provided by the more posteriorly acting gene(s) [235, 236]. However, it is also clear from these genetic experiments that the morphology of the axial skeleton regains wild-type patterns posterior to the affected region. Therefore, all of the *Hox* genes expressed in the posterior region of the early, developing embryo do not function in axial patterning. As little or no information exists regarding when or how *Hox* genes function at a mechanistic level to impart vertebral morphologies, the significance of the early, nested *Hox* expression pattern is not clear. Unequivocal experiments to test the molecular nature of the 'Hox code' and the model of posterior prevalence await the discovery of confirmed downstream targets in *Hox*-regulated axial patterning, knowledge of when *Hox*-

regulated axial patterning is imparted during embryogenesis, and details of Hox protein expression during critical axial patterning events.

This study also demonstrates that *Hox* genes are critical for patterning the lateral plate-derived, abaxial skeleton (the sternum and sternal ribs), that *Hox* gene function in the abaxial skeleton is independent of somite-derived patterning, and that this patterning is not colinear. Formation of the manubrium appears to be uniquely a *Hox5* regulated process (Figure 1E), however, the *Hox5*, *Hox6* and *Hox9* mutants all have patterning defects along the AP length of the sternum, inconsistent with a strictly colinear contribution to patterning this lateral plate-derived structure (Figure 6, blue-shaded abaxial defects). Further, defects are found with complete penetrance in first rib and sternabra formation in *Hox5*, *Hox6*, and *Hox9* paralogous mutants, *Hox5/Hox6* trans-triple heterozygotes, and *Hox7* and *Hox8* paralogous mutants [240, 253], as well as with incomplete penetrance in many of the *Hox5* through *Hox9* single mutant animals and *Hoxb5/Hoxb6* trans-heterozygotes [238, 249, 251, 252]. Taken together, the growth and formation of the first rib and sternabra is particularly sensitive to loss of *Hox5* through *Hox9* function. This phenotype is likely due to patterning disruptions in the lateral plate mesoderm that do not obey the colinear contribution to patterning that is clear in the somite-derived skeleton. Understanding the molecular details regarding *Hox* gene function in patterning the lateral plate-derived portion of the thoracic skeleton will require conditional analyses that can distinguish between the patterning contributions from these two distinct tissues in the development of the rib cage.

The combined genetic data on *Hox* paralogous phenotypes in the axial skeleton demonstrate clearly that *Hox* genes do not contribute to the total number of vertebral elements formed. Combined results from the *Hox4* triple mutants and the *Hox5* through the *Hox11* paralogous mutants ([240, 245, 253] and this report) demonstrate that while the morphology of AP-restricted regions display defects throughout the axial skeleton, the number of elements do not change.

In conclusion, the data reported herein contribute significantly to our genetic understanding of *Hox* function in vertebrate axial patterning. Loss of *Hox* paralogous function results in anterior homeotic transformations throughout the somite-derived axial skeleton, including the thoracic skeleton. The lateral plate-derived skeleton appears to be patterned independently from the somite-derived skeleton and lateral plate axial patterning is not colinear. By establishing that consistent genetic mechanisms operate in vertebrate axial patterning, it is hopeful that this framework will allow us to examine the molecular details of *Hox* function in this system.

Acknowledgments

This manuscript was written by Daniel C. McIntyre, Sabita Rakshit, Alisha R. Yallowitz, Luke Loken, Lucie Jeannotte, Mario R. Capecchi, Deneen M. Wellik. It was published August of 2007 in *Development*, Volume 134, Number 16, Pages 2981-2989.

We would like to thank J. Fallon, A. Boulet, and B. Bisgrove for critically reviewing previous versions of the manuscript. This work was supported in part by Research Grant No. 5-FY05-48 from the March of Dimes Birth Defects Foundation and by a University of Michigan's Organogenesis predoctoral fellowship award, T32-HD007505 (AY).

REFERENCES

1. Kaufman, T.C., M.A. Seeger, and G. Olsen, *Molecular and genetic organization of the antennapedia gene complex of Drosophila melanogaster*. *Adv Genet*, 1990. **27**: p. 309-62.
2. Sanchez-Herrero, E., et al., *Genetic organization of Drosophila bithorax complex*. *Nature*, 1985. **313**(5998): p. 108-13.
3. Gilbert, S.F., *Developmental biology*. 8th ed. 2006, Sunderland, Mass.: Sinauer Associates, Inc. Publishers. xviii, 817 p.
4. Lewis, E.B., *A gene complex controlling segmentation in Drosophila*. *Nature*, 1978. **276**(5688): p. 565-70.
5. Gehring, W.J., *Homeo boxes in the study of development*. *Science*, 1987. **236**(4806): p. 1245-52.
6. Gehring, W.J., *Exploring the homeobox*. *Gene*, 1993. **135**(1-2): p. 215-21.
7. Schneuwly, S., R. Klemenz, and W.J. Gehring, *Redesigning the body plan of Drosophila by ectopic expression of the homoeotic gene Antennapedia*. *Nature*, 1987. **325**(6107): p. 816-8.
8. Lappin, T.R., et al., *HOX genes: seductive science, mysterious mechanisms*. *Ulster Med J*, 2006. **75**(1): p. 23-31.
9. Holland, P.W. and T. Takahashi, *The evolution of homeobox genes: Implications for the study of brain development*. *Brain Res Bull*, 2005. **66**(4-6): p. 484-90.
10. Hueber, S.D. and I. Lohmann, *Shaping segments: Hox gene function in the genomic age*. *Bioessays*, 2008. **30**(10): p. 965-79.
11. Sharkey, M., Y. Graba, and M.P. Scott, *Hox genes in evolution: protein surfaces and paralog groups*. *Trends Genet*, 1997. **13**(4): p. 145-51.
12. Krumlauf, R., *Hox genes in vertebrate development*. *Cell*, 1994. **78**(2): p. 191-201.
13. Zakany, J. and D. Duboule, *Hox genes in digit development and evolution*. *Cell Tissue Res*, 1999. **296**(1): p. 19-25.
14. Pearson, J.C., D. Lemons, and W. McGinnis, *Modulating Hox gene functions during animal body patterning*. *Nat Rev Genet*, 2005. **6**(12): p. 893-904.
15. Chen, F. and M.R. Capecchi, *Paralogous mouse Hox genes, Hoxa9, Hoxb9, and Hoxd9, function together to control development of the mammary gland in response to pregnancy*. *Proc Natl Acad Sci U S A*, 1999. **96**(2): p. 541-6.
16. Chen, F., J. Greer, and M.R. Capecchi, *Analysis of Hoxa7/Hoxb7 mutants suggests periodicity in the generation of the different sets of vertebrae*. *Mech Dev*, 1998. **77**(1): p. 49-57.

17. Condie, B.G. and M.R. Capecchi, *Mice with targeted disruptions in the paralogous genes hoxa-3 and hoxd-3 reveal synergistic interactions.* Nature, 1994. **370**(6487): p. 304-7.
18. Davis, A.P., et al., *Absence of radius and ulna in mice lacking hoxa-11 and hoxd-11.* Nature, 1995. **375**(6534): p. 791-5.
19. Horan, G.S., et al., *Mutations in paralogous Hox genes result in overlapping homeotic transformations of the axial skeleton: evidence for unique and redundant function.* Dev Biol, 1995. **169**(1): p. 359-72.
20. Horan, G.S., et al., *Compound mutants for the paralogous hoxa-4, hoxb-4, and hoxd-4 genes show more complete homeotic transformations and a dose-dependent increase in the number of vertebrae transformed.* Genes Dev, 1995. **9**(13): p. 1667-77.
21. Rossel, M. and M.R. Capecchi, *Mice mutant for both Hoxa1 and Hoxb1 show extensive remodeling of the hindbrain and defects in craniofacial development.* Development, 1999. **126**(22): p. 5027-40.
22. St-Jacques, B. and A.P. McMahon, *Early mouse development: lessons from gene targeting.* Curr Opin Genet Dev, 1996. **6**(4): p. 439-44.
23. Studer, M., et al., *Genetic interactions between Hoxa1 and Hoxb1 reveal new roles in regulation of early hindbrain patterning.* Development, 1998. **125**(6): p. 1025-36.
24. Wellik, D.M. and M.R. Capecchi, *Hox10 and Hox11 genes are required to globally pattern the mammalian skeleton.* Science, 2003. **301**(5631): p. 363-7.
25. Wellik, D.M., P.J. Hawkes, and M.R. Capecchi, *Hox11 paralogous genes are essential for metanephric kidney induction.* Genes Dev, 2002. **16**(11): p. 1423-32.
26. Zakany, J., et al., *Regulation of number and size of digits by posterior Hox genes: a dose-dependent mechanism with potential evolutionary implications.* Proc Natl Acad Sci U S A, 1997. **94**(25): p. 13695-700.
27. Maconochie, M., et al., *Paralogous Hox genes: function and regulation.* Annu Rev Genet, 1996. **30**: p. 529-56.
28. Kmita, M. and D. Duboule, *Organizing axes in time and space; 25 years of colinear tinkering.* Science, 2003. **301**(5631): p. 331-3.
29. Duboule, D. and P. Dolle, *The structural and functional organization of the murine HOX gene family resembles that of Drosophila homeotic genes.* EMBO J, 1989. **8**(5): p. 1497-505.
30. Gaunt, S.J., *Expression patterns of mouse Hox genes: clues to an understanding of developmental and evolutionary strategies.* Bioessays, 1991. **13**(10): p. 505-13.
31. Graham, A., N. Papalopulu, and R. Krumlauf, *The murine and Drosophila homeobox gene complexes have common features of organization and expression.* Cell, 1989. **57**(3): p. 367-78.
32. Wellik, D.M., *Hox patterning of the vertebrate axial skeleton.* Dev Dyn, 2007. **236**(9): p. 2454-63.

33. Dolle, P., et al., *Coordinate expression of the murine Hox-5 complex homoeobox-containing genes during limb pattern formation*. Nature, 1989. **342**(6251): p. 767-72.
34. Izpisua-Belmonte, J.C., et al., *Murine genes related to the Drosophila AbdB homeotic genes are sequentially expressed during development of the posterior part of the body*. EMBO J, 1991. **10**(8): p. 2279-89.
35. Boulet, A.M. and M.R. Capecchi, *Targeted disruption of hoxc-4 causes esophageal defects and vertebral transformations*. Dev Biol, 1996. **177**(1): p. 232-49.
36. Chisaka, O. and M.R. Capecchi, *Regionally restricted developmental defects resulting from targeted disruption of the mouse homeobox gene hox-1.5*. Nature, 1991. **350**(6318): p. 473-9.
37. Condie, B.G. and M.R. Capecchi, *Mice homozygous for a targeted disruption of Hoxd-3 (Hox-4.1) exhibit anterior transformations of the first and second cervical vertebrae, the atlas and the axis*. Development, 1993. **119**(3): p. 579-95.
38. Davis, A.P. and M.R. Capecchi, *Axial homeosis and appendicular skeleton defects in mice with a targeted disruption of hoxd-11*. Development, 1994. **120**(8): p. 2187-98.
39. Fromental-Ramain, C., et al., *Specific and redundant functions of the paralogous Hoxa-9 and Hoxd-9 genes in forelimb and axial skeleton patterning*. Development, 1996. **122**(2): p. 461-72.
40. Horan, G.S., et al., *Homeotic transformation of cervical vertebrae in Hoxa-4 mutant mice*. Proc Natl Acad Sci U S A, 1994. **91**(26): p. 12644-8.
41. Jeannotte, L., et al., *Specification of axial identity in the mouse: role of the Hoxa-5 (Hox1.3) gene*. Genes Dev, 1993. **7**(11): p. 2085-96.
42. Kostic, D. and M.R. Capecchi, *Targeted disruptions of the murine Hoxa-4 and Hoxa-6 genes result in homeotic transformations of components of the vertebral column*. Mech Dev, 1994. **46**(3): p. 231-47.
43. Le Mouellic, H., Y. Lallemand, and P. Brulet, *Homeosis in the mouse induced by a null mutation in the Hox-3.1 gene*. Cell, 1992. **69**(2): p. 251-64.
44. McIntyre, D.C., et al., *Hox patterning of the vertebrate rib cage*. Development, 2007. **134**(16): p. 2981-9.
45. Small, K.M. and S.S. Potter, *Homeotic transformations and limb defects in Hox A11 mutant mice*. Genes Dev, 1993. **7**(12A): p. 2318-28.
46. Suemori, H., N. Takahashi, and S. Noguchi, *Hoxc-9 mutant mice show anterior transformation of the vertebrae and malformation of the sternum and ribs*. Mech Dev, 1995. **51**(2-3): p. 265-73.
47. van den Akker, E., et al., *Axial skeletal patterning in mice lacking all paralogous group 8 Hox genes*. Development, 2001. **128**(10): p. 1911-21.
48. Manley, N.R. and M.R. Capecchi, *Hox group 3 paralogs regulate the development and migration of the thymus, thyroid, and parathyroid glands*. Dev Biol, 1998. **195**(1): p. 1-15.

49. Glover, J.C., *Correlated patterns of neuron differentiation and Hox gene expression in the hindbrain: a comparative analysis*. Brain Res Bull, 2001. **55**(6): p. 683-93.
50. Trainor, P.A. and R. Krumlauf, *Hox genes, neural crest cells and branchial arch patterning*. Curr Opin Cell Biol, 2001. **13**(6): p. 698-705.
51. Patterson, L.T. and S.S. Potter, *Hox genes and kidney patterning*. Curr Opin Nephrol Hypertens, 2003. **12**(1): p. 19-23.
52. Maeda, Y., V. Dave, and J.A. Whitsett, *Transcriptional control of lung morphogenesis*. Physiol Rev, 2007. **87**(1): p. 219-44.
53. Zakany, J. and D. Duboule, *The role of Hox genes during vertebrate limb development*. Curr Opin Genet Dev, 2007. **17**(4): p. 359-66.
54. Svingen, T. and K.F. Tonissen, *Hox transcription factors and their elusive mammalian gene targets*. Heredity, 2006. **97**(2): p. 88-96.
55. Ekker, S.C., D.P. von Kessler, and P.A. Beachy, *Differential DNA sequence recognition is a determinant of specificity in homeotic gene action*. EMBO J, 1992. **11**(11): p. 4059-72.
56. Gehring, W.J., et al., *Homeodomain-DNA recognition*. Cell, 1994. **78**(2): p. 211-23.
57. Peifer, M. and E. Wieschaus, *Mutations in the Drosophila gene extradenticle affect the way specific homeo domain proteins regulate segmental identity*. Genes Dev, 1990. **4**(7): p. 1209-23.
58. Chan, S.K., et al., *The DNA binding specificity of Ultrabithorax is modulated by cooperative interactions with extradenticle, another homeoprotein*. Cell, 1994. **78**(4): p. 603-15.
59. Mann, R.S. and M. Affolter, *Hox proteins meet more partners*. Curr Opin Genet Dev, 1998. **8**(4): p. 423-9.
60. Capovilla, M., M. Brandt, and J. Botas, *Direct regulation of decapentaplegic by Ultrabithorax and its role in Drosophila midgut morphogenesis*. Cell, 1994. **76**(3): p. 461-75.
61. Grieder, N.C., et al., *Synergistic activation of a Drosophila enhancer by HOM/EXD and DPP signaling*. EMBO J, 1997. **16**(24): p. 7402-10.
62. Ryoo, H.D. and R.S. Mann, *The control of trunk Hox specificity and activity by Extradenticle*. Genes Dev, 1999. **13**(13): p. 1704-16.
63. Ryoo, H.D., et al., *Regulation of Hox target genes by a DNA bound Homothorax/Hox/Extradenticle complex*. Development, 1999. **126**(22): p. 5137-48.
64. Ferretti, E., et al., *Hoxb1 enhancer and control of rhombomere 4 expression: complex interplay between PREP1-PBX1-HOXB1 binding sites*. Mol Cell Biol, 2005. **25**(19): p. 8541-52.
65. Ferretti, E., et al., *Segmental expression of Hoxb2 in r4 requires two separate sites that integrate cooperative interactions between Prep1, Pbx and Hox proteins*. Development, 2000. **127**(1): p. 155-66.
66. Moens, C.B. and L. Selleri, *Hox cofactors in vertebrate development*. Dev Biol, 2006. **291**(2): p. 193-206.

67. Popperl, H., et al., *Segmental expression of Hoxb-1 is controlled by a highly conserved autoregulatory loop dependent upon exd/pbx*. Cell, 1995. **81**(7): p. 1031-42.
68. Tumpel, S., et al., *Expression of Hoxa2 in rhombomere 4 is regulated by a conserved cross-regulatory mechanism dependent upon Hoxb1*. Dev Biol, 2007. **302**(2): p. 646-60.
69. Capellini, T.D., et al., *Pbx1/Pbx2 requirement for distal limb patterning is mediated by the hierarchical control of Hox gene spatial distribution and Shh expression*. Development, 2006. **133**(11): p. 2263-73.
70. Di Rosa, P., et al., *The homeodomain transcription factor Prep1 (pKnox1) is required for hematopoietic stem and progenitor cell activity*. Dev Biol, 2007. **311**(2): p. 324-34.
71. DiMartino, J.F., et al., *The Hox cofactor and proto-oncogene Pbx1 is required for maintenance of definitive hematopoiesis in the fetal liver*. Blood, 2001. **98**(3): p. 618-26.
72. Hisa, T., et al., *Hematopoietic, angiogenic and eye defects in Meis1 mutant animals*. Embo J, 2004. **23**(2): p. 450-9.
73. Selleri, L., et al., *Requirement for Pbx1 in skeletal patterning and programming chondrocyte proliferation and differentiation*. Development, 2001. **128**(18): p. 3543-57.
74. Brendolan, A., et al., *A Pbx1-dependent genetic and transcriptional network regulates spleen ontogeny*. Development, 2005. **132**(13): p. 3113-26.
75. Kim, S.K., et al., *Pbx1 inactivation disrupts pancreas development and in lpf1-deficient mice promotes diabetes mellitus*. Nat Genet, 2002. **30**(4): p. 430-5.
76. Dressler, G.R., *The cellular basis of kidney development*. Annu Rev Cell Dev Biol, 2006. **22**: p. 509-29.
77. Mauch, T.J., et al., *Signals from trunk paraxial mesoderm induce pronephros formation in chick intermediate mesoderm*. Dev Biol, 2000. **220**(1): p. 62-75.
78. Kuure, S., R. Vuolteenaho, and S. Vainio, *Kidney morphogenesis: cellular and molecular regulation*. Mech Dev, 2000. **92**(1): p. 31-45.
79. Sainio, K. and A. Raatikainen-Ahokas, *Mesonephric kidney--a stem cell factory?* Int J Dev Biol, 1999. **43**(5): p. 435-9.
80. Saxen, L. and H. Sariola, *Early organogenesis of the kidney*. Pediatr Nephrol, 1987. **1**(3): p. 385-92.
81. Cullen-McEwen, L.A., G. Caruana, and J.F. Bertram, *The where, what and why of the developing renal stroma*. Nephron Exp Nephrol, 2005. **99**(1): p. e1-8.
82. Levinson, R. and C. Mendelsohn, *Stromal progenitors are important for patterning epithelial and mesenchymal cell types in the embryonic kidney*. Semin Cell Dev Biol, 2003. **14**(4): p. 225-31.
83. Vainio, S. and U. Muller, *Inductive tissue interactions, cell signaling, and the control of kidney organogenesis*. Cell, 1997. **90**(6): p. 975-8.

84. Pichel, J.G., et al., *Defects in enteric innervation and kidney development in mice lacking GDNF*. Nature, 1996. **382**(6586): p. 73-6.
85. Hellmich, H.L., et al., *Embryonic expression of glial cell-line derived neurotrophic factor (GDNF) suggests multiple developmental roles in neural differentiation and epithelial-mesenchymal interactions*. Mech Dev, 1996. **54**(1): p. 95-105.
86. Moore, M.W., et al., *Renal and neuronal abnormalities in mice lacking GDNF*. Nature, 1996. **382**(6586): p. 76-9.
87. Sainio, K., et al., *Glial-cell-line-derived neurotrophic factor is required for bud initiation from ureteric epithelium*. Development, 1997. **124**(20): p. 4077-87.
88. Sanchez, M.P., et al., *Renal agenesis and the absence of enteric neurons in mice lacking GDNF*. Nature, 1996. **382**(6586): p. 70-3.
89. Cacalano, G., et al., *GFRalpha1 is an essential receptor component for GDNF in the developing nervous system and kidney*. Neuron, 1998. **21**(1): p. 53-62.
90. Costantini, F. and R. Shakya, *GDNF/Ret signaling and the development of the kidney*. Bioessays, 2006. **28**(2): p. 117-27.
91. Enomoto, H., et al., *GFR alpha1-deficient mice have deficits in the enteric nervous system and kidneys*. Neuron, 1998. **21**(2): p. 317-24.
92. Pachnis, V., B. Mankoo, and F. Costantini, *Expression of the c-ret proto-oncogene during mouse embryogenesis*. Development, 1993. **119**(4): p. 1005-17.
93. Schuchardt, A., et al., *Defects in the kidney and enteric nervous system of mice lacking the tyrosine kinase receptor Ret*. Nature, 1994. **367**(6461): p. 380-3.
94. Schuchardt, A., et al., *Renal agenesis and hypodysplasia in ret-k- mutant mice result from defects in ureteric bud development*. Development, 1996. **122**(6): p. 1919-29.
95. Brophy, P.D., et al., *Regulation of ureteric bud outgrowth by Pax2-dependent activation of the glial derived neurotrophic factor gene*. Development, 2001. **128**(23): p. 4747-56.
96. Kreidberg, J.A., et al., *WT-1 is required for early kidney development*. Cell, 1993. **74**(4): p. 679-91.
97. Nishinakamura, R., et al., *Murine homolog of SALL1 is essential for ureteric bud invasion in kidney development*. Development, 2001. **128**(16): p. 3105-15.
98. Torres, M., et al., *Pax-2 controls multiple steps of urogenital development*. Development, 1995. **121**(12): p. 4057-65.
99. Xu, P.X., et al., *Eya1-deficient mice lack ears and kidneys and show abnormal apoptosis of organ primordia*. Nat Genet, 1999. **23**(1): p. 113-7.
100. Grieshammer, U., et al., *SLIT2-mediated ROBO2 signaling restricts kidney induction to a single site*. Dev Cell, 2004. **6**(5): p. 709-17.
101. Kume, T., K. Deng, and B.L. Hogan, *Murine forkhead/winged helix genes Foxc1 (Mf1) and Foxc2 (Mfh1) are required for the early organogenesis of the kidney and urinary tract*. Development, 2000. **127**(7): p. 1387-95.

102. Pepicelli, C.V., et al., *GDNF induces branching and increased cell proliferation in the ureter of the mouse*. Dev Biol, 1997. **192**(1): p. 193-8.
103. Vega, Q.C., et al., *Glial cell line-derived neurotrophic factor activates the receptor tyrosine kinase RET and promotes kidney morphogenesis*. Proc Natl Acad Sci U S A, 1996. **93**(20): p. 10657-61.
104. Dudley, A.T., R.E. Godin, and E.J. Robertson, *Interaction between FGF and BMP signaling pathways regulates development of metanephric mesenchyme*. Genes Dev, 1999. **13**(12): p. 1601-13.
105. Dudley, A.T., K.M. Lyons, and E.J. Robertson, *A requirement for bone morphogenetic protein-7 during development of the mammalian kidney and eye*. Genes Dev, 1995. **9**(22): p. 2795-807.
106. Luo, G., et al., *BMP-7 is an inducer of nephrogenesis, and is also required for eye development and skeletal patterning*. Genes Dev, 1995. **9**(22): p. 2808-20.
107. Carroll, T.J., et al., *Wnt9b plays a central role in the regulation of mesenchymal to epithelial transitions underlying organogenesis of the mammalian urogenital system*. Dev Cell, 2005. **9**(2): p. 283-92.
108. Schmidt-Ott, K.M. and J. Barasch, *WNT/beta-catenin signaling in nephron progenitors and their epithelial progeny*. Kidney Int, 2008. **74**(8): p. 1004-8.
109. Kispert, A., S. Vainio, and A.P. McMahon, *Wnt-4 is a mesenchymal signal for epithelial transformation of metanephric mesenchyme in the developing kidney*. Development, 1998. **125**(21): p. 4225-34.
110. Stark, K., et al., *Epithelial transformation of metanephric mesenchyme in the developing kidney regulated by Wnt-4*. Nature, 1994. **372**(6507): p. 679-83.
111. Mendelsohn, C., et al., *Stromal cells mediate retinoid-dependent functions essential for renal development*. Development, 1999. **126**(6): p. 1139-48.
112. Hatini, V., et al., *Essential role of stromal mesenchyme in kidney morphogenesis revealed by targeted disruption of Winged Helix transcription factor BF-2*. Genes Dev, 1996. **10**(12): p. 1467-78.
113. Levinson, R.S., et al., *Foxd1-dependent signals control cellularity in the renal capsule, a structure required for normal renal development*. Development, 2005. **132**(3): p. 529-39.
114. Batourina, E., et al., *Vitamin A controls epithelial/mesenchymal interactions through Ret expression*. Nat Genet, 2001. **27**(1): p. 74-8.
115. Cui, S., L. Schwartz, and S.E. Quaggin, *Pod1 is required in stromal cells for glomerulogenesis*. Dev Dyn, 2003. **226**(3): p. 512-22.
116. Quaggin, S.E., et al., *The basic-helix-loop-helix protein pod1 is critically important for kidney and lung organogenesis*. Development, 1999. **126**(24): p. 5771-83.
117. Raatikainen-Ahokas, A., et al., *BMP-4 affects the differentiation of metanephric mesenchyme and reveals an early anterior-posterior axis of the embryonic kidney*. Dev Dyn, 2000. **217**(2): p. 146-58.
118. Angulo, J.C. and J.I. Lopez, *Pathogenetical considerations on a case of bilateral pelvic renal ectopia*. Minerva Urol Nefrol, 1994. **46**(4): p. 261-4.

119. Patterson, L.T. and S.S. Potter, *Atlas of Hox gene expression in the developing kidney*. Dev Dyn, 2004. **229**(4): p. 771-9.
120. Kobayashi, A., et al., *Six2 defines and regulates a multipotent self-renewing nephron progenitor population throughout mammalian kidney development*. Cell Stem Cell, 2008. **3**(2): p. 169-81.
121. Self, M., et al., *Six2 is required for suppression of nephrogenesis and progenitor renewal in the developing kidney*. Embo J, 2006. **25**(21): p. 5214-28.
122. Yu, J., A.P. McMahon, and M.T. Valerius, *Recent genetic studies of mouse kidney development*. Curr Opin Genet Dev, 2004. **14**(5): p. 550-7.
123. Patterson, L.T., M. Pembaur, and S.S. Potter, *Hoxa11 and Hoxd11 regulate branching morphogenesis of the ureteric bud in the developing kidney*. Development, 2001. **128**(11): p. 2153-61.
124. Ekker, S.C., et al., *Optimal DNA sequence recognition by the Ultrabithorax homeodomain of Drosophila*. Embo J, 1991. **10**(5): p. 1179-86.
125. Di Giacomo, G., et al., *Spatio-temporal expression of Pbx3 during mouse organogenesis*. Gene Expr Patterns, 2006.
126. Schnabel, C.A., R.E. Godin, and M.L. Cleary, *Pbx1 regulates nephrogenesis and ureteric branching in the developing kidney*. Dev Biol, 2003. **254**(2): p. 262-76.
127. Schnabel, C.A., et al., *Expression of Pbx1b during mammalian organogenesis*. Mech Dev, 2001. **100**(1): p. 131-5.
128. Treanor, J.J., et al., *Characterization of a multicomponent receptor for GDNF*. Nature, 1996. **382**(6586): p. 80-3.
129. Trupp, M., et al., *Functional receptor for GDNF encoded by the c-ret proto-oncogene*. Nature, 1996. **381**(6585): p. 785-9.
130. Brodbeck, S. and C. Englert, *Genetic determination of nephrogenesis: the Pax/Eya/Six gene network*. Pediatr Nephrol, 2004. **19**(3): p. 249-55.
131. Ohto, H., et al., *Cooperation of six and eya in activation of their target genes through nuclear translocation of Eya*. Mol Cell Biol, 1999. **19**(10): p. 6815-24.
132. Pignoni, F., et al., *The eye-specification proteins So and Eya form a complex and regulate multiple steps in Drosophila eye development*. Cell, 1997. **91**(7): p. 881-91.
133. Rebay, I., S.J. Silver, and T.L. Tootle, *New vision from Eyes absent: transcription factors as enzymes*. Trends Genet, 2005. **21**(3): p. 163-71.
134. Rupp, R.A., L. Snider, and H. Weintraub, *Xenopus embryos regulate the nuclear localization of XMyoD*. Genes Dev, 1994. **8**(11): p. 1311-23.
135. Turner, D.L. and H. Weintraub, *Expression of achaete-scute homolog 3 in Xenopus embryos converts ectodermal cells to a neural fate*. Genes Dev, 1994. **8**(12): p. 1434-47.
136. Lechner, M.S. and G.R. Dressler, *Mapping of Pax-2 transcription activation domains*. J Biol Chem, 1996. **271**(35): p. 21088-93.
137. Dressler, G.R., et al., *Pax2, a new murine paired-box-containing gene and its expression in the developing excretory system*. Development, 1990. **109**(4): p. 787-95.

138. Hostikka, S.L. and M.R. Capecchi, *The mouse Hoxc11 gene: genomic structure and expression pattern*. Mech Dev, 1998. **70**(1-2): p. 133-45.
139. Hsieh-Li, H.M., et al., *Hoxa 11 structure, extensive antisense transcription, and function in male and female fertility*. Development, 1995. **121**(5): p. 1373-85.
140. Xu, P.X., et al., *Mouse Eya homologues of the Drosophila eyes absent gene require Pax6 for expression in lens and nasal placode*. Development, 1997. **124**(1): p. 219-31.
141. Brophy, P.D., K.M. Lang, and G.R. Dressler, *The secreted frizzled related protein 2 (SFRP2) gene is a target of the Pax2 transcription factor*. J Biol Chem, 2003. **278**(52): p. 52401-5.
142. Phelps, D.E. and G.R. Dressler, *Identification of novel Pax-2 binding sites by chromatin precipitation*. J Biol Chem, 1996. **271**(14): p. 7978-85.
143. Cheng, W., et al., *Lineage infidelity of epithelial ovarian cancers is controlled by HOX genes that specify regional identity in the reproductive tract*. Nat Med, 2005. **11**(5): p. 531-7.
144. Nagy, A., M. Gerstenstein, K. Vintersten, and R. Behringer (ed.), *Manipulating the mouse embryo: a laboratory manual, 3rd ed.* 2003, Cold Spring Harbor, N.Y.: Cold Spring Harbor Laboratory Press.
145. Brodbeck, S., B. Besenbeck, and C. Englert, *The transcription factor Six2 activates expression of the Gdnf gene as well as its own promoter*. Mech Dev, 2004. **121**(10): p. 1211-22.
146. Epstein, J., et al., *Identification of a Pax paired domain recognition sequence and evidence for DNA-dependent conformational changes*. J Biol Chem, 1994. **269**(11): p. 8355-61.
147. McConnell, M.J., et al., *Differential regulation of the human Wilms tumour suppressor gene (WT1) promoter by two isoforms of PAX2*. Oncogene, 1997. **14**(22): p. 2689-700.
148. Pfeffer, P.L., M. Bouchard, and M. Busslinger, *Pax2 and homeodomain proteins cooperatively regulate a 435 bp enhancer of the mouse Pax5 gene at the midbrain-hindbrain boundary*. Development, 2000. **127**(5): p. 1017-28.
149. Oliver, G., et al., *Homeobox genes and connective tissue patterning*. Development, 1995. **121**(3): p. 693-705.
150. Xu, P.X., et al., *Six1 is required for the early organogenesis of mammalian kidney*. Development, 2003. **130**(14): p. 3085-94.
151. James, R.G., et al., *Odd-skipped related 1 is required for development of the metanephric kidney and regulates formation and differentiation of kidney precursor cells*. Development, 2006. **133**(15): p. 2995-3004.
152. James, R.G. and T.M. Schultheiss, *Bmp signaling promotes intermediate mesoderm gene expression in a dose-dependent, cell-autonomous and translation-dependent manner*. Dev Biol, 2005. **288**(1): p. 113-25.
153. Chisaka, O., T.S. Musci, and M.R. Capecchi, *Developmental defects of the ear, cranial nerves and hindbrain resulting from targeted disruption of the mouse homeobox gene Hox-1.6*. Nature, 1992. **355**(6360): p. 516-20.

154. Lufkin, T., et al., *Disruption of the Hox-1.6 homeobox gene results in defects in a region corresponding to its rostral domain of expression*. Cell, 1991. **66**(6): p. 1105-19.
155. Di Rocco, G., et al., *The recruitment of SOX/OCT complexes and the differential activity of HOXA1 and HOXB1 modulate the Hoxb1 autoregulatory enhancer function*. J Biol Chem, 2001. **276**(23): p. 20506-15.
156. Jacobs, Y., C.A. Schnabel, and M.L. Cleary, *Trimeric association of Hox and TALE homeodomain proteins mediates Hoxb2 hindbrain enhancer activity*. Mol Cell Biol, 1999. **19**(7): p. 5134-42.
157. Maconochie, M.K., et al., *Cross-regulation in the mouse HoxB complex: the expression of Hoxb2 in rhombomere 4 is regulated by Hoxb1*. Genes Dev, 1997. **11**(14): p. 1885-95.
158. Halder, G., et al., *Eyeless initiates the expression of both sine oculis and eyes absent during Drosophila compound eye development*. Development, 1998. **125**(12): p. 2181-91.
159. Hollander, G., et al., *Cellular and molecular events during early thymus development*. Immunol Rev, 2006. **209**: p. 28-46.
160. Kawakami, K., et al., *Six family genes--structure and function as transcription factors and their roles in development*. Bioessays, 2000. **22**(7): p. 616-26.
161. Benassayag, C., et al., *Evidence for a direct functional antagonism of the selector genes proboscipedia and eyeless in Drosophila head development*. Development, 2003. **130**(3): p. 575-86.
162. Plaza, S., et al., *Molecular basis for the inhibition of Drosophila eye development by Antennapedia*. Embo J, 2001. **20**(4): p. 802-11.
163. Manley, N.R. and M.R. Capecchi, *The role of Hoxa-3 in mouse thymus and thyroid development*. Development, 1995. **121**(7): p. 1989-2003.
164. Xu, P.X., et al., *Eya1 is required for the morphogenesis of mammalian thymus, parathyroid and thyroid*. Development, 2002. **129**(13): p. 3033-44.
165. Zou, D., et al., *Patterning of the third pharyngeal pouch into thymus/parathyroid by Six and Eya1*. Dev Biol, 2006. **293**(2): p. 499-512.
166. Neubuser, A., H. Koseki, and R. Balling, *Characterization and developmental expression of Pax9, a paired-box-containing gene related to Pax1*. Dev Biol, 1995. **170**(2): p. 701-16.
167. Poleev, A., et al., *PAX8, a human paired box gene: isolation and expression in developing thyroid, kidney and Wilms' tumors*. Development, 1992. **116**(3): p. 611-23.
168. Wallin, J., et al., *Pax1 is expressed during development of the thymus epithelium and is required for normal T-cell maturation*. Development, 1996. **122**(1): p. 23-30.
169. Christ, S., et al., *Hearing loss in athyroid pax8 knockout mice and effects of thyroxine substitution*. Audiol Neurootol, 2004. **9**(2): p. 88-106.
170. Gendron-Maguire, M., et al., *Hoxa-2 mutant mice exhibit homeotic transformation of skeletal elements derived from cranial neural crest*. Cell, 1993. **75**(7): p. 1317-31.

171. Ozaki, H., et al., *Six1 controls patterning of the mouse otic vesicle*. Development, 2004. **131**(3): p. 551-62.
172. Rijli, F.M., et al., *A homeotic transformation is generated in the rostral branchial region of the head by disruption of Hoxa-2, which acts as a selector gene*. Cell, 1993. **75**(7): p. 1333-49.
173. Kutejova, E., et al., *Hoxa2 downregulates Six2 in the neural crest-derived mesenchyme*. Development, 2005. **132**(3): p. 469-78.
174. Berger, M.F., et al., *Variation in homeodomain DNA binding revealed by high-resolution analysis of sequence preferences*. Cell, 2008. **133**(7): p. 1266-76.
175. Ekker, S.C., et al., *The degree of variation in DNA sequence recognition among four Drosophila homeotic proteins*. Embo J, 1994. **13**(15): p. 3551-60.
176. Noyes, M.B., et al., *Analysis of homeodomain specificities allows the family-wide prediction of preferred recognition sites*. Cell, 2008. **133**(7): p. 1277-89.
177. Gibson, G., et al., *The specificities of Sex combs reduced and Antennapedia are defined by a distinct portion of each protein that includes the homeodomain*. Cell, 1990. **62**(6): p. 1087-103.
178. Kuziora, M.A. and W. McGinnis, *Autoregulation of a Drosophila homeotic selector gene*. Cell, 1988. **55**(3): p. 477-85.
179. Kuziora, M.A. and W. McGinnis, *A homeodomain substitution changes the regulatory specificity of the deformed protein in Drosophila embryos*. Cell, 1989. **59**(3): p. 563-71.
180. Kuziora, M.A. and W. McGinnis, *Altering the regulatory targets of the Deformed protein in Drosophila embryos by substituting the Abdominal-B homeodomain*. Mech Dev, 1990. **33**(1): p. 83-93.
181. Lin, L. and W. McGinnis, *Mapping functional specificity in the Dfd and Ubx homeo domains*. Genes Dev, 1992. **6**(6): p. 1071-81.
182. Mann, R.S. and D.S. Hogness, *Functional dissection of Ultrabithorax proteins in D. melanogaster*. Cell, 1990. **60**(4): p. 597-610.
183. Zeng, W., et al., *Ectopic expression and function of the Antp and Scr homeotic genes: the N terminus of the homeodomain is critical to functional specificity*. Development, 1993. **118**(2): p. 339-52.
184. Gong, K.Q., et al., *A Hox-Eya-Pax Complex Regulates Early Kidney Developmental Gene Expression*. Mol Cell Biol, 2007. **21**(27): p. 7661-7668.
185. Kutejova, E., et al., *Six2 functions redundantly immediately downstream of Hoxa2*. Development, 2008. **135**(8): p. 1463-70.
186. Huppert, S.S., et al., *Analysis of Notch function in presomitic mesoderm suggests a gamma-secretase-independent role for presenilins in somite differentiation*. Dev Cell, 2005. **8**(5): p. 677-88.
187. Gong, K.Q., et al., *A Hox-Eya-Pax complex regulates early kidney developmental gene expression*. Mol Cell Biol, 2007. **27**(21): p. 7661-8.
188. Laughon, A., *DNA binding specificity of homeodomains*. Biochemistry, 1991. **30**(48): p. 11357-67.

189. Fromental-Ramain, C., et al., *Hoxa-13 and Hoxd-13 play a crucial role in the patterning of the limb autopod*. *Development*, 1996. **122**(10): p. 2997-3011.
190. Kmita, M., et al., *Early developmental arrest of mammalian limbs lacking HoxA/HoxD gene function*. *Nature*, 2005. **435**(7045): p. 1113-6.
191. Krumlauf, R. and A. Gould, *Homeobox cooperativity*. *Trends Genet*, 1992. **8**(9): p. 297-300.
192. McGinnis, W. and R. Krumlauf, *Homeobox genes and axial patterning*. *Cell*, 1992. **68**(2): p. 283-302.
193. Dessain, S., et al., *Antp-type homeodomains have distinct DNA binding specificities that correlate with their different regulatory functions in embryos*. *EMBO J*, 1992. **11**(3): p. 991-1002.
194. Malicki, J., K. Schughart, and W. McGinnis, *Mouse Hox-2.2 specifies thoracic segmental identity in Drosophila embryos and larvae*. *Cell*, 1990. **63**(5): p. 961-7.
195. McGinnis, N., M.A. Kuziora, and W. McGinnis, *Human Hox-4.2 and Drosophila deformed encode similar regulatory specificities in Drosophila embryos and larvae*. *Cell*, 1990. **63**(5): p. 969-76.
196. Neuteboom, S.T., et al., *The hexapeptide LFPWMR in Hoxb-8 is required for cooperative DNA binding with Pbx1 and Pbx2 proteins*. *Proc Natl Acad Sci U S A*, 1995. **92**(20): p. 9166-70.
197. Passner, J.M., et al., *Structure of a DNA-bound Ultrabithorax-Extradenticle homeodomain complex*. *Nature*, 1999. **397**(6721): p. 714-9.
198. Phelan, M.L., I. Rambaldi, and M.S. Featherstone, *Cooperative interactions between HOX and PBX proteins mediated by a conserved peptide motif*. *Mol Cell Biol*, 1995. **15**(8): p. 3989-97.
199. Piper, D.E., et al., *Structure of a HoxB1-Pbx1 heterodimer bound to DNA: role of the hexapeptide and a fourth homeodomain helix in complex formation*. *Cell*, 1999. **96**(4): p. 587-97.
200. Knoepfler, P.S., et al., *A conserved motif N-terminal to the DNA-binding domains of myogenic bHLH transcription factors mediates cooperative DNA binding with pbx-Meis1/Prep1*. *Nucleic Acids Res*, 1999. **27**(18): p. 3752-61.
201. Ebner, A., et al., *Recognition of distinct target sites by a unique Labial/Extradenticle/Homothorax complex*. *Development*, 2005. **132**(7): p. 1591-600.
202. Tour, E., C.T. Hittinger, and W. McGinnis, *Evolutionarily conserved domains required for activation and repression functions of the Drosophila Hox protein Ultrabithorax*. *Development*, 2005. **132**(23): p. 5271-81.
203. Gebelein, B., D.J. McKay, and R.S. Mann, *Direct integration of Hox and segmentation gene inputs during Drosophila development*. *Nature*, 2004. **431**(7009): p. 653-9.
204. Walsh, C.M. and S.B. Carroll, *Collaboration between Smads and a Hox protein in target gene repression*. *Development*, 2007. **134**(20): p. 3585-92.

205. Cobb, J. and D. Duboule, *Comparative analysis of genes downstream of the Hoxd cluster in developing digits and external genitalia*. Development, 2005. **132**(13): p. 3055-67.
206. Hedlund, E., et al., *Identification of a Hoxd10-regulated transcriptional network and combinatorial interactions with Hoxa10 during spinal cord development*. J Neurosci Res, 2004. **75**(3): p. 307-19.
207. Hersh, B.M., et al., *The UBX-regulated network in the haltere imaginal disc of D. melanogaster*. Dev Biol, 2007. **302**(2): p. 717-27.
208. Leemans, R., et al., *Identification of candidate downstream genes for the homeodomain transcription factor Labial in Drosophila through oligonucleotide-array transcript imaging*. Genome Biol, 2001. **2**(5): p. RESEARCH0015.
209. Mohit, P., et al., *Modulation of AP and DV signaling pathways by the homeotic gene Ultrabithorax during haltere development in Drosophila*. Dev Biol, 2006. **291**(2): p. 356-67.
210. Rohrschneider, M.R., G.E. Elsen, and V.E. Prince, *Zebrafish Hoxb1a regulates multiple downstream genes including prickle1b*. Dev Biol, 2007. **309**(2): p. 358-72.
211. Schwab, K., et al., *Comprehensive microarray analysis of Hoxa11/Hoxd11 mutant kidney development*. Dev Biol, 2006. **293**(2): p. 540-54.
212. Valerius, M.T., et al., *Microarray analysis of novel cell lines representing two stages of metanephric mesenchyme differentiation*. Mech Dev, 2002. **112**(1-2): p. 219-32.
213. McCabe, C.D. and J.W. Innis, *A genomic approach to the identification and characterization of HOXA13 functional binding elements*. Nucleic Acids Res, 2005. **33**(21): p. 6782-94.
214. Alcorn, D., C. Maric, and J. McCausland, *Development of the renal interstitium*. Pediatr Nephrol, 1999. **13**(4): p. 347-54.
215. Little, M.H., et al., *A high-resolution anatomical ontology of the developing murine genitourinary tract*. Gene Expr Patterns, 2007. **7**(6): p. 680-99.
216. Schuster, V.L., *Function and regulation of collecting duct intercalated cells*. Annu Rev Physiol, 1993. **55**: p. 267-88.
217. Cho, E.A., et al., *Differential expression and function of cadherin-6 during renal epithelium development*. Development, 1998. **125**(5): p. 803-12.
218. Brenner-Anantharam, A., et al., *Tailbud-derived mesenchyme promotes urinary tract segmentation via BMP4 signaling*. Development, 2007. **134**(10): p. 1967-75.
219. Cebrian, C., et al., *Morphometric index of the developing murine kidney*. Dev Dyn, 2004. **231**(3): p. 601-8.
220. Lang, R.J., M.E. Davidson, and B. Exintaris, *Pyeloureteral motility and ureteral peristalsis: essential role of sensory nerves and endogenous prostaglandins*. Exp Physiol, 2002. **87**(2): p. 129-46.
221. Chevalier, R.L., *Perinatal obstructive nephropathy*. Semin Perinatol, 2004. **28**(2): p. 124-31.
222. Mendelsohn, C., *Functional obstruction: the renal pelvis rules*. J Clin Invest, 2004. **113**(7): p. 957-9.

223. Nelson, L.T., et al., *Generation and expression of a Hoxa11eGFP targeted allele in mice*. Dev Dyn, 2008. **237**(11): p. 3410-6.
224. Niederreither, K., et al., *Differential expression of retinoic acid-synthesizing (RALDH) enzymes during fetal development and organ differentiation in the mouse*. Mech Dev, 2002. **110**(1-2): p. 165-71.
225. Niederreither, K., et al., *Restricted expression and retinoic acid-induced downregulation of the retinaldehyde dehydrogenase type 2 (RALDH-2) gene during mouse development*. Mech Dev, 1997. **62**(1): p. 67-78.
226. Leimeister, C., A. Bach, and M. Gessler, *Developmental expression patterns of mouse sFRP genes encoding members of the secreted frizzled related protein family*. Mech Dev, 1998. **75**(1-2): p. 29-42.
227. Trevant, B., et al., *Expression of secreted frizzled related protein 1, a Wnt antagonist, in brain, kidney, and skeleton is dispensable for normal embryonic development*. J Cell Physiol, 2008. **217**(1): p. 113-26.
228. Lewis, E.B., *Genes and developmental pathways*. American Zoology, 1963. **3**: p. 33-56.
229. Lewis, E.B., *A gene complex controlling segmentation in Drosophila*. Nature, 1978. **276**: p. 565-570.
230. Colberg-Poley, A.M., et al., *Clustered homeo boxes are differentially expressed during murine development*. Cell, 1985. **43**(39-45).
231. Duboule, D. and P. Dolle, *The structural and functional organization of the murine HOX gene family resembles that of Drosophila homeotic genes*. EMBO Journal, 1989. **8**(5): p. 1497-505.
232. Gruss, P. and M. Kessel, *Axial specification in higher vertebrates*. Current Opinion in Genetics and Development, 1991. **1**: p. 204-210.
233. Kessel, M. and P. Gruss, *Murine developmental control genes*. Science, 1990. **249**: p. 374-9.
234. Bachiller, D., et al., *Conservation of a functional hierarchy between mammalian and insect Hox/HOM genes*. EMBO Journal, 1994. **13**: p. 1930-41.
235. Duboule, D., *Patterning in the vertebrate limb*. Current Opinion in Genetics and Development, 1991. **1**(2): p. 211-216.
236. Duboule, D. and G. Morata, *Colinearity and functional hierarchy among genes of the homeotic complexes*. TIG, 1994. **10**(10): p. 358-364
237. Kmita, M. and D. Duboule, *Organizing Axes in Time and Space; 25 Years of Colinear Tinkering*. Science, 2003. **301**: p. 331-333.
238. Chen, F. and M.R. Capecchi, *Targeted mutations in hoxa-9 and hoxb-9 reveal synergistic interactions*. Developmental Biology, 1997. **181**(2): p. 186-196.
239. Chen, F. and M.R. Capecchi, *Paralogous mouse Hox genes, Hoxa9, Hoxb9, and Hoxd9, function together to control development of the mammary gland in response to pregnancy*. Proceedings of the National Academy of Sciences, USA, 1999. **96**: p. 541-546.

240. Chen, F., J. Greer, and M.R. Capecchi, *Analysis of Hoxa7/Hoxb7 mutants suggests periodicity in the generation of the different sets of vertebrae*. *Mechanisms of Development*, 1998. **77**: p. 49-57.
241. Davis, A.P., et al., *Absence of radius and ulna in mice lacking hoxa-11 and hoxd-11*. *Nature*, 1995. **375**: p. 791-795.
242. Horan, G.S.B., et al., *Compound mutants for the paralogous hoxa-4, hoxb-4, and hoxd-4 genes show more complete homeotic transformations and a dose-dependent increase in the number of vertebrae transformed*. *Genes & Development*, 1995. **9**: p. 1667-1677.
243. Rossel, M. and M.R. Capecchi, *mice mutant for both Hoxa1 and Hoxb1 show extensive remodeling of the hindbrain and defects in craniofacial development*. *Development*, 1999. **126**: p. 5027-5040.
244. Patterson, L.T., M. Pembaur, and S.S. Potter, *Hoxa11 and Hoxd11 regulate branching morphogenesis of the ureteric bud in the developing kidney*. *Development*, 2001. **128**: p. 2153-2161.
245. Wellik, D.M. and M.R. Capecchi, *Hox10 and Hox11 Genes Are Required to Globally Pattern the Mammalian Skeleton*. *Science*, 2003. **301**: p. 363-366.
246. Wellik, D.M., P.J. Hawkes, and M.R. Capecchi, *Hox11 paralogous genes are essential for metanephric kidney induction*. *Genes & Development*, 2002. **16**: p. 1423-1432.
247. Wahba, G.M., S.L. Hostikka, and E.M. Carpenter, *The Paralogous Hox Genes Hoxa10 and Hoxd10 Interact to Pattern the Mouse Hindlimb Peripheral Nervous System and Skeleton*. *Developmental Biology*, 2001. **231**: p. 87-102.
248. Greer, J., et al., *Maintenance of functional equivalence during paralogous Hox gene evolution*. *Nature*, 2000. **403**(6770): p. 661-5.
249. Garcia-Gasca, A. and D.D. Spyropoulos, *Differential mammary morphogenesis along the anteroposterior axis in Hoxc6 gene targeted mice*. *Developmental Dynamics*, 2000. **219**(2): p. 261-276.
250. Jeannotte, L., et al., *Specification of axial identity in the mouse: role of the Hoxa-5 (Hox1.3) gene*. *Genes & Development*, 1993. **7**(11): p. 2085-96.
251. Kostic, D. and M.R. Capecchi, *Targeted disruptions of the murine Hoxa-4 and Hoxa-6 genes result in homeotic transformations of components of the vertebral column*. *Mechanisms of Development*, 1994. **46**(3): p. 231-47.
252. Rancourt, D.E., T. Tsuzuki, and M.R. Capecchi, *Genetic interaction between hoxb-5 and hoxb-6 is revealed by nonallelic noncomplementation*. *Genes & Development*, 1995. **9**(1): p. 108-22.
253. vandenAkker, E., et al., *Axial skeletal patterning in mice lacking all paralogous group 8 Hox genes*. *Development*, 2001. **128**: p. 1911-1921.
254. Nowicki, J.L. and A.C. Burke, *Hox genes and morphological identity: axial patterning versus lateral patterning in the vertebrate mesoderm*. *Development*, 2000. **127**: p. 4265-4275.

255. Nowicki, J.L., R. Takimoto, and A.C. Burke, *The lateral somitic frontier: dorso-ventral aspects of antero-posterior regionalization in avian embryos*. *Mechanisms of Development*, 2003. **120**: p. 227-240.
256. Burke, A.C. and J.L. Nowicki, *A New View of Patterning Domains in the Vertebrate Mesoderm*. *Developmental Cell*, 2003. **4**: p. 159-165.
257. Boulet, A.M. and M.R. Capecchi, *Targeted Disruption of hoxc-4 Causes Esophageal Defects and Vertebral Transformations*. *Developmental Biology*, 1996. **177**: p. 232-249.
258. Huppert, S.S., et al., *Analysis of Notch function in presomitic mesoderm suggests a gamma-secretase-independent role for presenilins in somite differentiation*. *Developmental Cell*, 2005. **8**(5): p. 677-88.
259. Burke, A.C., et al., *Hox genes and the evolution of vertebrate axial morphology*. *Development* 1995. **121**(2): p. 333-46.
260. Gaunt, S.J., et al., *Mouse Hox-3.4: homeobox sequence and embryonic expression patterns compared with other members of the Hox gene network*. *Development*, 1990. **109**(2): p. 329-39.
261. Toth, L.E., et al., *Region-specific expression of mouse homeobox genes in the embryonic mesoderm and central nervous system*. *Proceedings of the National Academy of Sciences, U.S.A.*, 1987. **84**(19): p. 6790-4.
262. Chen, F. and M.R. Capecchi, *Targeted mutations in hoxa-9 and hoxb-9 reveal synergistic interactions*. *Developmental Biology*, 1997. **181**: p. 186-196.
263. Erselius, J.R., M.D. Goulding, and P. Gruss, *Structure and expression pattern of the murine Hox-3.2 gene*. *Development*, 1990. **110**(2): p. 629-42.